Modeling the potential influence of subsurface tile drainage systems on downstream flooding in a midwestern agricultural watershed

by

Heather White

B.S., Kansas State University, 2023

A THESIS

submitted in partial fulfillment of the requirements for the degree

MASTER OF SCIENCE

Carl and Melinda Helwig Department of Biological and Agricultural Engineering
Carl R. Ice College of Engineering

KANSAS STATE UNIVERSITY
Manhattan, Kansas

2023

Approved by:

Major Professor
Vaishali Sharda

Copyright

Abstract

Subsurface drainage systems are common in agricultural regions of the Midwestern United States. Drainage systems remove excess water from the surface and soil profile of agricultural fields, allowing crop production in previously unsuitable locations. However, drainage systems impact watershed hydrology and could, depending on site-specific factors, influence flooding events. Therefore, this study determines whether subsurface tile drainage systems influence daily downstream flooding from a midwestern, agricultural watershed: Skunk Creek watershed.

In this study, the Soil and Water Assessment Tool (SWAT) model is used to simulate the hydrologic processes of Skunk Creek Watershed for a period of 18 years (2004-2021). The model is calibrated and validated using observed daily streamflow data with the SWAT Calibration and Uncertainty Program (SWAT-CUP) software, as well as through the manual addition of missed precipitation data. The statistical parameters Nash Sutcliffe Efficiency (NSE), Percent Bias (PBIAS), and RMSE-Observations Standard Deviation Ratio (RSR) are used to evaluate the fit and accuracy of the model, with the daily NSE ranging from 0.595 to 0.790, PBIAS ranging from -2.588 to 25.808, and RSR ranging from 0.636 to 0.458.

The calibrated and validated model is used as the baseline scenario, and five tile drainage scenarios—ranging from 15% to 75% tile-drained agricultural land—are individually incorporated into the model. It was observed that as the area of tile-drained land increases, the depth of tile flow contributing to daily streamflow increases. Additionally, surface runoff, groundwater flow, deep aquifer recharge, and percolation decrease, whereas lateral soil flow, tile flow, evapotranspiration, and water yield increase.

A comparison of tile drainage scenarios suggests that increasing the amount of tile-drained agricultural land decreases the total number of flood events (flood days). However, the impact of tile drainage systems on downstream flood peak flows was found to vary by event. Large precipitation events (greater than 300 mm/day) were found to initiate flood days with similar peak flows across all scenarios. Future studies can replicate the approach with a sub-daily time-step for simulating hourly flood events with various tile drainage scenarios.

Table of Contents

List of Figures

List of Tables

Acknowledgments

It is my pleasure to express my sincerest thanks and gratitude to those who helped me accomplish my Master's thesis work. This accomplishment would not have been possible without the continuous support and guidance offered to me before and throughout my time at Kansas State University.

First of all, I would like to thank my advisor, Dr. Vaishali Sharda for the continuous feedback and support throughout my study. The mentorship, knowledge, encouragement, and patience allowed me to grow into a more independent scholar and researcher. I sincerely appreciate the time made for me to stop by and talk, no matter how small my problem or concern. I truly cannot imagine having a better advisor and mentor for my study.

I would also like to thank my research committee members, Dr. Aleksey Sheshukov and Dr. Laurent Ahiablame for their immense expertise and support. I truly appreciate their willingness to meet and answer questions while guiding me through this study.

I am thankful to all faculty members of the Carl and Melinda Helwig Department of Biological and Agricultural Engineering for teaching and shaping me throughout my undergraduate and graduate degrees. I would also like to thank my friends and research group members for being with me from start to finish.

I would like to thank Mrs. Sandy Wanklyn, who helped me make it to both Kansas State University and the College of Engineering. I would also like to thank my Uncle John for both teaching and helping me to improve my writing.

Finally, I would like to thank my family for their continuous, steadfast support.

Dedication

To my parents, Tom and Darla, and my sisters, Rachel and Sara for the encouragement and support. To Khai, for the patience. To my dog, Tonks, for the companionship and unconditional love.

Chapter 1 - Introduction

1.1 Background

Over 100 years ago, farmers in the United States began to adopt subsurface drainage as a production management practice (Cooke et al., 2001; Guo et al., 2018; Rahman & Lin, 2013; Woo et al., 2019). The practice is often referred to as tile drainage because historically, producers used clay or concrete tiles to construct the drainage systems. In the 1960s, agriculturalists developed plastic pipelines for use in these systems. Originally, the plastic pipes were straight and had smooth walls; however, over several years of development, corrugated plastic pipes soon replaced straight, smooth-walled pipes. Since the 1970s, corrugated, plastic pipelines have been regularly used and installed in place of clay and concrete tiles (Jha; NDSU).

Despite the transition to plastic pipelines, the function of subsurface tile drainage systems remains the same: to remove excess water from the surface, or the soil profile, of agricultural fields (Guo et al., 2018; Rahman et al., Sloan, 2013; 2011; Woo et al., 2019). The removal of such water alters (or controls) the depth of the natural water table (Boles, 2013; Cihacek et al., 2020; Hofstrand, 2010; Moriasi et al., 2013; Rahman et al., 2011; Sloan et al., 2015). When groundwater is near the soil surface, salt accumulates and soil oxygen levels decrease, resulting in inadequate conditions for crop production (Cihacek et al., 2020; NDSU). Therefore, in agricultural production, it is imperative that the water table is maintained. Management of the water table has enabled crop growth and production in previously unsuitable locations (Cooke et al., 2001; Sloan, 2013; Sloan et al., 2015).

Water table management allows crops to be planted earlier in the growing season, reducing overall plant stress. Fields with subsurface drainage systems have increased infiltration, increased soil aeration, and increased soil water storage (SWS) capacity (Pakuska, 2018; Woo et

al., 2019). When crops have access to adequate oxygen in the root zone, fewer plants are affected by disease, and crop stands are improved (Hofstrand, 2010; Thomas, 2015; Woo et al., 2019). Correspondingly, soil health is maintained and improved by drainage systems. When producers drain farm ground, the soil is less vulnerable to compaction from heavy machinery, and surface runoff is reduced. With less surface runoff, topsoil is conserved (Panuska, 2018), field erosion is mitigated, and freshwater contamination is decreased. Due to these benefits, subsurface drainage systems have allowed regions in the Midwest to flourish, becoming some of the most productive agricultural land in the world (Guo et al., 2018).

In the early 2000s, landowners rapidly accelerated their installation of drainage systems to improve crop yields and expand agricultural land cover (Werner et al., 2016). Currently, more than 30% of farm ground in the Midwest has subsurface drainage systems (Sloan et al., 2015; Woo et al., 2019), which ultimately impacts both the hydrologic and ecological regime (Sloan, 2013). Consequences of drainage systems include the loss of wetland and floodplain ecosystems; the alteration of instream habitats, riparian habitats, and nutrient cycles (Sloan et al., 2015); and the increased risk of floods and droughts (Thomas, 2015). Drainage systems convey effluent that often carries contaminants, pollutants, and chemical species from agricultural systems into drainage ditches, streams, and wetlands (Cooke et al., 2001; Golmohammadi et al., 2017; Guo et al., 2018; Thomas, 2015). Eventually, the effluent merges with various stream networks and contributes to downstream pollutant concentrations (Sloan et al., 2015; Woo et al., 2019). Likewise, the addition of excess water from drainage systems alters streamflow regimes, which in turn, transform stream morphology and watershed hydrology (Cooke et al., 2001; Gupta et al., 2015; Rahman et al., 2011; Rahman et al., 2014; Sloan et al., 2015). In the Midwest,

despite such impacts, landowners continue to increase the implementation and use of subsurface drainage systems (Sloan et al., 2015).

1.2 Problem Statement

At the watershed scale, observers have long raised concerns regarding the role of subsurface drainage in downstream flow alterations and subsequent flooding events. Despite decades of research, there is still significant controversy regarding the impacts of drainage systems on watershed hydrology (Sloan, 2013). Two schools of thought have often been debated regarding the hydrologic and environmental impacts of subsurface drainage (Blann et al., 2009). One school argues that with changes in the amount and timing of water leaving the field, surface runoff may decrease (Zucker & Brown, 1998; Macrae et al., 2007; Maalim & Melesse, 2013), while peak flow rates may increase (Konyha et al., 1992; Blann et al., 2009; Wesström et al., 2014), leading to downstream flooding through the acceleration of water delivery to receiving rivers (Whiteley, 1979; Blann et al., 2009). The other school argues that subsurface drainage removes extra moisture from the soil profile, allowing increased infiltration, decreased surface runoff, and decreased downstream flood flow (Irwin & Whiteley, 1983; Fraser et al., 2001; King et al., 2014). Considering the two conflicting points of view, a logical question is to explore the extent to which streamflow changes and downstream flooding can be explained by subsurface drainage.

1.3 Research Objectives

The objective of this study is to use the hydrologic Soil and Water Assessment Tool (SWAT) model to quantitatively analyze the impact of subsurface drainage systems on streamflow in the Skunk Creek watershed in southeastern South Dakota. Daily streamflow is

analyzed to determine whether subsurface tile drainage systems influence daily flooding events at the outlet of the watershed. More specific objectives of the study are as follows:

(i) Building a SWAT model, and calibrating and validating the model with the SWAT-Calibration and Uncertainty Program (SWAT-CUP) software to accurately simulate daily streamflow in the Skunk Creek watershed;

(ii) Performing scenario analysis by modeling subsurface tile drainage systems on varied extents of agricultural land in the watershed while simulating reasonable, expected ranges of tile flow;

(iii) Analyzing the impacts of increased tile-drained agricultural land on watershed hydrology; and

(iv) Evaluating the influence of tile drainage scenarios on daily downstream flooding from the Skunk Creek watershed.

1.4 Significance of Thesis

Given the continual installation of subsurface drainage systems in the Midwestern United States (Sloan et al., 2015), this case study could be used to provide beneficial information to support and maintain stream systems, environments, and ecosystems at the outlet of similar drained, Midwestern, agricultural watersheds.

Chapter 2 - Literature Review

2.1 Studies Conducted in Skunk Creek Watershed

This study was conducted in Skunk Creek watershed, located in southeastern South Dakota. Several studies have been conducted in the Skunk Creek watershed, including the coupling of calibration methods to improve streamflow simulations (Mehan et al., 2017), as well as the evaluation of streamflow and water quality impacts caused by land-use conversion and climatic changes (Ahiablame et al., 2019; Hong, 2017; Paul, 2016; Paul et al., 2016; Rajib et al., 2016).

In a study conducted by Mehan et al., (2017), a Soil and Water Assessment Tool (SWAT) model for Skunk Creek watershed was constructed with 7 sub-basins and 364 hydrologic response units (HRUs). The model was calibrated and validated from 1980-2000 with 24 hydrologic parameters. The model warm-up period occurred from 1980-1986, with the calibration period from 1987-1994, and the validation period from 1995-2000. The model was evaluated with the NSE, PBIAS, RMSE, and R^2 statistics, ranging from 0.56 to 0.55, -9.70 to -16.3, 411.39 to 292.75, and 0.7 to 0.44 at the daily time-step during the calibration and validation time periods, respectively. The global sensitivity analysis, performed by the SWAT-Calibration and Uncertainty Program (SWAT-CUP) software, determined the most sensitive parameter to be the available water capacity of the soil layer (SOL_AWC) for both 500 and 2,000 simulations. The authors concluded that the coupling of the SWAT model and SWAT-CUP software allowed the reliable simulation of watershed hydrology within the Skunk Creek watershed.

In another study, Hong, (2017), constructed a SWAT model for the Skunk Creek watershed with 31 sub-basins and 1,097 HRUs. The model was calibrated and validated from 1994 to 2014 for daily streamflow, monthly sediment load, monthly dissolved phosphorous load,

and monthly nitrate load. The model warm-up period occurred from 1994-1995, calibration occurred from 2005-2014 (the years 2001-2003 were excluded due to missing observed streamflow data), and validation occurred from 1996-2000. The SWAT model was used to evaluate 24 hypothetical scenarios including time-static land use change, time-variant land use change, and grassland management in the watershed. The model was evaluated with the R^2, NSE, and PBIAS statistics. For the calibration and validation time periods, streamflow statistics ranged from 0.57 to 0.51 (R^2), 0.57 to 0.50 (NSE), and -4.14 to 3.90 (PBIAS) at the daily time step (please see Hong, (2017) for monthly sediment load, monthly dissolved phosphorous load, and monthly nitrate load calibration and validation statistics). The author found that the conversion of grassland to cropland, with the simultaneous implementation of heavy grazing regimes, likely results in water quality degradation. More specifically, the author observed a 7% increase in streamflow and sediment loading, a 9% increase in dissolved phosphorous loading, and a 25% decrease in nitrate loading. Similarly, scenarios with a grass-crop rotation indicate a 12% increase in streamflow, a 19% increase in sediment loads, a 13% decrease in nitrate loads, and a decrease in dissolved phosphorous loading. Long-term grassland establishment scenarios result in an 18% reduction in nitrate loads and less than a 1% increase in dissolved phosphorous loads. With these results, the author concluded that the best watershed location for water quality benefits (through grassland establishment) is dependent on the nutrient of interest as well as the cropping systems.

In a study by Ahiablame et al., (2019), a similar SWAT model was constructed for Skunk Creek watershed with 31 sub-basins and 1,097 HRUs. Eighteen parameters were selected for streamflow model calibration and validation, with the warm-up period from 1994-1995, calibration from 2005-2014, and validation from 1996-2000. The calibrated model served as the

baseline scenario, which depicted existing land use conditions in the watershed. Seven hypothetical land use change scenarios were developed and compared with the baseline scenario to analyze streamflow changes from grassland to cropland (and vice versa) conversion. The model was evaluated with the R^2, NSE, and PBIAS statistics, with monthly values ranging from 0.62 to 0.70, 0.62 to 0.65, and -4.24 to 3.92 during the calibration and validation time periods, respectively. The authors found that in the watershed, the conversion from grassland to cropland (and vice versa) would alter both low- and high-flow regimes, with average annual flow increasing with grassland-to-cropland conversion, and average annual flow decreasing with cropland-to-grassland conversion.

In a study by Paul et al., (2017), three South Dakota watersheds, including the Skunk Creek watershed, were evaluated. The Skunk Creek watershed was calibrated and validated with 19 selected parameters for two discrete time periods (1981-1990 and 2005-2014) to provide comparisons between annual and seasonal runoff, available soil water content, evapotranspiration, water yield, and percolation. The model was calibrated and validated on the daily time step with the R^2, NSE, and PBIAS statistics. Calibration and validation statistics for the 1981-1990 study period ranged from 0.57 to 0.65 (R^2), 0.55 to 0.63 (NSE), and -20.80 to 0.85 (PBIAS). Similarly, for the 2005-2014 study period, daily calibration and validation statistics ranged from 0.56 to 0.75 (R^2), 0.56 to 0.48 (NSE), and -7.60 to -42.60 (PBIAS). The authors found that when comparing the average annual water budget between the two study periods, surface runoff, available soil water content, water yield, and percolation increased; therefore, providing insight regarding the changes in hydrological process induced by both land use conversion and climate change.

As demonstrated by several previous studies (Ahiablame et al., 2019; Hong, 2017; Mehan et al., 2017; Paul et al., 2017), the Skunk Creek watershed has continual research interests. Further examination of the watershed through hydrologic modeling will allow a deeper understanding of the hydrologic processes, water quantity, and water quality relationships within the watershed. Additionally, as no reviewed study focuses on subsurface tile drainage systems or daily downstream flood events, this study could provide additional, valuable information to contribute to scientific knowledge regarding these studied events within the watershed, as well as similar Midwestern, agricultural watersheds.

2.2 Subsurface Drainage System Design

The design of subsurface tile drainage systems influences hydrograph peaks (Frankenberger et al., 2013) as well as streamflow regimes (Sloan, 2013). These systems are designed and installed based on the unique properties of agricultural fields. Factors influencing system arrangement include dominant soil types, soil surface conditions, average field slope, and preexisting crop variety (Woo et al., 2019). Due to the multitude of variables influencing system arrangement, several common designs of subsurface tile drainage systems exist. Standard drainage designs include parallel, herringbone, double-main, and random (targeted) systems (Figure 2-1; USDA SCS, 1971). Parallel systems consist of lateral lines that enter the main drainage line perpendicularly. These systems are generally installed in flat fields with uniform soil types. Herringbone systems consist of parallel lines that enter the main line at an angle. The main line generally runs along the major hillslope of the field with the lateral lines angled upstream. Double-main systems include a combination of parallel and herringbone systems; these systems are generally installed in fields divided by large depressions. Finally, random systems include various combinations of drainage designs. These systems are often installed in

fields with isolated wet areas, with lateral lines arranged according to the size of surface depressions (Figure 2-1; Cooke et al., n.d.; Hofstrand, 2010; USDA SCS, 1971).

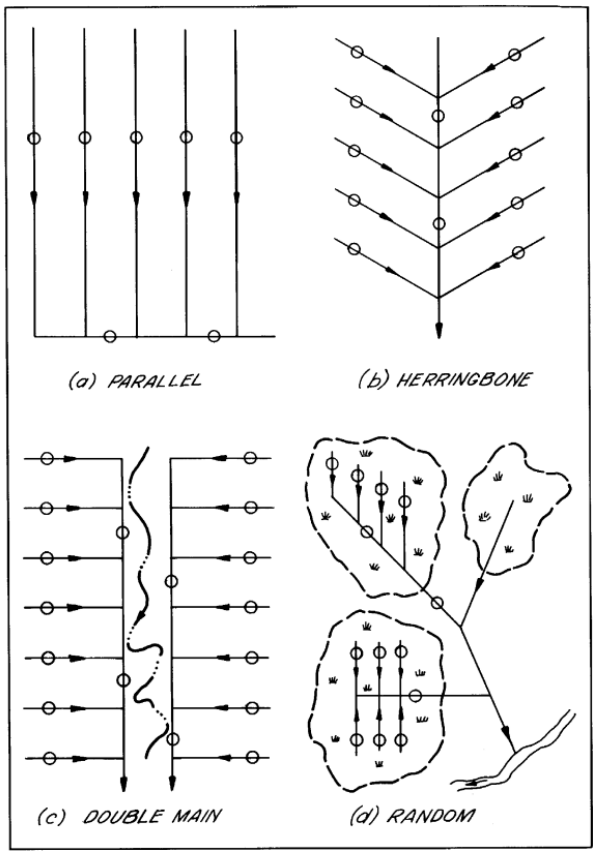

Figure 2-1: Subsurface tile drainage system design, where (A) Parallel, (B) Herringbone, (C) Double Main, and (D) Random (USDA SCS, 1971).

In all drainage systems, water first enters the pipeline (lateral lines) through holes in, or cracks between, adjacent tiles (Guo et al., 2018; NDSU). The water is then directed to the main line (Cooke et al., n.d.; Hofstrand, 2010), and is routed to the system outlet. The outlet then discharges the water into an open ditch, stream system, or other conveyance structure. The effectiveness of the drainage system is dependent on the outlet's ability to remove water from the field; therefore, the placement of the outlet is crucial (Figure 2-2; Stika, 2019; Hofstrand, 2010).

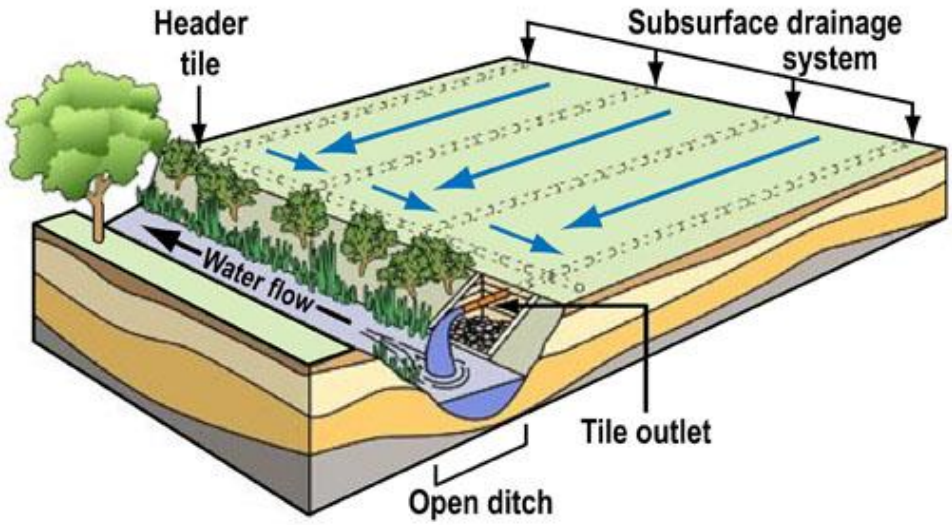

Figure 2-2: Transportation of excess field water through lateral lines, main lines, and the system outlet through a subsurface tile drainage system (Stika, 2019).

In tile systems, drainage pipelines (or laterals) are generally placed approximately one-to-two meters below the soil surface. This depth allows the performance of routine tilling and planting operations; the complete development of crop root systems (NDSU; Sloan et al., 2015); and the maintenance of the water table depth (Boles, 2013; Cihacek et al., 2020; Hofstrand, 2010; Moriasi et al., 2013; Rahman et al., 2011; Sloan et al., 2015). In undrained fields, the water table is near the soil surface, with excess water ponding in surface depressions (Figure 2-3a). In contrast, in drained fields, the water table depth is lowered to the depth of the tile drains (Figure 2-3b; Eller, 2015). The respective spacing (distance between parallel laterals) of tile drains is considered relative to drainage depth and is based on both soil properties and crop type (Thomas, 2015; University of Minnesota Extension, 2018).

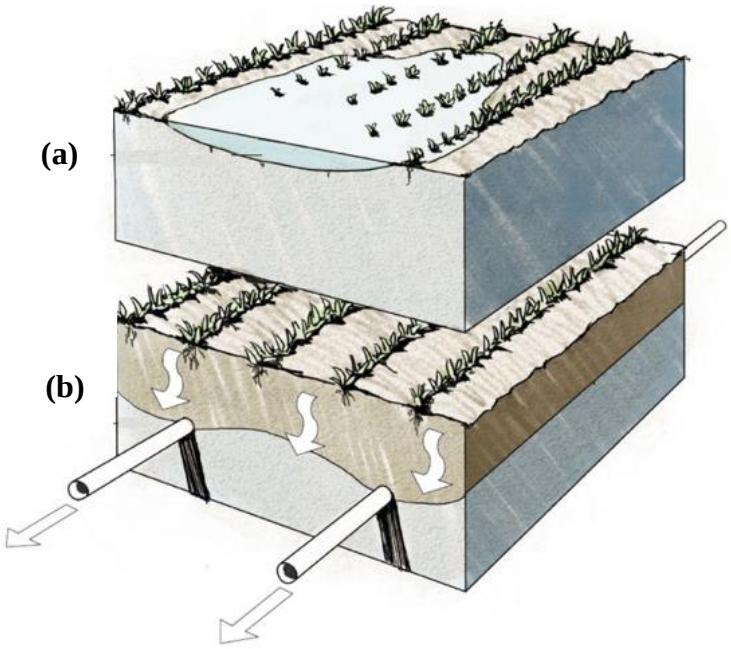

Figure 2-3: Subsurface tile drainage system control on water table depth, where (a) undrained condition and (b) drained condition (Adapted from Eller, 2015).

Coarse soils, such as sands and silts, often have wider spacings, whereas finer soils, such as clays and loams, often have narrower spacings (Scherer et al., 2015). As soil types often vary across agricultural fields, optimal performance is determined by the ability of the system to remove excess field water within 24 hours of a precipitation event (Hofstrand, 2010). To ensure drainage systems achieve optimal performance, design criteria exist for several Midwestern states (Boles, 2013; University of Minnesota Extension, 2018; Schilling et al., 2019). These criteria improve the maintenance of agricultural fields, as well as allow more accurate hydrologic modeling through the appropriate representation of subsurface tile drainage systems.

2.3 Impacts of Subsurface Drainage on Watershed Water Balance

In natural landscapes, there are several pathways in which water flows. Primary routines include surface runoff and baseflow, which direct and transport water throughout the watershed. When subsurface drainage systems are installed, an additional (or alternative) flow path is added

to the water balance, modifying the natural hydrologic regime (Boles, 2013; Guo et al., 2018; Schilling et al., 2019; Thomas, 2015). Specific impacts of subsurface drainage on the hydrologic regime are characterized by changes in the water balance, including increased infiltration, increased soil water storage, decreased surface runoff, and increased evapotranspiration (ET) (Sloan et al., 2016; Vidon and Cuadra, 2011; Yang et al., 2017).

When considering changes in the water balance, in the Upper Red River of the North Basin (URRNB; located in part of Minnesota, North Dakota, and South Dakota, USA; as well as Manitoba, and Saskatchewan, Canada), Rahman & Lin, (2013) observed the impacts of tile drainage. With the implementation of these systems at the field scale, the authors found that the average surface runoff decreased by approximately 30%, whereas the water yield increased by approximately 10%. Additionally, following the installation of tile drainage systems, the average soil water content (SWC) decreased by approximately 10%; thus, causing an increase in soil water storage. Similarly, in another study in the URRNB, Rahman et al., (2011), found that with the implementation of tile drainage systems in the watershed, groundwater flow, deep aquifer recharge, and percolation decreased, whereas tile flow and water yield increased.

In a study conducted in Canagagigue Creek watershed in Ontario, Canada, Golmohammadi et al., (2017), used SWATDRAIN (i.e., a watershed model developed through the incorporation of DRAINMOD into SWAT) to model tile drainage scenarios, including a no tile drainage scenario and an existing conventional tile drainage scenario. The Canagagigue Creek watershed has an existing (or current) condition of approximately 65% tile-drained agricultural land. When comparing the average annual water balance of the no drainage scenario with the existing drainage scenario, evapotranspiration decreased by approximately 8.3% (40 mm), percolation decreased by approximately 8.2% (3.7 mm), and streamflow decreased by

approximately 3.6% (16.6 mm). Similarly, when comparing the individual streamflow components (i.e., surface runoff, groundwater flow, lateral flow, and tile flow) between the no drainage and existing drainage scenarios, surface runoff decreased by approximately 34% (124.3 mm) and groundwater flow decreased by approximately 31% (16.8 mm), whereas lateral flow increased by approximately 4.8% (2.3 mm) and tile flow increased by 113.1 mm (Figure 2-4).

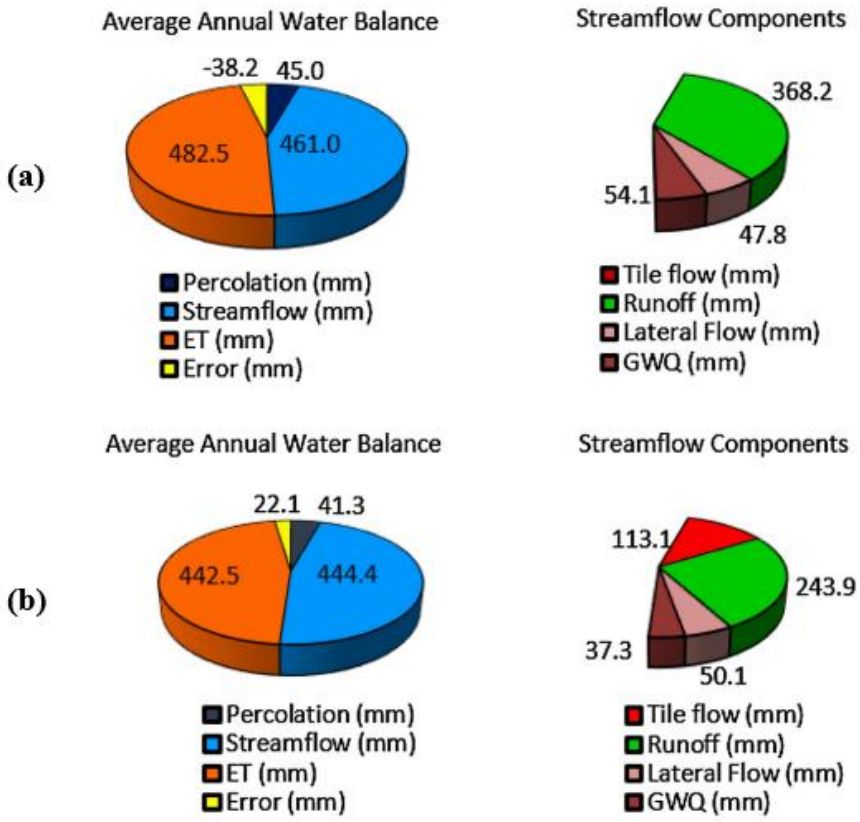

Figure 2-4: Impact of subsurface tile drainage systems on average annual water balance and individual stream components where (a) no drainage and (b) existing drainage (Adapted from Golmohammadi et al., 2017).

These observed impacts of subsurface drainage on individual water balance components (Rahman et al., 2011; Rahman & Lin, 2013; Golmohammadi et al., 2017) may lead to homogeneity in responses across different soil types (Sloan et al., 2016). For example, under relatively small storm events with dry antecedent moisture conditions, increased infiltration and

decreased surface runoff will likely prevail on drained soils compared to undrained soils (Sloan et al., 2016). In contrast, subsurface drainage may not considerably impact infiltration under large and intense rainfall events (Balnn et al., 2009; Sloan, 2013). The conversion of land and installation of drainage systems for intensive agricultural use has been shown to decrease in-field runoff but increase peak flow rates in streams (Blann et al., 2009; Skaggs et al., 1994; Wiskow and van der Ploeg, 2003). The reduction of in-field runoff has been attributed to the increased capacity of drained soils to temporarily store moisture, allowing more water to infiltrate into the soil profile (Fraser et al., 2001; Zucker and Brown, 1998), which in turn reduces local flooding (i.e., in the field) but may contribute to increased annual downstream flows (King et al., 2014).

Between 2005 and 2010, King et al., (2014), found that subsurface drainage accounted for approximately 47% of the total monthly discharge in the Upper Big Walnut Creek watershed near Columbus, Ohio. In Strawberry Creek watershed in Ontario, Canada, Macrae et al., (2007), found the contribution of subsurface drainage to be between 0 and 90% of seasonal discharge and 40% of annual discharge of the watershed. In Matson Ditch watershed, in Dekalb County, Indiana, Boles, (2013), found subsurface drainage to account for approximately 20 to 48% of the annual water yield. Similarly, in the Boone River watershed and Lyons Creek watershed of north-central Iowa, Schilling et al., (2019), found subsurface drainage to account for 46 to 66% of the annual water yield. Another study in Iowa, conducted by Thomas, (2015), in Beaver Creek watershed, found subsurface drainage to account for 6 to 71% of the average annual water yield. Due to the substantial impact of subsurface drainage systems on the hydrologic regime, approximately 20 to 87% of peak flow reductions in the Midwest have been linked to drainage systems. However, these reductions are often dependent on both soil type and antecedent moisture conditions (Fraser et al., 2001; Skaggs & Broadhead, 1982; Vidon & Cuadra, 2010).

Regarding soil type, at a field-scale study in the United Kingdom, Robinson and Rycroft (1999), observed reductions in peak flow rates in clayey soils and increased peak flow rates in sandy soils. Using advanced ET mapping techniques based on remote sensing, Yang et al., (2017), determined that subsurface drainage systems appear to decrease ET during the early growing season, but substantially increase crop water use during the mature crop growth stage. The authors linked the differences in ET water losses to the existence of higher soil moisture content (from winter snowmelt and early spring rainfall events) in the early growth stage, versus the elevated crop water demand during the peak growing season.

2.3.1 Impacts of Subsurface Drainage on Flooding

Research has shown that subsurface tile drainage systems substantially impact the natural hydrologic water balance. The specific impact of drainage systems on streamflow, however, has been a source of debate for nearly a century. The issue is complex due to its high variability; the effect of drainage systems on streamflow is dependent on several site-specific factors (Rahman & Lin, 2013).

Drainage systems have been found to both increase and decrease peak streamflow depending on topography, climate, and management characteristics (Sloan et al., 2015). Additionally, the influence of subsurface drainage systems on peak flows is dependent on scale, as the amount of contributing tile flow is relative to specific properties of the drainage area (Thomas, 2015). For example, at the field scale, soil type is the primary factor influencing streamflow. In contrast, at the watershed scale, a combination of factors including soil type, precipitation, drainage networks, channel routing, and drainage network distribution influence streamflow. Similarly, the magnitude of the impact of tile drainage systems differs between the

field scale and watershed scale. At the watershed scale, the impact is lessened, as the percentage of tile-drained land is typically much smaller than at the field scale (Rahman & Lin, 2013).

While the effect of subsurface drainage systems on streamflow is highly variable, research has indicated that drainage systems decrease peak flows in waterlogged, clay soils, and increase peak flows in dry, permeable soils (Rahman & Lin, 2013; Rahman et al., 2014). In clay soils, peak flows decrease due to increased infiltration, while in permeable soils, peak flows increase due to a greater hydraulic gradient accelerating the subsurface flow rate. The high permeability of sandy and silty soils allows precipitation to rapidly infiltrate into the soil profile, whereas the low permeability of clayey and loamy soils allows surface runoff to be the primary mechanism in fields. Such results, however, have been primarily concluded from field studies and modeling reviews in North America and Europe (Rahman & Lin, 2013; Rahman et al., 2014; Sloan, 2013).

To better understand the impact of subsurface tile drainage systems on the hydrologic regime, Sloan (2013) used DRAINMOD to simulate tile scenarios in Iowa from 1981-2010. Seven drainage scenarios were simulated, including Original (i.e., all hillslopes with row crop agriculture were drained), All Drained, and All Undrained. The summer of 1993 was selected for detailed analysis, as it was a wet year in the state of Iowa with several flooding events. During the summer, two distinct patterns emerged among the scenario hydrographs. For example, the August 10, 1993, hydrograph depicted a minimal difference between the three drainage scenarios, whereas the August 17, 1993, hydrograph depicted the drainage scenarios with similar shapes, but varying magnitudes (Figure 2-5). When considering the later hydrograph (i.e., August 17, 1993), results indicated that the addition of tile drainage reduces peak flows at the watershed outlet.

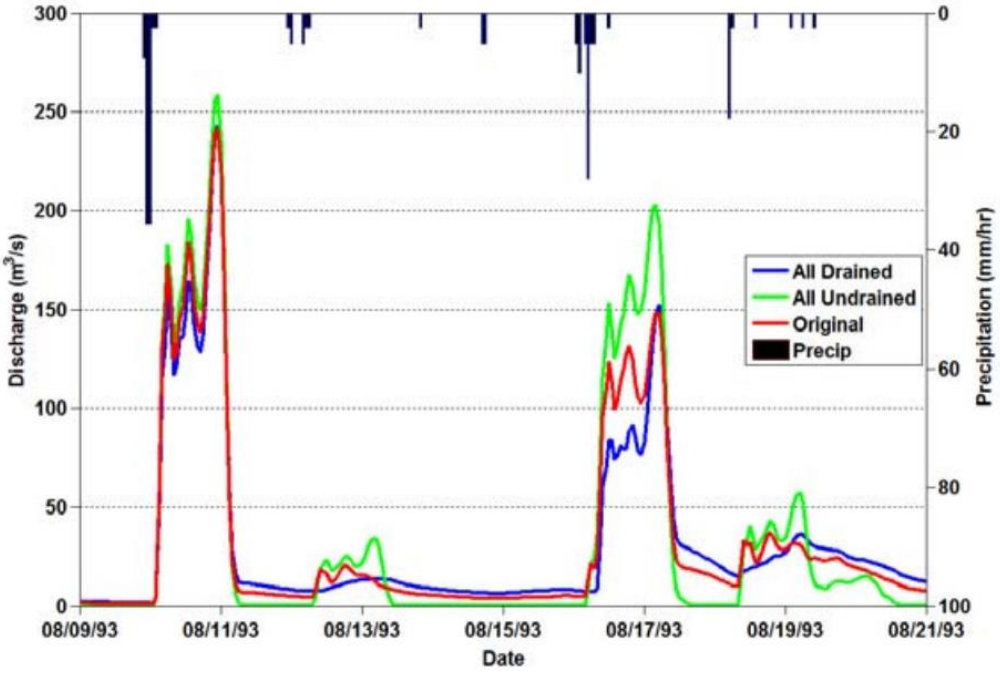

Figure 2-5: August 1993 hydrographs for Original, All Drained, and All Undrained Scenarios showing two distinct behaviors (Sloan, 2013).

More specifically, the soil component hydrographs of the August 17, 1993, event depict a difference in the magnitude of daily discharge with respect to the tile drainage scenarios. For example, in the Original and All Drained Scenario, the additional storage caused by drainage caused increased infiltration, allowing a more gradual hydrograph (Figure 2-6a; Figure 2-6b). In contrast, in the All-Undrained scenario, surface runoff prevailed, causing a more abrupt hydrograph (Figure 2-6c).

(a)

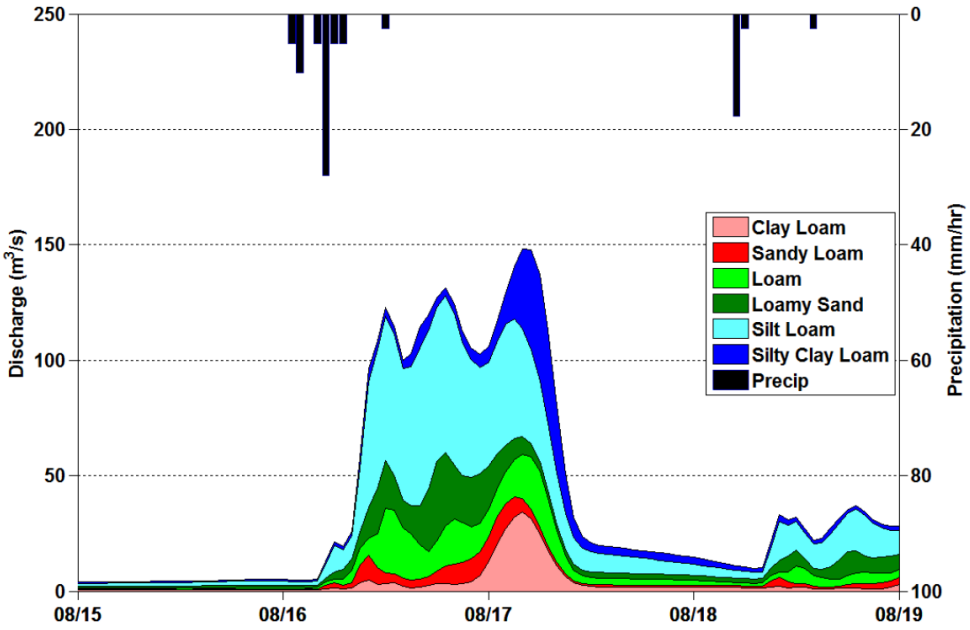
250
200
150
100
50
0
Discharge (m3/s)
0
20
40
60
80
100
Precipitation (mm/hr)
08/15
08/16
08/17
08/18
08/19
Clay Loam
Sandy Loam
Loam
Loamy Sand
Silt Loam
Silty Clay Loam
Precip

(b)

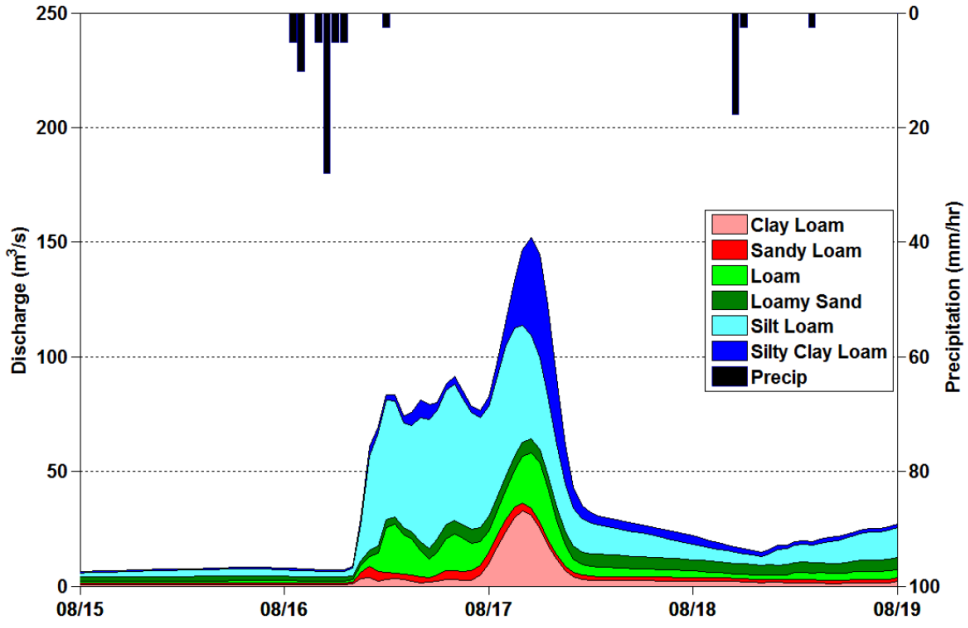
250
200
150
100
50
0
Discharge (m3/s)
0
20
40
60
80
100
Precipitation (mm/hr)
08/15
08/16
08/17
08/18
08/19
Clay Loam
Sandy Loam
Loam
Loamy Sand
Silt Loam
Silty Clay Loam
Precip

(c)

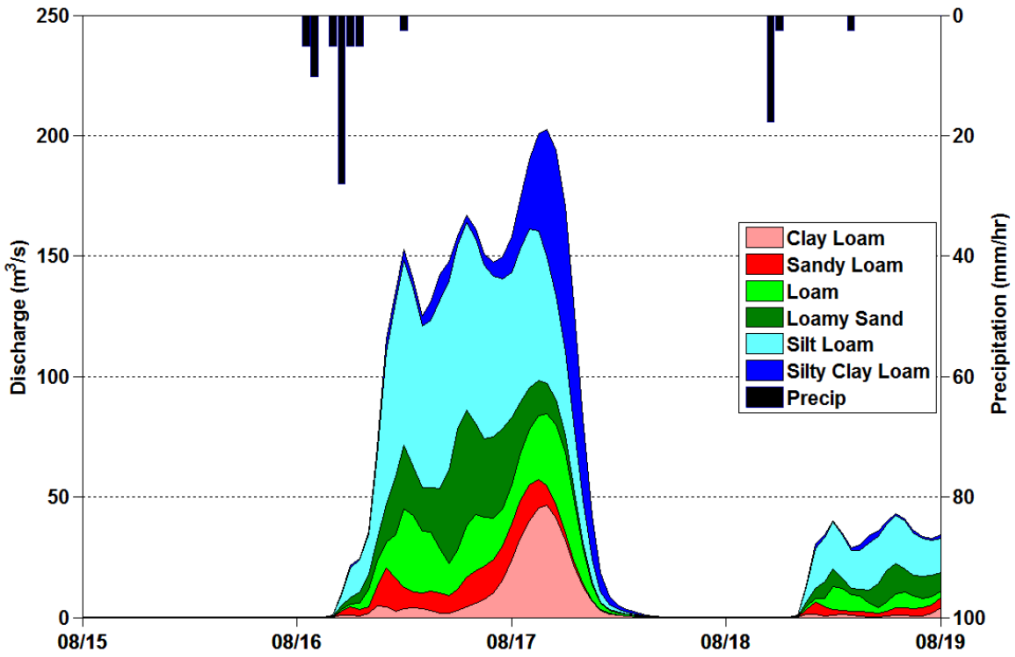

Figure 2-6: August 1993 soil component hydrographs where (a) Original scenario, (b) All Drained scenario, and (c) All Undrained scenario (Adapted from Sloan, 2013).

In addition to hydrographs, Sloan (2013) analyzed annual hourly peak flows and the Richard-Baker Flashiness Index for the Clear Creek watershed during the study period. From analysis, the author found that in approximately two-thirds of the years, the All-Undrained scenario had larger peak flows than the Original and All Drained scenarios (Figure 2-7) due to the reduction in peak flows through the rerouting of surface runoff to drainage systems. In contrast, approximately one-third of the years had a constant annual hourly peak flow with respect to the drainage scenarios (Figure 2-7).

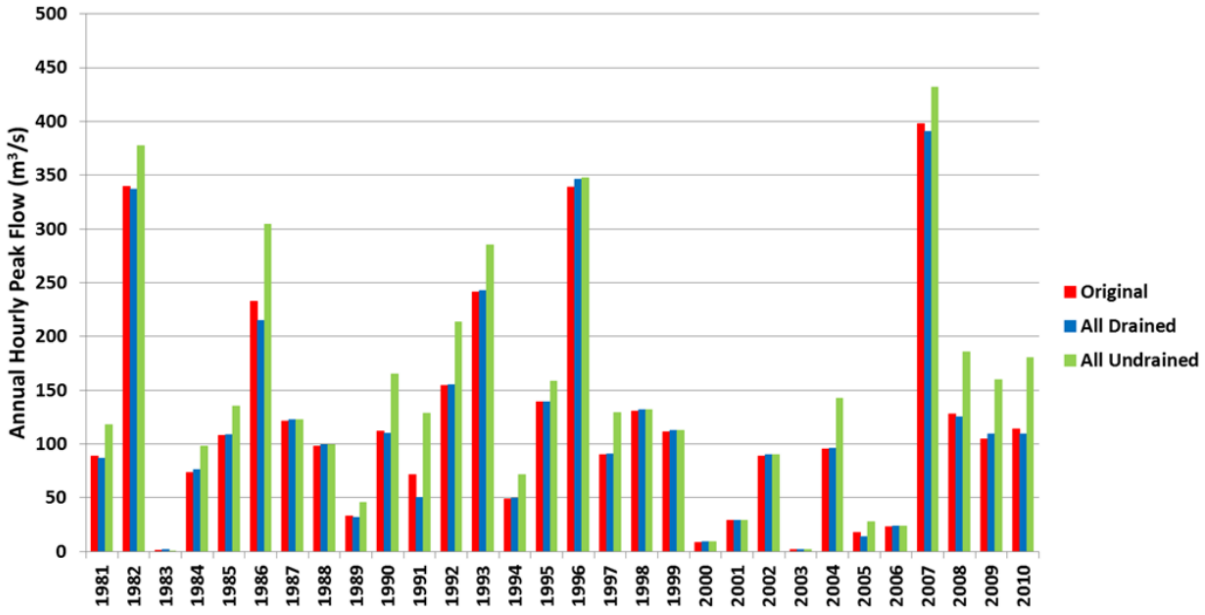

Figure 2-7: Annual hourly peak flows during the 1981-2010 study period in the Clear Creek watershed (Adapted from Sloan, 2013).

Similarly, when considering the Flashiness Index (i.e., how quickly the systems respond to a precipitation event), the author found the All Drained scenario to be the least flashy, whereas the All Undrained scenario was the most flashy. While the scenarios had several similar reactions to precipitation events (i.e., 1999-2004), generally, the All Undrained scenario produced more surface runoff, hence, a flashier hydrograph (Figure 2-8).

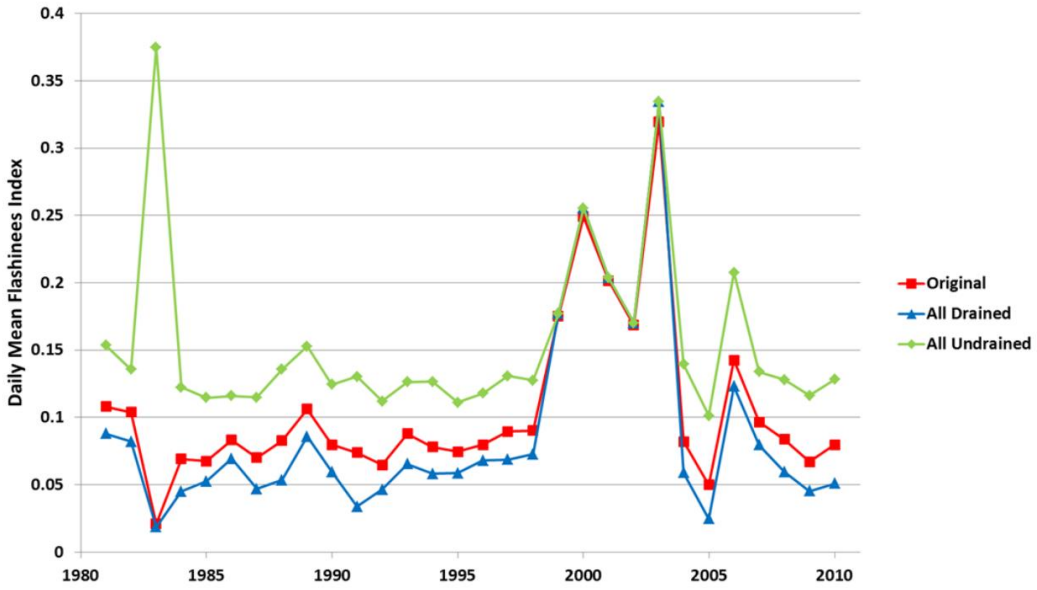

Figure 2-8: Richard-Baker Flashiness Index for the Clear Creek watershed during the 1981-2010 study period (Adapted from Sloan, 2013).

From analysis, Sloan (2013) determined the effect of subsurface drainage systems on streamflow to be a function of the size of the precipitation event. During small events, drainage systems were found to increase or decrease peak flow as a function of antecedent moisture conditions. During medium-sized events, peak flows generally decreased, and during large events, peak flows were not substantially impacted. Therefore, the author suggests that in the state of Iowa, during flood-causing storm events, subsurface drainage systems have little to no impact on flooding. However, it was noted that such results are valid in landscapes with defined surface runoff to the watershed outlet.

In the Upper Red River of the North Basin (URRNB), Rahman & Lin (2013) and Rahman et al., (2014) performed a field scale and basin scale study to determine the relationship between subsurface drainage and late-spring snowmelt flood events. At the field scale, tile flow composed approximately 37% of the water yield. At the basin scale, three drainage scenarios were developed, including the Baseline (0.7% URRNB tile-drained), D Soil (5.6% URRNB tile-

drained, and C+D Soil (16.8% URRNB tile-drained) scenarios. Results of the annual peak flow frequency analysis demonstrated that the Baseline and D Soil scenarios caused no difference in flood frequency, whereas the C+D Soil scenario will likely increase the magnitude of smaller peak flows while decreasing the magnitude of larger peak flows (Figure 2-9).

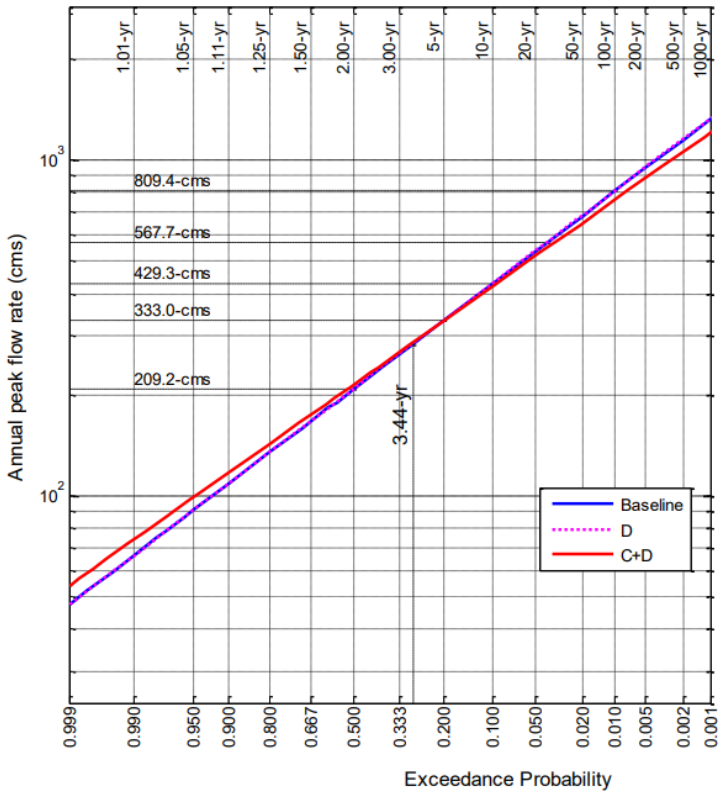

Figure 2-9: Annual peak flow frequency analysis for Upper Red River of the North Basin (Adapted from Rahman & Lin, 2013).

Additionally, the authors performed a seasonal streamflow analysis for the entire study period (i.e., 1993-2010) as well as the seven wettest years (i.e., 1997, 1998, 2001, 2005, 2006, 2009, and 2010). Results of the entire study period analysis indicated that the C+D Soil scenario results in an increased average monthly flow from March to July (excluding the month of May) (Figure 2-10). In contrast, results of the seven wettest year analysis indicated that the C+D Soil

scenario results in a decreased average monthly flow from April to June (and increased flows in March) (Figure 2-10).

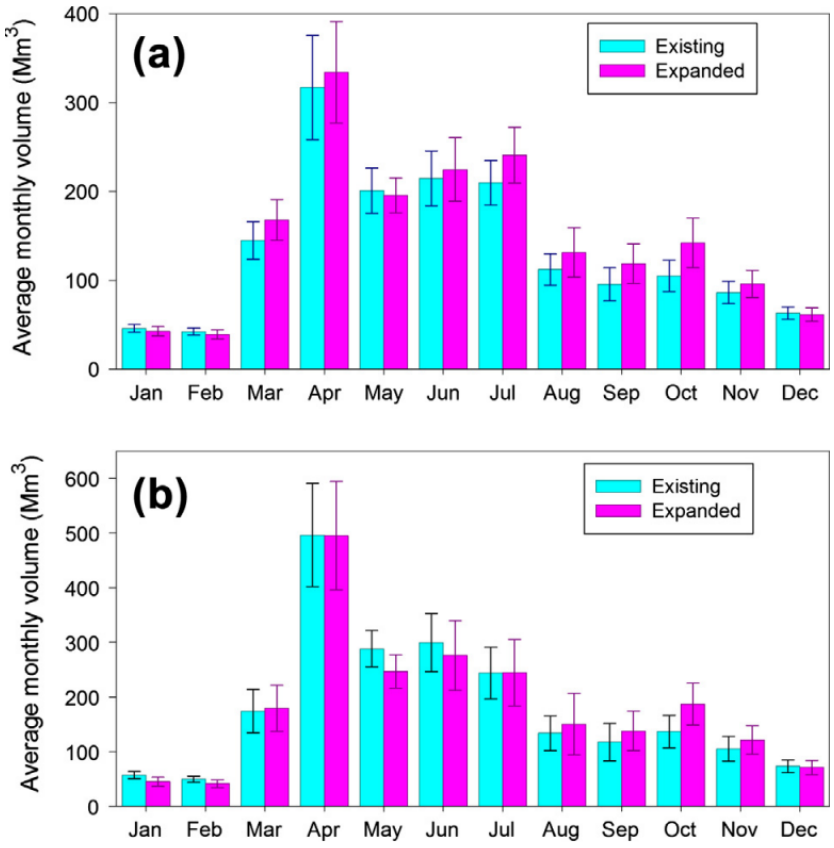

Figure 2-10: Average monthly flow volume in the Upper Red River of the North Basin, where (a) entire study period (1993-2010), and (b) seven wettest years (1997, 1998, 2001, 2005, 2006, 2009, 2010) (Adapted from Rahman & Lin, 2013).

Research has indicated that there is no definitive rule for the influence of subsurface tile drainage on downstream peak flows and subsequent flooding events. To better understand these impacts in the Midwest, additional studies are required to evaluate watersheds with various climates, topographies, soil types, and management characteristics.

Chapter 3 - Materials and Methods

3.1 Study Area

Serving as a tributary to the Big Sioux River, the Skunk Creek watershed is located in southeastern South Dakota, United States (Figure 3-1). The watershed (lying within 96.74º and 97.35°W latitude and 43.45° and 44.13° N longitude) drains approximately 1,606 km^2 of predominantly agricultural land. The watershed produces primarily corn and soybean crops, accounting for roughly 35% and 29% of the respective watershed area (Ahiablame et al., 2019; Hong, 2017). The Skunk Creek watershed encompasses portions of six counties, including Lake, Lincoln, Moody, McCook, Minnehaha, and Turner Counties.

The dominant soil types in the Skunk Creek watershed include gently sloping Egan and Moody silty clay loams. These soil types belong to hydrologic soil group B, which is composed of approximately 10% to 20% clay and 50% to 90% sand. Such soils, when saturated, have a relatively low runoff potential and allow unrestricted water transmission through the soil profile (Soil Survey Staff, 2022; USDA-NRCS, 2007).

During the 2007-2021 study period, the Skunk Creek watershed received an average annual precipitation of 729.14 mm (PRISM Climate Group; Rupp et al., 2022). Relatively, the average annual streamflow at the outlet of the watershed (Figure 3-1) was 5.80 m^3/s. During the study period, the maximum streamflow occurred on March 14, 2019, when the streamflow was approximately 195 m^3/s. The minimum streamflow occurred from February 23 through February 27, 2014, and from March 2 through March 3, 2014, when the streamflow was approximately 0.04 m^3/s (U.S. Geological Survey, 2022). The average daily temperature in the Skunk Creek watershed ranged from -34.4℃ during the winter to 40.7℃ during the summer throughout the 2007-2021 study period (PRISM Climate Group; Rupp et al., 2022).

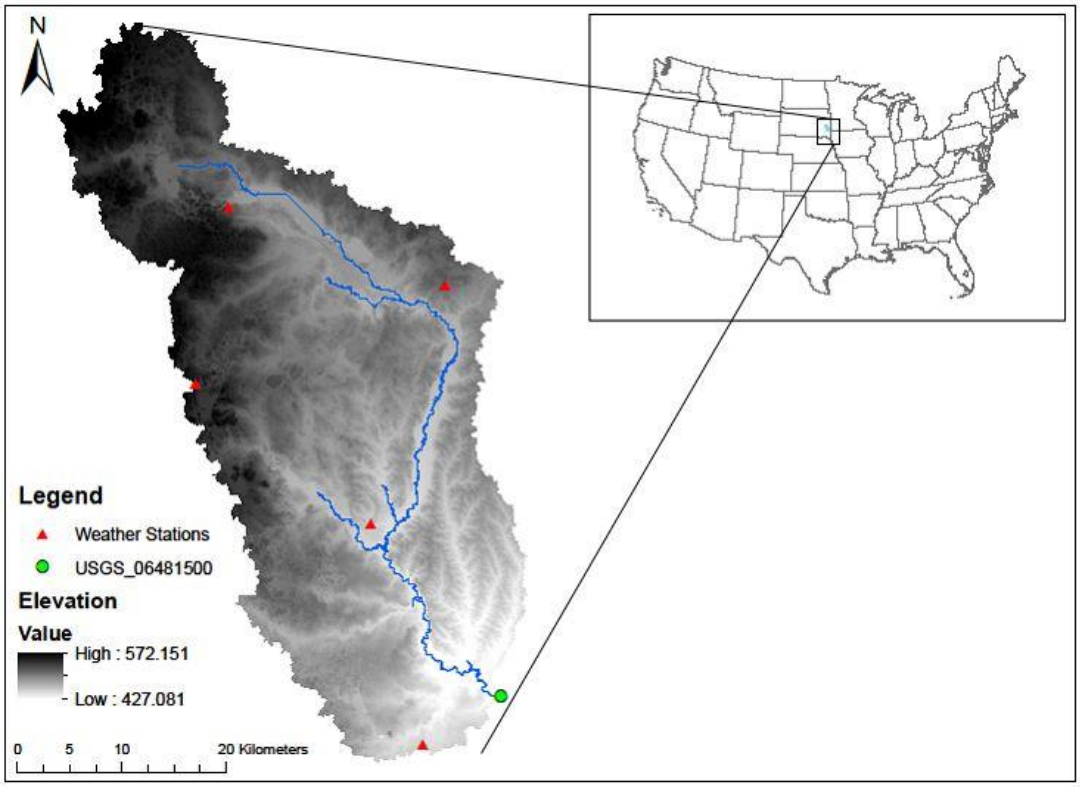

Figure 3-1: Location of Skunk Creek watershed in southeastern South Dakota, United States; USGS Stream Gauge Station at watershed outlet; and defined Weather Stations.

3.2 SWAT Model

The Soil and Water Assessment Tool (SWAT) is a comprehensive, physically based, semi-distributed, continuous-time, watershed-scale, ecohydrological model (Abbaspour et al., 2015; Guo et al., 2018; Hutchinson & Christiansen, 2013; Moriasi et al., 2013; Rahman et al., 2011; Rahman et al., 2013; Rahman et al., 2014; Teshanger et al., 2016). The SWAT model was developed by the United States Department of Agriculture (USDA) Agricultural Research Service (ARS) to predict and assess the impact of climate change and agricultural land use management practices on water quality and quantity and sediment and nutrient yields in large watersheds with a variety of soil types, land uses, and management strategies (Guo et al., 2018; Hutchinson & Christiansen, 2013; Moriasi et al., 2013; Rahman, et al., 2011; Rahman, et al., 2013; Rahman et al., 2014; Teshanger et al., 2016). The Arc-GIS extension, ArcSWAT, allows

the SWAT model to be executed within a geographic information system (GIS) while providing tools to develop and run the model (Hutchinson & Christiansen, 2013). In this study, ArcGIS version 10.7.1 was used with SWAT 2012 version 681.

In the SWAT model, a watershed is first delineated into multiple subbasins—connected by stream networks—based on digital elevation model (DEM) data (Abbaspour et al., 2015; Hutchinson & Christiansen, 2013; Rahman et al., 2011; Rahman et al., 2013; Teshanger et al., 2016). A single reach (stream) is created in each subbasin based on the principles of flow accumulation and flow direction (Hutchinson & Christiansen, 2013; Rahman et al., 2011). The outlet of the delineated watershed is manually defined, allowing the comparison of observed and simulated streamflow data (Rahman, 2011).

Upon watershed delineation, the SWAT model further discretizes every subbasin into hydrologic response units, or HRUs. HRUs consist of unique combinations of land use, soil, and surface slope and are the smallest modeling units used in the SWAT model. HRU discretization allows the model to account for watershed spatial variability while reducing overall running time (Abbaspour et al., 2015; Hutchinson & Christiansen; Rahman et al., 2011; Rahman et al., 2013; Teshanger et al., 2016).

The SWAT model has multiple variables to simulate hydrologic processes, including runoff, percolation, lateral subsurface flow, groundwater flow, evapotranspiration, snow melt, transmission losses, ponds, and weather (precipitation, air temperature, solar radiation, wind speed, and humidity). In the SWAT model, the hydrologic cycle is simulated based on the daily water balance equation:

$$SW_t = SW_0 + \sum_{i=1}^{t}(P - Q_{surf} - ET - w_{seep} - Q_{gw})$$

where SW_t is the soil water content (mm) on day t, SW_0 is the initial soil water content (mm) on day $i=1$, t is the time in days, P is the precipitation (mm) on day i, Q_{surf} is the surface runoff (mm) on day i, ET is the evapotranspiration (mm) on day i, w_{seep} is the deep aquifer recharge (mm) on day i, and Q_{gw} is return subsurface flow (mm) on day i (Hong, 2017; Saha et al., 2019).

The SWAT model divides watershed hydrology into two phases: (i) hydrology at the HRU level and (ii) channel routing. First, the SWAT model estimates the hydrologic components (flow, sediment, nutrient, and pesticide loadings) in each HRU, as well as the hydrologic components generated by each HRU. The hydrologic components generated by all HRUs in an individual subbasin are summed, representing the total load for that subbasin. From this, the model determines the amount of available water for streamflow (water yield). Next, the water yield is routed through channel networks, ponds, and reservoirs to the watershed outlet (Jha et al., 2004; Rahman, 2011). The SWAT model outputs values for all water balance components—precipitation, surface runoff flow, lateral flow, groundwater flow, percolation, tile drainage flow, and evapotranspiration—and presents them on the daily, monthly, and annual time steps (Rahman, 2011; Tyagi & Rao, n.d.).

One of the critical parameters evaluated in this study is water yield. Water yield is equivalent to the sum of water leaving an HRU and entering the primary channel. The SWAT model calculates water yield as:

$$W_{yld} = Q_{surf} + Q_{gw} + Q_{lat} - T_{loss}$$

where W_{yld} is the measure of the water yield (mm), Q_{surf} is the surface runoff (mm), Q_{gw} is the groundwater flow (mm), Q_{lat} is the lateral flow contribution to the stream (mm), and T_{loss} is the transmission losses (mm) from the tributary in the HRU by means of transmission through the bed (Ayivi & Jha, 2018).

In this study, the Soil Conservation Service (SCS) Curve Number (CN) method was used to estimate surface runoff. The SCS CN method relies on land use, soil properties, and antecedent soil moisture conditions to estimate surface runoff. It is calculated using the equation:

$$Q_{surf} = \frac{(R_{day} - I_a)^2}{(R_{day} - I_a + S)}$$

where Q_{surf} is the accumulated runoff or rainfall excess (mm H_2O), R_{day} is the rainfall depth for the day (mm H_2O), I_a is the initial abstractions, including surface storage, interception, and infiltration prior to runoff (mm H_2O), and S is the retention parameter (mm H_2O). Initial abstractions (I_a) are commonly approximated as $0.2S$, and runoff will occur when $R_{day} > I_a$. The retention parameter, S, was calculated using the following equation:

$$S = \frac{25400}{CN} - 254$$

where CN is the curve number for the day. The retention parameter, S, is spatially variable and is primarily based on land use type and soil water content (Mehan et al., 2016; Mehan et al., 2017).

When considering groundwater flow, the SWAT model divides underground storage into the shallow aquifer or the deep aquifer in each sub-basin. The shallow aquifer is unconfined and contributes to flow in the main channel. The deep aquifer is confined and is assumed to contribute to flow outside of the watershed. The water balance for the shallow aquifer is calculated as:

$$aq_{sh,i} = aq_{sh,i-1} + w_{rchrg,sh} - Q_{gw} - w_{revap} - w_{pump,sh}$$

where $aq_{sh,i}$ is the amount of water stored in the shallow aquifer on day i (mm H_2O), $aq_{sh,i-1}$ is the amount of water stored in the aquifer on day $i-1$ (mm H_2O), $w_{rchrg,sh}$ is the amount of recharge entering the shallow aquifer on day i (mm H_2O), Q_{gw} is the groundwater flow, or baseflow in the

main channel on day *i* (mm H_2O), w_{revap} is the amount of water moving into the soil zone in response to water deficiencies on day *i* (mm H_2O), and $w_{pump,sh}$ is the amount of water removed from the shallow aquifer by pumping on day *i* (mm H_2O).

The recharge to both aquifers on a given day is calculated as:

$$w_{rchrg,i} = \left(1 - e^{\left[\frac{-1}{\delta_{gw}}\right]}\right) * w_{seep} + e^{\left[\frac{-1}{\delta_{gw}}\right]} * w_{rchrg,i-1}$$

where $w_{rchrg,i}$ is the amount of recharge entering the aquifers on day *i* (mm H_2O), δ_{gw} is the delay time or drainage time of the overlying geologic formations (days), w_{seep} is the total amount of water exiting the bottom of the soil profile on day *i* (mm H_2O), and $w_{rchrg,i-1}$ is the amount of recharge entering the aquifers on day *i-1* (mm H_2O).

The groundwater flow (Q_{gw}) for each HRU is calculated using simplified equations of groundwater flow and water table fluctuations. The change in groundwater flow (i.e., baseflow) is calculated by the following equation:

$$\frac{dQ_{gw}}{dt} = \left(\frac{800 * K}{L_{gw}^2}\right) * \left(\frac{w_{rchrg,sh} - Q_{gw}}{800 * S_y}\right)$$

where *K* is the hydraulic conductivity of the aquifer material (mm/day), L_{gw} is the distance (m) between the groundwater divide and the main channel within the subbasin, and S_y is the specific yield of the shallow aquifer (m/m) (i.e., the ratio of the volume of water that drains by gravity to the total bulk volume of the porous medium).

The baseflow recession constant, α_{gw}, relating a recharge event to baseflow, is calculated by the following equation:

$$\frac{dQ_{gw}}{dt} = \left(10\frac{K}{L_{gw}^2 * S_y}\right) * \left(w_{rchrg,sh} - Q_{gw}\right) = \alpha_{gw}(w_{rchrg,sh} - Q_{gw})$$

and is then integrated to solve for $Q_{gw,}$ where:

$$Q_{gw,i} = \left[Q_{gw,i-1} * e^{(-\alpha_{gw})}\right] + \left[w_{rchrg,sh} * \left(1 - e^{(-\alpha_{gw})}\right)\right].$$

This equation is used if groundwater storage exceeds a user-defined value (Bailey et al., 2020; Lou et al., 2012; Neitsch et al., 2005).

The SWAT model approximation of lateral flow assumes that the flow in the saturated zone is parallel to the impermeable boundary, and that the hydraulic gradient is equal to the slope of the bed. The drainable volume of water stored in the saturated zone of the hillslope segment is calculated using the following equation:

$$SW_{ly,excess} = \frac{1000 * H_o * \phi_d * L_{hill}}{2}$$

where $SW_{ly,excess}$ is the drainable volume of water stored in the saturated zone of the hillslope per unit area (mm H_2O), H_o is the saturated thickness normal to the hillslope at the outlet expressed as a fraction of the total thickness (mm/mm), ϕ_d is the drainable porosity of the soil (mm/mm), L_{hill} is the hillslope length (m), and *1000* is a factor used to convert m to mm.

The velocity of flow at the hillslope outlet is calculated using the following equation:

$$v_{lat} = K_{sat} * \tan(\alpha_{hill}) = K_{sat} * slp$$

where v_{lat} is the velocity of flow at the outlet (mm/hour), K_{sat} is the saturated hydraulic conductivity (mm/hour), α_{hill} is the slope of the hillslope segment, and *slp* is the model input for slope.

Combining the previous two equations, lateral flow is calculated by the following equation:

$$Q_{lat} = 0.024 * \left(\frac{2 * SW_{ly,excess} * K_{sat} * slp}{\phi_d * L_{hill}}\right)$$

where Q_{lat} is the water discharged from the hillslope outlet (mm H_2O/day) (Neitsch et al., 2005).

Finally, transmission losses are calculated using the following equation:

$$t_{loss} = K_{ch} * TT * P_{ch} * L_{ch}$$

where t_{loss} are the channel transmission losses (m^3 H_2O), K_{ch} is the effective hydraulic conductivity of the channel alluvium (mm/hr), TT is the flow travel time (hr), P_{ch} is the wetted perimeter (m), and L_{ch} is the channel length (km) (Neitsch et al., 2005).

Additionally, in this study, the Variable Storage method was used for simulating channel routing and the Penman-Monteith (PM) equation was used for estimating potential evapotranspiration (ET) in the watershed.

3.2.1 Tile Drainage in SWAT

The SWAT model has been used to model tile drainage systems at both the basin and watershed scales (Rahman, et al. 2011). Tile drainage algorithms were introduced in early versions of the SWAT model (version 98.1), and Arnold et al., (1999) further improved early simulations in SWAT 2000 with the following algorithm:

$$tile_{wtr} = \left(SW_{ly} - FC_{ly}\right) \times \left(1 - e^{\left[\frac{-24}{t_{drain}}\right]}\right) \text{ if } SW_{ly} > FC_{ly},$$

where $tile_{wtr}$ is the amount of water removed from the soil layer (mm H_2O) on a given day by tile drainage, SW_{ly} is the water content of the soil layer (mm H_2O) on a given day, FC_{ly} is the field capacity water content of the soil layer (mm H_2O), and t_{drain} is the time (hours) required to drain the soil to field capacity.

The algorithm was successfully tested at the field scale with the improved SWAT 2002 model. However, in SWAT 2002, pothole impacts were not included, and subsurface tile drainage routines were old. Therefore, researchers determined that SWAT 2002 was

inappropriate for modeling subsurface tile drainage systems at the watershed scale (Guo et al., 2018).

Research further improved subsurface tile drainage algorithms, which were incorporated into SWAT 2005 (Boles, 2013; Schilling et al., 2019). In SWAT 2005, a restrictive soil layer (or impermeable depth) is set at the bottom of the soil profile and water table dynamics are more accurately simulated (Guo et al., 2018; Rahman & Lin, 2013). The impermeable depth allows the soil above the restrictive layer to fill to field capacity and the excess water to fill the soil profile upward from the saturated bottom layer (Rahman & Lin, 2013). To simulate subsurface tile drainage in SWAT 2005, the values are user-defined for tile drainage depth (DDRAIN), time to drain soils to field capacity (TDRAIN), and tile drainage lag time (GDRAIN) (Boles, 2013; Guo et al., 2018; Hutchinson & Christiansen, 2013). In the algorithm, in order for subsurface tile flow to begin, the value of DDRAIN must be greater than zero, and the impervious depth (DEP_IMP) must be approximately the same value as DDRAIN (Boles, 2013; Hutchinson & Christiansen, 2013). The parameter GDRAIN is then used as the quantity of daily tile flow contribution to stream systems and TDRAIN is used to determine flow rate (Boles, 2013; Guo et al., 2018). The tile drainage algorithm used in SWAT 2005 is:

$$tile_{wtr} = \left(\frac{h_{wtbl} - h_{drain}}{h_{wtbl}}\right) \times (SW - FC) \times \left(1 - e^{\left[\frac{-24}{t_{drain}}\right]}\right) \text{ if } h_{wtbl} > h_{drain},$$

where $tile_{wtr}$ is the amount of water removed from the layer (mm H_2O) on a given day by tile drainage, h_{wtbl} is the height of the water table (mm) above the impervious zone, *SW* is the water content (mm H_2O) of the profile on a given day, *FC* is the field capacity water content (mm H_2O) of the profile, and t_{drain} is the time required (hours) to drain the soil to field capacity. It is

important to note that t_{drain} is a user-defined value, based on management, land cover, soil type, and other watershed properties (Guo et al., 2018; Neitsch et al., 2005).

The SWAT 2005 tile drainage routine is based on drawdown time, or the time to drain soils to field capacity. However, TDRAIN is a static parameter; thus, no matter the size of the storm event, the drawdown time is the same (Frankenberger et al., 2013; Guo et al., 2018). Additionally, the SWAT 2005 algorithm does not account for tile drain size or spacing (Rahman, 2011), which reduces the models' accuracy.

To more accurately model and reflect real-world tile drainage systems, Moriasi et al., (2007) developed a new tile drainage simulation method using the more robust, physically based Hooghoudt (1940) and Kirkham (1957) drainage equations (Boles, 2013; Frankenberger et al., 2013; Guo et al., 2018; Rahman, 2011; Rahman et al., 2011; Schilling et al., 2019). These drainage equations, as well as a drainage coefficient, were incorporated into SWAT 2012, beginning with version 531 (Boles, 2013; Frankenberger et al., 2013; Schilling et al., 2019). The principal assumption for the Hooghoudt and Kirkham tile drainage algorithms is that when the upper soil layer is saturated, tile flow will occur laterally (Rahman, 2011). There are three conditions in which the Hooghoudt and Kirkham drainage equations simulate subsurface tile drainage flux (flow). They are as follows:

Condition I: If the groundwater table is below the soil surface and the depth of ponded water in surface depressions is less than maximum depressional storage (S_1), the Hooghoudt steady-state equation simulates drainage flux:

$$q = \frac{8K_e d_e m + 4K_e m^2}{CL^2}$$

where q is drainage flux (mm/hr), K_e is effective lateral hydraulic conductivity (mm/hr), d_e is the equivalent depth substituted for d (height of the drain from the impervious layer) to correct the

convergence near the drains (mm), *m* is the midpoint water table height above the drain (mm), *C* is the ratio of the average flux between the drains to the flux midway between the drains and is assumed to be unity (*C* = 1) in this model, and *L* is the distance between the drains (mm).

Condition II: If the ponded depth in surface depressions is greater than S_1, and the water table rises over the soil surface and lingers, the Kirkham equation is used to calculate drainage flux:

$$q = \frac{4\pi K_e(t + b - r)}{gL}$$

where *t* is the depth of ponded water (mm), *b* is the depth from the soil surface to the center line of the drain (mm), and *g* is a dimensionless factor expressed as a function of d, *L*, the actual depth of the soil profile (h), and the radius of the tile tube (r).

Condition III: If the estimated drainage flux by the previous two equations is greater than the drainage coefficient (*DC*, mm/day), the flux (mm/day) will be equal to the *DC*:

$$q = DC$$

Additionally, the maximum depressional storage (S_1) is calculated by the equation of Onstad (1984):

$$S_1 = 0.112RR + 0.031RR^2 - 0.012RR * S$$

where *RR* is the random roughness (cm) and *S* is the slope (%) of the land (Boles, 2013; Guo et al., 2018; Rahman, 2011; Rahman et al., 2011).

In addition to the previously discussed equations and variables, there are several additional tile drainage parameters used by the SWAT model. Parameters in the SWAT model Subbasin Drainage (.sdr) File, as well as their respective definition and default values are shown below, in Table 3-1.

Table 3-1: Tile drainage parameters in the Subbasin Drainage File in the SWAT model (Adapted from Frankenberger et al., 2013)

Drainage Parameter	Definition	Default SWAT Value
RE	Effective radius of drains (mm)	15.0
SDRAIN	Distance between two drain tiles (mm)	15000.0
DRAIN_CO	Drainage coefficient (mm)	10.0
PC	Pump capacity (mm/hr)	0.00
LATKSATF	Multi factor for lateral conductivity	1.00
SSTMAXD	Static maximum depressional storage (mm)	12.50

In addition to the .sdr file, the Management (.mgt) SWAT Input File contains the previously discussed tile drainage parameters DDRAIN, TDRAIN, and GDRAIN (Table 3-2).

Table 3-2: Tile drainage parameters in the Management File in the SWAT model.

Drainage Parameter	Definition	Default SWAT Value
DDRAIN	Depth to subsurface drain (mm)	0.00
TDRAIN	Time to drain soil to field capacity (hr)	0.00
GDRAIN	Drain tile lag time (hr)	0.00

3.3 Input Data

In this study, a baseline scenario of the Skunk Creek watershed was first constructed. The baseline scenario encompasses a period of 18 years (2004-2021) and models the watershed with no subsurface tile drainage. The purpose of the baseline scenario is to provide comparisons between the streamflow hydrology with and without the five tile drainage scenarios and their impact on daily downstream flooding events.

The required inputs of the SWAT model include topography, land use, soil, and weather data. From these data inputs, the SWAT model simulates streamflow in the watershed. To evaluate the accuracy of the simulated streamflow, it is compared with observed streamflow data during model calibration and validation.

3.3.1 Topography Data

In this study, a 10-meter DEM for South Dakota was downloaded from the USDA Natural Resources Conservation Service (USDA-NRCS, 2022). In Skunk Creek watershed, the elevation ranges from approximately 427.1 m to 572.1 m above sea level, with higher elevations being near the headwater of the watershed, and lower elevations being near the watershed outlet (Figure 3-2).

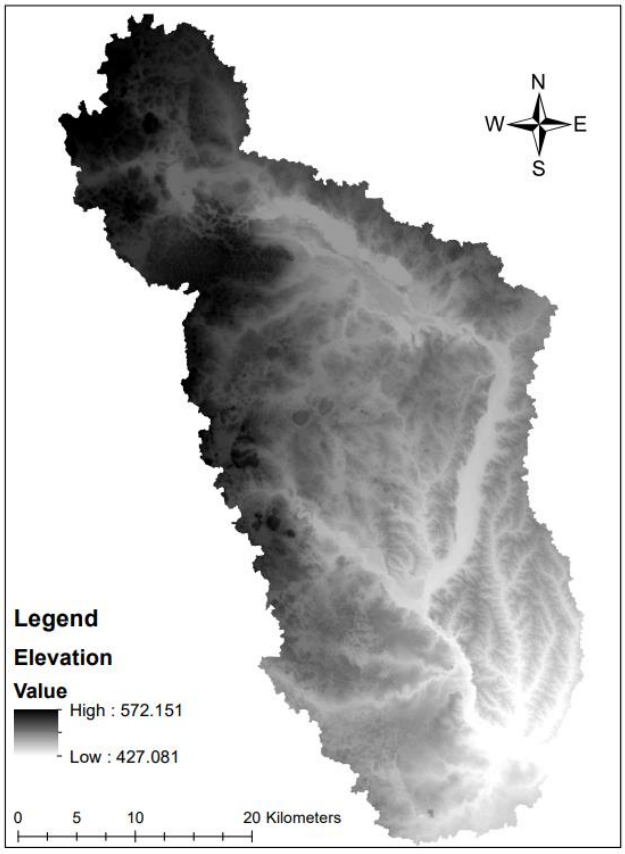

Figure 3-2: Digital Elevation Model of Skunk Creek watershed, with darker color indicating higher elevation and lighter color indicating lower elevation.

3.3.2 Soil Data

Soil Survey Geographic Database (SSURGO) data was downloaded from the USDA-NRCS Web Soil Survey for all six counties within the Skunk Creek watershed (Soil Survey Staff, 2022). The watershed consists of a total of 230 unique soil types, ranging from less than 0.00% of the watershed area to approximately 10.11% of the watershed area. The Hydrologic Soil Group (HSG) classification of these soils were observed. Group A soils were found to cover approximately 0.84% of the watershed area, Group B covered approximately 72.9% of the watershed area, Group C covered approximately 15% of the watershed area, and Group D covered the remaining 11.3% of the watershed area (Figure 3-3).

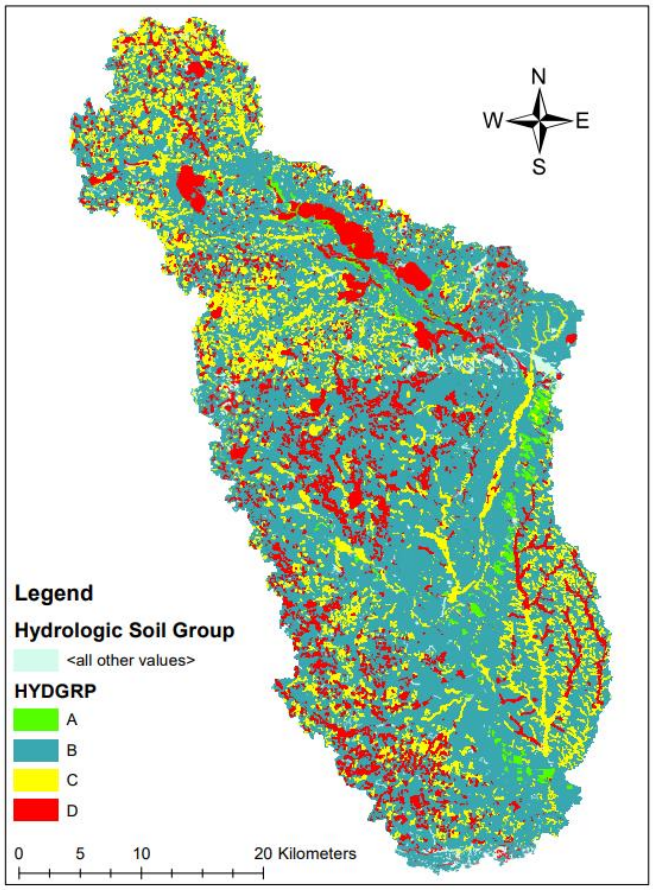

Figure 3-3: Hydrologic Soil Group classification of soils in Skunk Creek watershed.

3.3.3 Land Use Data

The 2019 National Land Cover Dataset (NLCD) was downloaded from the Multi-Resolution Land Characteristics Consortium. The watershed area consists of approximately 2.93% Non-Forested Wetlands (WETN), 3.40% Water (WATR), 1.29% Residential-Medium Density (URMD), 4.03% Residential-Low Density (URLD), 1.23% Residential-High Density (URHD), 0.07% Southwestern US (Arid) Range (SWRN), 3.73% Range (Grasses) (RNGE), 10.24% Hay (HAY), 0.67% Forest-Deciduous (FRSD), and 72.41% Agricultural Land-Row Crops (AGRR) (Figure 3-4).

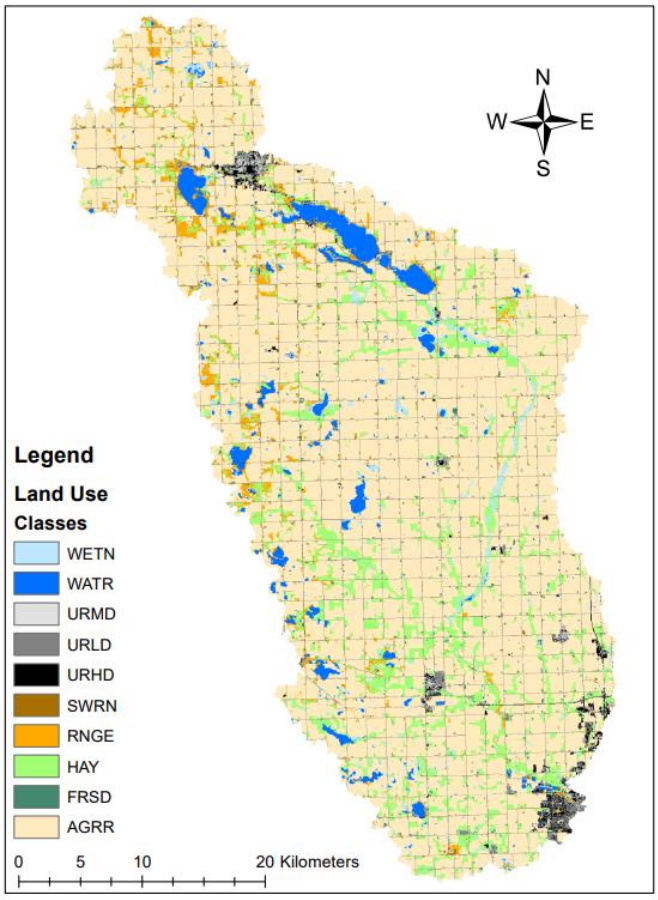

Figure 3-4: Land Use / Land Cover classes in Skunk Creek watershed.

3.3.4 Weather Data

Weather data requirements of the SWAT model include minimum temperature, maximum temperature, and daily precipitation for the period of interest. Such data was obtained from the PRISM Climate Group Northwest Alliance for Computational Science and Engineering (Rupp et al., 2022)—managed by Oregon State University—for the years 2004-2021.

PRISM climatic data was downloaded at a 4 km x 4 km grid for five counties within Skunk Creek watershed—Lake, Lincoln, McCook, Minnehaha, and Moody. Gridded data was downloaded for only the area of each county that lay within the watershed. The values for minimum daily temperature, maximum daily temperature, and total daily precipitation were averaged across the respective county (i.e., an area weighted average was computed for each county). The average value was then indicated at the county's centroid as a weather station. All other climatic components required by SWAT—solar radiation, windspeed, and relative humidity—were simulated using the built-in SWAT model weather generator (i.e., WGEN_US_COOP_1980_2010; Winchell et al., 2013).

3.3.5 Observed Streamflow Data

Observed daily streamflow data was downloaded from streamflow gauge station USGS 06481500 located at the outlet of the watershed (latitude 43°32'01" and longitude 96°47'26") (U.S. Geological Survey, 2022). Daily discharge data (ft^3/s) was downloaded from January 1, 2004, through December 31, 2021. It is interesting to note that the station has a record of discharge data beginning June 1, 1948, through present day. In contrast, daily stage data (ft) was downloaded from May 5, 2018, through December 31, 2021. Data was downloaded for only this period, as the station stage data record begins May 1, 2018, and extends through the present day.

Daily discharge and stage data were converted in Excel from the English units of ft^3/s and ft to the Metric units of m^3/s and m.

The quality of the downloaded daily discharge and stage data were analyzed, as the USGS notes data qualification codes with published station data. These qualification codes include A and A:e, where A indicates the value has been approved for publication, and e indicates that the value was estimated. Of the downloaded 6,575 days of discharge data, 4,375 days (66.5%) were indicated as an A, whereas the remaining 2,200 days (33.5%) were indicated as an A:e. In comparison, of the downloaded 1,253 days of stage data, 1,204 days (96.1%) were indicated as an A, whereas the remaining 49 days (3.90%) were missing, or blank (U.S. Geological Survey, 2022). It is important to note that the SWAT model was calibrated and validated with observed daily discharge data from 2004-2021.

3.4 Model Set-Up

In developing the SWAT model and defining the watershed delineation, an area of 12,000 Ha (120 km^2) was specified. Out of this area, a total of eight sub-basins were discretized. The larger sub-basins are located in the headwaters of the watershed, whereas the middle and lower watershed sub-basins are relatively similar in size (Figure 3-5). The areas of the sub-basins in Skunk Creek watershed range from approximately 122.11 km^2 to 373.25 km^2 (Table 3-3).

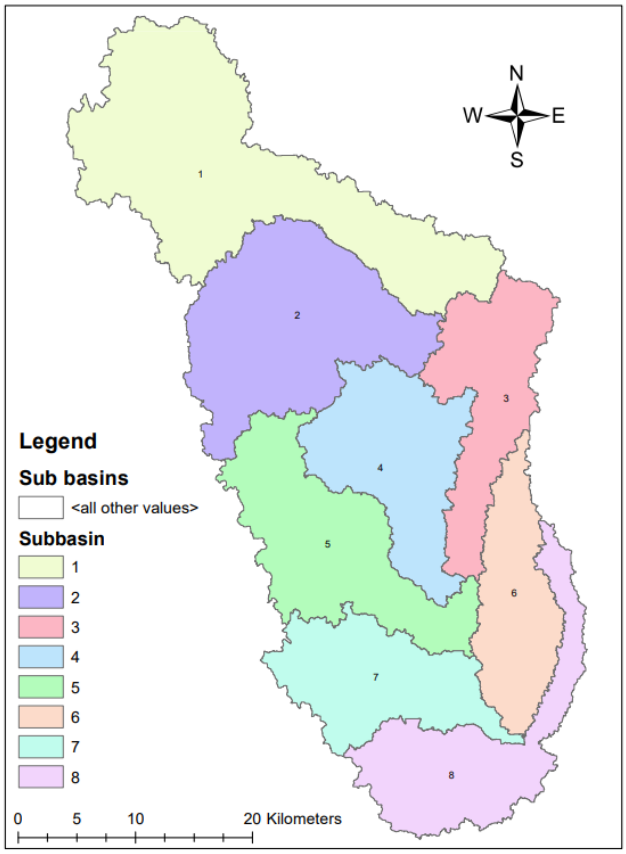

Figure 3-5: Delineation of sub basins in Skunk Creek watershed, with sub-basin 1 located the furthest away from the watershed outlet and sub-basin 8 containing the outlet.

Table 3-3: Respective area of each delineated sub basin in Skunk Creek watershed.

Subbasin	Area (km^2)
1	373.25
2	254.77
3	145.15
4	167.17
5	198.90
6	122.11
7	146.18
8	159.52

In addition to sub-basins, during the HRU analysis, the initial inputs of land use, soil, and slope gave rise to over 9,000 HRUs. To reduce the number of HRUs in the SWAT model, the NLCD2001 Look-Up table (nlcd2001_lu in SWAT2012.mdb) was manually aggregated. If a land use was found to comprise less than 1% of the total watershed area, the SWAT look-up value was manually changed to correspond to a similar land use. In addition to the manual aggregation of the land use look-up table, an HRU threshold for soil class was specified as 1%, respectively. With the land use aggregation and soil thresholds, the model used a total of 10 unique land uses and 137 soil classes. One slope class (0-9999) was used as well. With this, Skunk Creek watershed was discretized into a total of 1,288 unique HRUs (Figure 3-6).

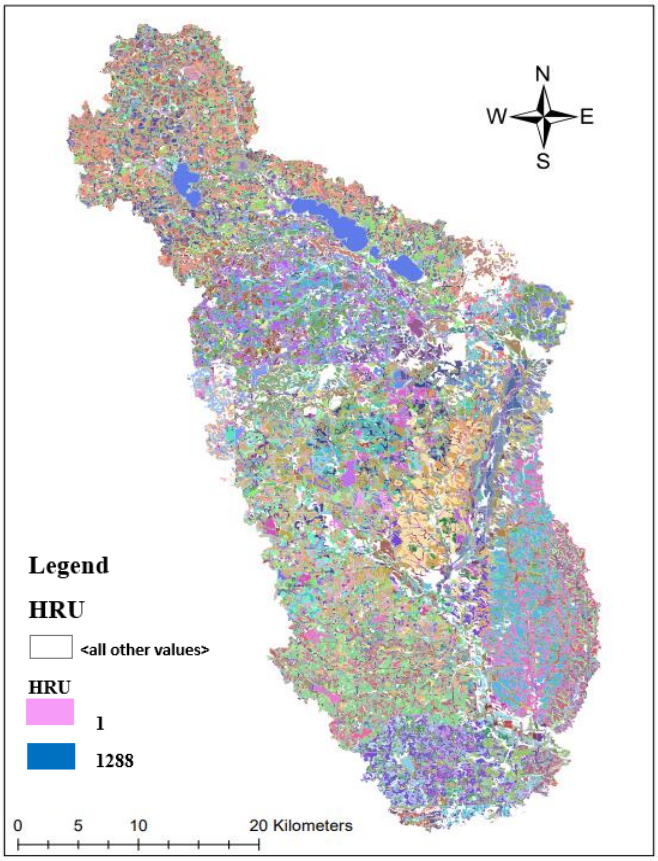

Figure 3-6: Final delineation of 1288 Hydrologic Response Units in Skunk Creek watershed.

Upon HRU analysis, similar studies (as well as operational standards) were used to determine practical land-management operations and schedules for corn and soybean crops in the watershed. In the ".mgt table" of SWAT, the tillage operation was selected as no till for both corn and soybeans (USDA-NRCS, 2014; Rajib et al., 2016). The date for planting (Hall et al., 2016; Hong, 2017; Rajib et al., 2016) and harvest and kill (Hong et al., 2016; Rajib et al., 2016; South Dakota's Conservation Districts, n.d.) were scheduled by date. Also scheduled by date were fertilizer type, application frequency, and amount (Table 3-4; Carlson et al., 2016; Hong, 2017; Mengel, 1996; Rajib et al., 2016; Ransom, 2020; Sanghum & Reicks, 2013). It is important to note that no tile drainage management operations were scheduled, as the baseline scenario has no tile drainage (see Section 3.7 for further discussion regarding scenarios).

Table 3-4: Land management operations in Skunk Creek watershed, as used in this study.

Management Operation	Date	Applications	Rate/Crop Year (kg/ha)
Corn			
Tillage			
No Till			
Planting	May 7		
Fertilizer Application			
Urea (N)	June 4	1	85
Monoammonium Phosphate (P)	June 4	1	40
Harvest and Kill	October 7		
Soybeans			
Tillage			
No Till			
Planting	May 15		
Fertilizer Application			
Monoammonium Phosphate (P)	May 10	1	40
Harvest and Kill	October 1		

3.5 Calibration and Validation

The SWAT model was executed from 2007-2021, or a total simulation period of 18 years. To minimize uncertainty while stabilizing the model before simulation, the first three years (2004-2006) were used as the model warm-up period (Mehan et al., 2017). The next twelve years (2007-2018) were used as the calibration period, and the final three years (2019-2021) were used as the validation period.

The SWAT model was calibrated and validated using observed daily streamflow data from the outlet of Skunk Creek watershed. The stand-alone SWAT Calibration and Uncertainty Program (SWAT-CUP; Abbaspour, 2015) software was used and the Sequential Uncertainty Fitting 2 (SUFI-2) approach was selected for model calibration and validation. The SUFI-2 method has been widely and successfully used for SWAT calibration in recent SWAT studies in Skunk Creek watershed and surrounding watersheds (Mehan et al., 2016; Teshager et al., 2016) due to its ability to calibrate the model in less time compared to other SWAT-CUP methods (Yang et al., 2008). The SUFI-2 approach conducts model parameterization, sensitivity analysis, uncertainty analysis, calibration, and validation on the daily and monthly time steps. In the SUFI-2 approach, the objective function is defined, then the algorithm optimizes the absolute maximum and minimum ranges of the selected parameters (Abbaspour, 2015; Mehan et al., 2017).

In this study, the objective function was defined as the maximization of the Nash Sutcliffe Efficiency (NSE). To assess the similarity between the observed and simulated streamflow, the percent bias (PBIAS) and root mean square error (RMSE) observations standard deviation ratio (RSR) were evaluated as well.

The NSE determines the relative magnitude of the residual variance ("noise") between the observed and simulated data. The NSE is computed as:

$$NSE = 1 - \left[\frac{\sum_{i=1}^{n}(Y_i^{obs} - Y_i^{sim})^2}{\sum_{i=1}^{n}(Y_i^{obs} - Y^{mean})^2}\right]$$

where Y_i^{obs} is the *i*th observation of the data being evaluated, Y_i^{sim} is the *i*th simulated value of the data being evaluated, Y^{mean} is the average of the observed data for the data being evaluated, and *n* is the total number of observations. The acceptable range of NSE varies between 0 and 1.

The PBIAS measures the average tendency of the simulated data to be larger than or smaller than the observed data, or the deviation between the values. PBIAS, which measures the percentage of bias in a simulation, is calculated as follows:

$$PBIAS = \left[\frac{\sum_{i=1}^{n}(Y_i^{obs} - Y_i^{sim}) * (100)}{\sum_{i=1}^{n}(Y_i^{obs})}\right]$$

The optimal value of PBIAS is zero. A positive value of PBIAS indicates over-prediction of the model while a negative value indicates underprediction of the model.

The RSR is the ratio of the RMSE to the standard deviation of the observation. RSR is calculated as follows:

$$RSR = \frac{RMSE}{STDEV_{obs}} = \left[\frac{\sqrt{\sum_{i=1}^{n}(Y_i^{obs} - Y_i^{sim})^2}}{\sqrt{\sum_{i=1}^{n}(Y_i^{obs} - Y^{mean})^2}}\right]$$

The lower the value of RSR, the lower the RMSE, and the better the model simulation performance (Moriasi et al., 2007; Sharma, 2018).

To evaluate SWAT model outputs, Moriasi et al. (2007) suggested the performance ratings of "Very Good," "Good," and "Satisfactory," each of which has its respective statistical

index. In this study, the recommended satisfactory statistical indices for streamflow at a monthly time step were used, as they were considered valid for daily output comparison (Table 3-5).

Table 3-5: Satisfactory statistical indices for monthly streamflow SWAT model calibration and validation (Adapted from Moriasi et al., 2007).

Model Performance Evaluation Statistic	Satisfactory Range
NSE	≥ 0.50
PBIAS	-25% to +25%
RSR	≤ 0.7

In addition to the statistical indices, qualitative information was used to evaluate the performance of the model (Moriasi et al., 2007; 2015). This information was based on plotting the time series of daily simulated and observed streamflow. In addition, streamflow calibrations were constrained using soft, or qualitative, data (Arnold et al., 2015) such that the SWAT-CUP parameters, simulated ET values, and baseflow values were realistic and representative of the study area. Soft data were used to minimize the potential for false positive outcomes in the model (obtaining good statistics for the wrong reasons; Moriasi et al., 2015). In this study, the model was constrained such that simulated values were within 15% of the average annual ET soft data value of 630 mm (Paul et al., 2016) and were within the expected range of 22% to 29% of baseflow contribution to streamflow (USGS, 2003).

In this study, nineteen parameters were selected for the calibration and validation of daily streamflow data at the outlet of the watershed. Parameters were selected based on previous studies conducted in and around the study area, as well as other midwestern, agricultural watersheds (Ahiablame et al., 2019; Hong, 2017; Mehan et al., 2017). The selected model

parameters, along with their minimum values, maximum values, and best-fitted values are shown below in Table 3-6.

Table 3-6: Parameters used in daily streamflow SWAT model calibration and validation.

Parameter	Definition	Minimum Value	Maximum Value	Fitted Value
R_CN2	Curve number (moisture condition II)	-0.20	0.20	-0.108
V_ALPHA_BF	Baseflow alpha factor	0.00	1.00	0.389
V_GW_DELAY	Groundwater delay time (days)	30.0	450	49.86
V_GWQMN	Depth of water in shallow aquifer	0.00	2.00	300.4
V_CH_N2	Manning's "n" value for main channel	0.01	0.30	0.147
V_OV_N	Manning's "n" value for overland flow	0.01	1.00	0.339
V_SURLAG	Surface runoff lag coefficient	0.05	24.0	3.259
A_SOL_AWC	Available water capacity of soil layer	0.00	1.00	0.887
V_ESCO	Soil evaporation compensation factor	0.00	1.00	0.900
V_EPCO	Plant uptake compensation factor	0.00	1.00	0.724
V_SMTMP	Snow melt base temperature	-5.00	5.00	0.283
V_SFTMP	Snowfall temperature	-5.00	5.00	-1.681
V_SMFMX	Melt factor for snow on June 21 (mm H_2O/°C-day)	1.40	7.50	4.358
V_TIMP	Snow pack temperature lag factor	0.00	1.00	0.475
V_SMFMN	Melt factor for snow on December 31 (mm H_2O/°C-day)	1.40	7.50	2.299
V_CH_K2	Effective hydraulic conductivity in main channel (mm/hr)	-0.01	500	79.53
V_GW_REVAP	Groundwater "revap" coefficient	0.02	0.20	0.087
V_REVAPMN	Threshold depth of water in shallow aquifer	0.00	500	170.1

V_CANMX	Maximum canopy storage (mm H_2O)	0.01	25.0	6.935

Note. "V" indicates that the original value was replaced by a value from the range; "A" indicates that the original value was added to a value within the range; and "R" indicates that the original value was multiplied by 1+ a value from the range.

The respective sensitivity of each parameter used for model calibration and validation was determined by performing a Global Sensitivity Analysis. A Global Sensitivity Analysis assesses the complete range of parameter values used during the simulation process. In this analysis, all parameter values are simultaneously altered, which captures the full range of parameter values, showcases the interaction among the parameters, and determines their influence on model outputs (Mehan et al., 2017). A multiple regression analysis is then used to determine the sensitivity of each parameter, including the t-stat and p-value statistics. The t-stat indicates the level of sensitivity of each parameter, whereas the p-value determines the significance of the sensitivity (a value close to 0 has more significance) (Pandey et al., 2021). During a Global Sensitivity Analysis, the larger the absolute value of t-stat and the smaller the p-value, the more sensitive the parameter (Figure 3-7; Abbaspour, 2015). In this study, the most sensitive parameters include ESCO, CN2, CH_K2, CH_N2, ALPHA_BF, and CANMX, whereas the least sensitive parameters include GWQMN, OV_N, SMFMX, GW_DELAY, SOL_AWC, and REVAPMN (Figure 3-7).

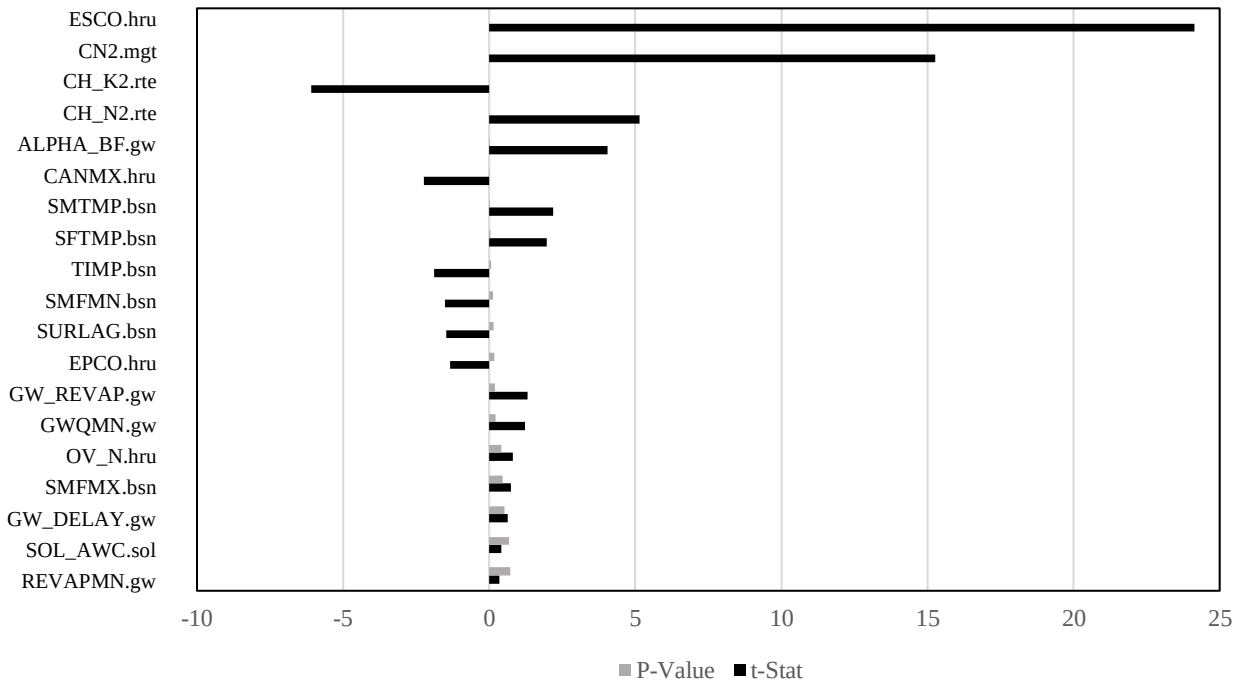

Figure 3-7: Global sensitivity analysis of parameters used in daily streamflow calibration and validation based on output from SWAT-CUP, in which the length of the bar depicts the level of sensitivity of the parameter.

To further analyze the most sensitive (Figure 3-8) and least sensitive (Figure 3-9) parameters in this study, dotty plots were observed. In SWAT-CUP, dotty plots show parameter values or relative changes versus the objective function (i.e., NSE). These plots show the distribution of sampling points, as well as give a general idea of parameter sensitivity (Abbaspour, 2015). If the points on dotty plots are scattered, the sensitivity of the parameter is lower, whereas if the points follow a trend, the sensitivity is higher (Mehan et al., 2017).

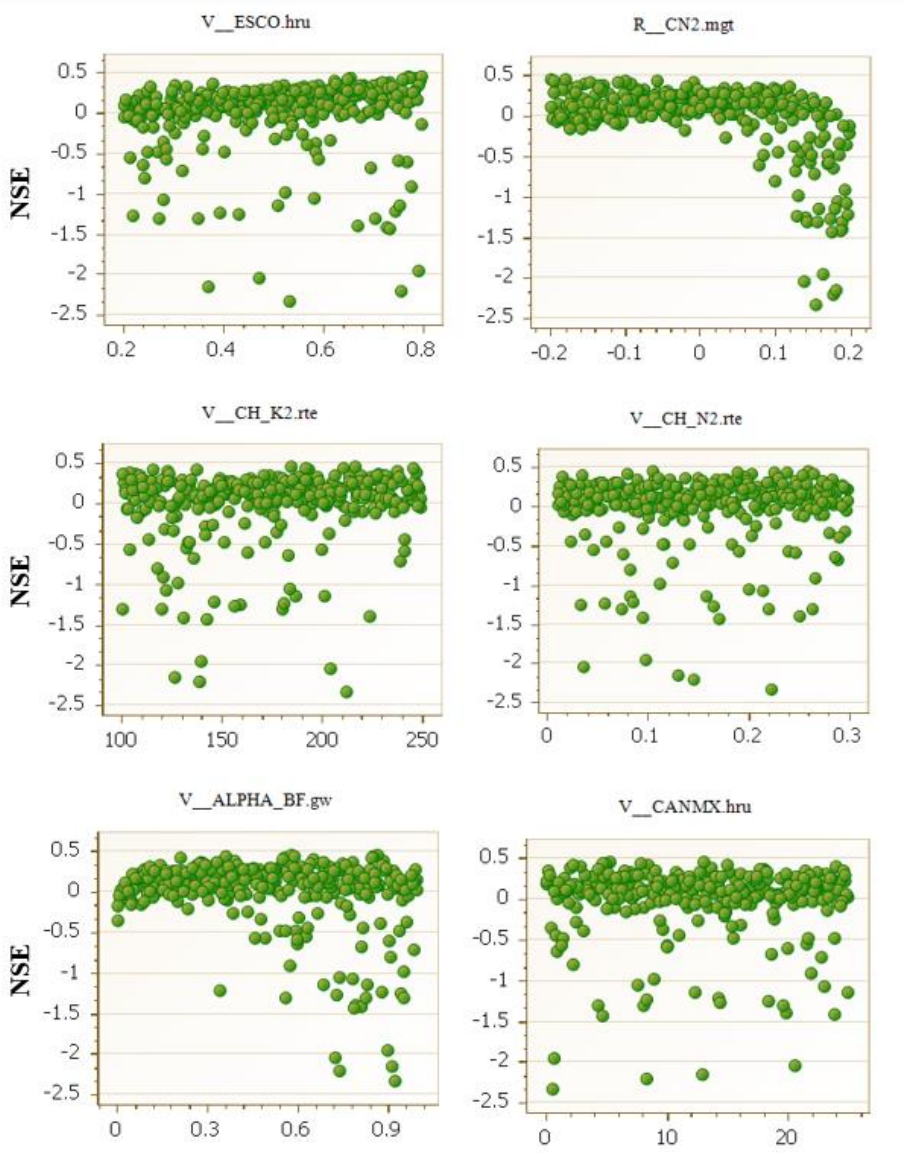

Figure 3-8: Dotty plots derived from SWAT-CUP for most sensitive parameters during model calibration.

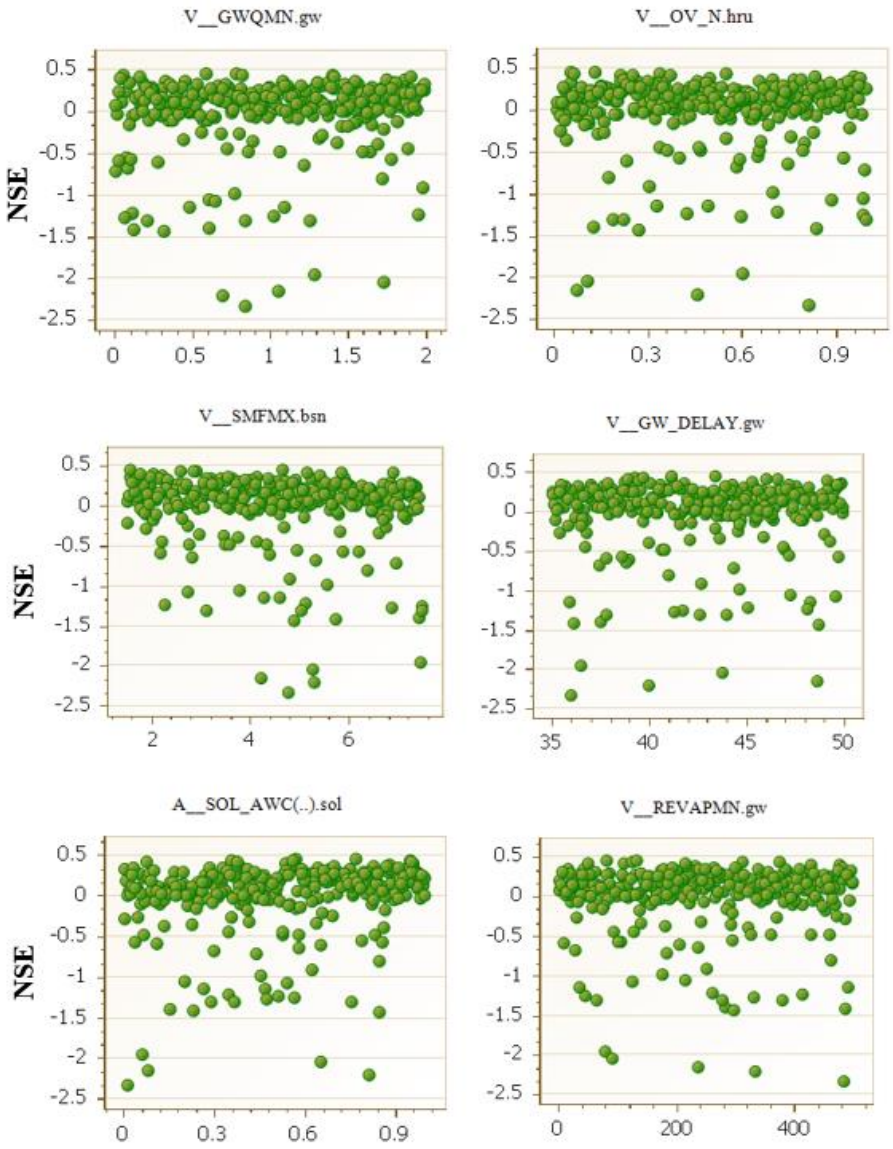

Figure 3-9: Dotty plots derived from SWAT-CUP for least sensitive parameters during model calibration.

3.5.1 Precipitation Assessment

Upon calibration and validation of the nineteen selected parameters in SWAT-CUP, additional manual calibration was performed. Manual calibration was necessary, as the model failed to capture several peak flow (flood) events. To increase the validity of the model (as well as the reliability of the results), it was essential that the model accurately simulated peak flow

events. To simulate daily peak flow events more accurately, an assessment of observed precipitation data was performed.

Originally, the values of precipitation were averaged and indicated at the centroid of each county as a weather station. Due to this representation of weather stations in the watershed, it was hypothesized that precipitation levels were misrepresented or missed (due to the size and variability of the watershed). Therefore, PRISM precipitation data was redownloaded on the basis of SWAT discretized sub-basins and averaged at the centroid of each sub-basin as a weather station. Additionally, data from several land-based stations located in and around the watershed were collected. The collection and comparison of data from land based stations were essential to ensure that the PRISM data appropriately represented large precipitation, hence runoff, events (Figure 3-10).

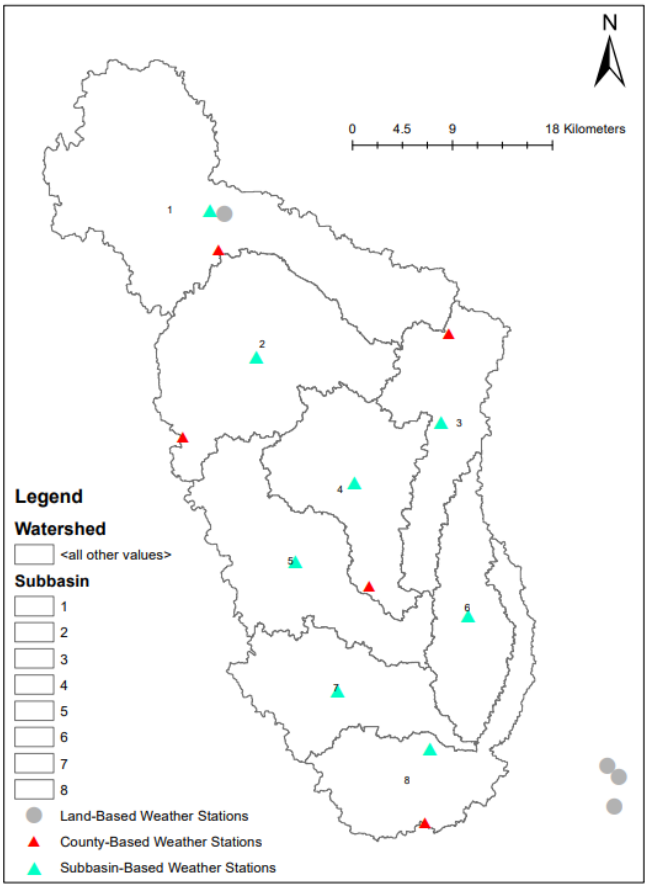

Figure 3-10: Location of land-based weather stations, PRISM county-based weather stations, and PRISM subbasin-based weather stations used in manual calibration of Skunk Creek watershed.

Upon the investigation of county-based precipitation stations, it was found that sub-basins 4, 5, 6, and 7 received precipitation inputs from the Minnehaha Weather Station (the red flag located within Subbasin 4; Figure 3-10). Due to this distribution of precipitation in the watershed, daily county-based precipitation data were compared to and supplemented with daily observed subbasin- and land station-based precipitation data. Using these supplemental precipitation data sources, missing values of precipitation were manually replaced in the project's precipitation (i.e., pcp1.pcp) file (located in Scenarios, Default, TxtInOut folder). The focus of the precipitation analysis was the high peak-flow years; therefore, the years modified were only 2007, 2010, 2011, 2018, 2019, and 2020 (Table 3-7). In some instances, (e.g., March

2019 and September 2019), precipitation data was redistributed throughout the watershed (i.e., the value of observed precipitation in Subbasin 1 was swapped with the value of observed precipitation in Subbasin 8 for a particular event). This methodology of redistribution ensured the same amount of observed precipitation fell on the watershed during a given event.

Table 3-7: Total annual watershed precipitation, as modified by manual calibration of observed subbasin-based PRISM data and land station-based data for 2007, 2010, 2011, 2018, 2019, and 2020.

Year	Original Precipitation	Modified Precipitation	Percent Change (%)
2007	3856.8	3920.5	1.65
2010	4642.4	4756.1	2.45
2011	3357.0	3367.1	0.30
2018	4877.9	4914.5	0.75
2019	5569.2	5907.9	6.08
2020	2235.1	2307.1	3.22

3.5.2 Indicators of Hydrologic Alteration

The Indicators of Hydrologic Alteration (IHA) tool is a software program developed by Richter et al., (1996) of the United States Nature Conservancy to evaluate the degree of hydrologic alterations caused by human activities (Gao et al., 2009; Kim et al., 2011; The Nature Conservancy, n.d.). The IHA software calculates a total of 67 parameters from daily runoff data, with 33 hydrologic parameters and 34 environmental parameters (Gao et al., 2009; Mathews et al., 2007; Kim et al., 2011). These parameters were developed based on both ecological importance and their ability to reflect human-induced alterations of the natural flow regime (Gao et al., 2009). The hydrologic parameters characterize intra- and inter-annual variability of water

conditions, such as magnitude, frequency, duration, timing, and the rate of change of flows. In the IHA software, five major components of flow are considered, including extreme low flows, low flows, high flow pulses, small floods, and large floods. In the IHA, small floods are classified as events in which river flows are greater than or equal to bankfull, and occur frequently (e.g., every 2 to 10 years). In contrast, large floods occur rarely and are classified as events greater than or equal to the 10-year flood event (Mathews et al., 2007).

The IHA software was used as a method to double-check the calibration and validation of the SWAT model to ensure flood events were appropriately simulated. In the IHA, a custom analysis was developed to ensure simulated peak flow events were representative of observed flood days in the watershed. A small flood event was defined as a peak flow greater than 78.0 m^3/s, while a large flood event was defined as a peak flow greater than 144.0 m^3/s (see Section 3.6 for a discussion regarding these values).

3.6 Flood Risk Modelling

Flood hazard, or risk, is the probability that a specific magnitude (depth, velocity, or discharge) flood event will occur (National Research Council of the National Academies, 2015). Following Schilling et al., (2014), this work defines a flood event as a simulated stream discharge at the watershed outlet which exceeds a specified flood stage. A flood stage is a predetermined gauge height—specific to a creek or river—at the elevation in which stormwater overflows the natural banks of the system (Fahlquist & Hopkins, 2023). The event may last a few minutes to hours and days, and represents any flood type (i.e., action, minor, moderate, and major). Flood duration is the number of minutes, hours, and days a given flood event lasts on occurrence (i.e., the total number of minutes, hours, and days a given flood event stays above the defined flood stage in a year over the study period; (Schilling et al., 2014)). Due to observed

streamflow data limitations, only daily flood events (streamflow events that exceed the defined flood stage and maintain the stage for a complete 24-hour period) were considered during analysis.

The USGS has established flood stages at the outlet of Skunk Creek watershed (USGS gauge station 06481500) for action, minor, moderate, and major flood types. During an action flood event, the water level of the stream is below the flood stage but near "bankfull"—the height at which additional rise would result in water overflowing onto the flood plain. At the minor flood stage, minor flooding occurs as water begins to overtop streambanks. At the moderate flood stage, some inundation to roads, minor to moderate damage to infrastructure, and moderate erosion occurs. Finally, if streamflow reaches the major flood stage, it produces extensive inundation of roads, severe damage to infrastructure, and extreme erosion (National Weather Service, n.d.; Susquehanna Flood Forecast and Warning System, n.d.). For Skunk Creek, the "Action Flood Stage" is defined as 2.90 m, the "Minor Flood Stage" is defined as 3.51 m, the "Moderate Flood Stage" is defined as 4.57 m, and the "Major Flood Stage" is defined as 5.18 m (National Weather Service, 2022: NOAA, 2022).

In this study, observed daily flood stage values were obtained from USGS gauge station 06481500 from May 1, 2018, through December 5, 2022 (with several missing values). Observed daily streamflow data from 2004-2021 were used as well (U.S. Geological Survey, 2022) and a relationship was developed between observed daily streamflow and river stage (Figure 3-11). It is interesting to note that in the stage-discharge relationship (rating) curve, there are two distinct splits in the data. This split could be attributed to changes in the streambed due to erosion or deposition, or the growth of riparian vegetation. Changes in the stage-discharge curve are called shifts. Shifts may cause a short- or long-term change in the stage-discharge

relationship curve for the stream gauge (USGS, 2023). However, by following the average trend depicted by the curve, the stage-discharge relationship was used to determine the stream discharge that corresponds to the defined flood stages of Skunk Creek (Figure 3-11).

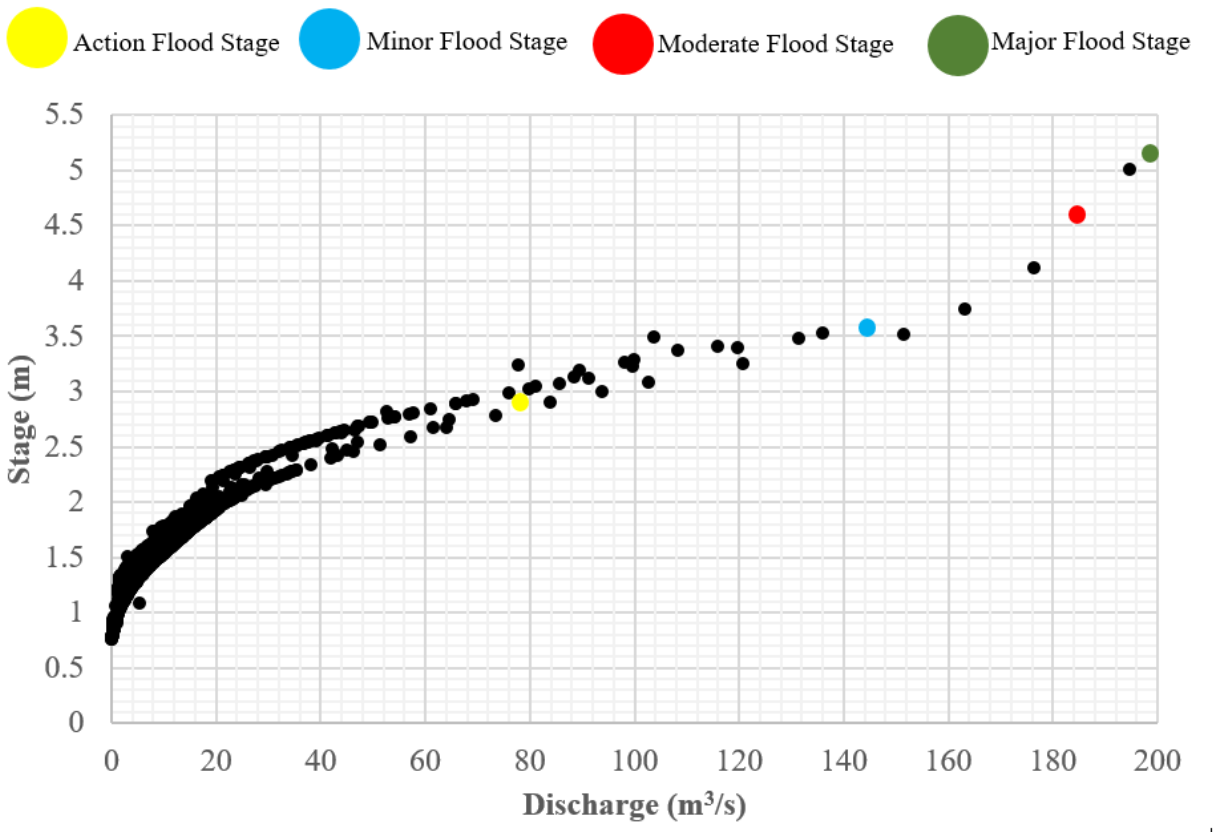

Figure 3-11: Gauge station USGS 06481500 stage-discharge relationship, used to determine discharge associated with corresponding flood stage at watershed outlet.

From the stage-discharge relationship curve developed for Skunk Creek, the stage heights of 2.90 m, 3.51 m, 4.57 m, and 5.18 m were found to correspond with stream discharge values of approximately 78.0 m^3/s, 144 m^3/s, 184 m^3/s, and 197 m^3/s, respectively (Figure 3-11). Values of simulated streamflow in the baseline and tile drainage scenarios that exceeded the flood discharge threshold were considered as flood events. The frequency of such events was determined by counting the number of times, over the study period, that river discharge peaked above any defined flood stage and remained that way for one complete day (Figure 3-12).

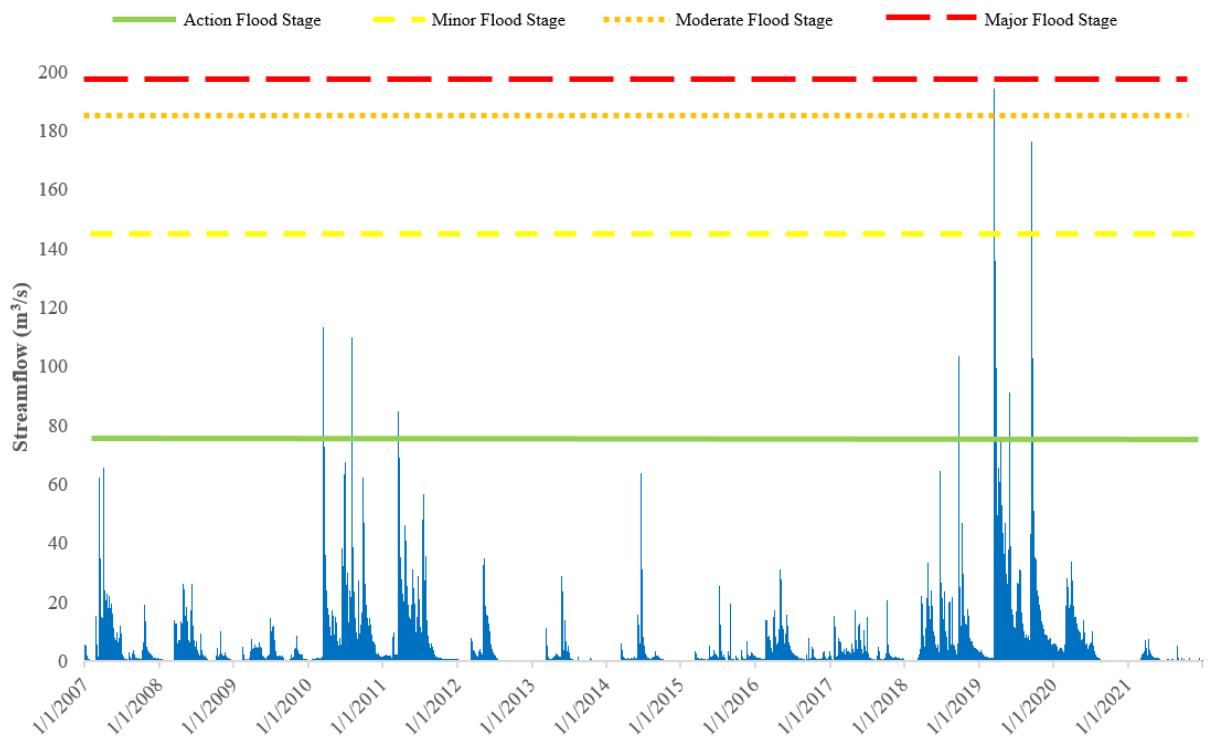

Figure 3-12: Observed hydrograph for daily streamflow (2007-2021) for Skunk Creek watershed showing "Action Flood Stage" at 78 m^3/s, "Minor Flood Stage" at 144 m^3/s, "Moderate Flood Stage" at 184 m^3/s, and "Major Flood Stage" at 197 m^3/s.

3.6.1 Flood Evaluation

To evaluate (or count) the occurrence and magnitude of flood days during the study period, the K-State Calibration Utility for ArcSWAT tool was used. The K-State Calibration Utility for ArcSWAT is an Excel spreadsheet tool designed to aid with analyzing SWAT model outputs. The tool functions by reading the ArcSWAT database file and analyzing the default scenario (located in Scenarios, Default, TxtInOut folder). Simulated values for daily, monthly, and annual streamflow are compared with observed streamflow data series, and the tool calculates hydrologic statistics (e.g., NSE, PBIAS, and RSR) (Sheshukov, 2012). As the tool outputs a data series of daily discharge, the baseline and tile drainage scenarios were evaluated against predetermined flood stages for Skunk Creek. When values of daily discharge were

greater than or equal to the "Action Flood Stage" of 78 m^3/s, the respective magnitude of streamflow was collected and counted as a flood day.

3.7 Flood Assessment Scenarios

In this study, a total of five tile drainage scenarios were simulated to assess the impacts of subsurface tile drainage systems on daily downstream flooding events. A baseline scenario was constructed with the calibrated and validated parameters based on 2019 land use data and 2007-2021 climatic data. The baseline scenario has no subsurface tile drainage management operations and was created to provide comparisons between scenarios with varied extents of tile-drained agricultural land.

It is important to note that in all tile drainage scenarios, tile flow was simulated using the Kirkham and Hooghoudt drainage equations (i.e., ITDRN=1). Similarly, the five scenarios all have the same drainage depth (DDRAIN), drainage spacing (SDRAIN), and impermeable depth (DEP_IMP)—914.4 mm, 30,000 mm, and 1,000 mm, respectively—yet vary in their extent of agricultural land cover (Table 3-8). The values of drainage depth and spacing were determined from the literature (Kringen et al., 2021; University of Minnesota Extension, 2018) and the impermeable depth was set at a value slightly larger than DDRAIN (ArcSWAT Google Groups, 2014; Boles, 2013; Hutchinson & Christiansen, 2013). Additionally, the curve number (CN2) was reduced in all tile-drained HRUs by 30% to reflect infiltrated water contributing to tile flow (Frankenberger et al., 2013).

The tile drainage scenarios increase at increments of 15% and consist of 15% to 75% drained agricultural land in the watershed (see Table 3-8). The tile-drained agricultural land is based on total watershed area (e.g., 15% tile-drained agricultural land implies that 15% of the total watershed agricultural land is modeled with tile drainage), and is distributed throughout the

sub-watersheds (i.e., the total area of tile-drained HRUs in sub-watershed are non-uniform and sum to equal the respective scenario percentage).

Table 3-8: Tile drainage design scenarios simulated in this study.

Scenario Description	Scenario Notation
15% Tile-Drained Agricultural HRUs	Scenario 1
30% Tile-Drained Agricultural HRUs	Scenario 2
45% Tile-Drained Agricultural HRUs	Scenario 3
60% Tile-Drained Agricultural HRUs	Scenario 4
75% Tile-Drained Agricultural HRUs	Scenario 5

During scenario development, subsurface tile drainage systems were implemented in all agricultural HRUs despite the crop type and were randomly distributed throughout the watershed. To perform random selection, all agricultural HRUs were assigned a unique number in Excel. A script was written that selected a random number from the specified list of HRUs. The random selections were recorded until the respective tile drainage scenarios were obtained, that is, 15%, 30%, 45%, 60%, and 75% of the watershed agricultural area.

To ensure the Excel selection of agricultural HRUs were spatially random, the GIS Spatial Autocorrelation (Moran's Index (I)) tool was used (Getis & Ord, 1992). This tool measures spatial autocorrelation based on select feature locations and attribute values using the Global Moran's I statistic. The Moran's I tool determines whether the spatial pattern is clustered, dispersed, or random. The tool returns the Moran's Index value, the z-score, and the p-value, to indicate whether the null hypothesis (features are randomly distributed across the study area) can be rejected. The z-score represents the critical value and indicates spatial randomness with values

between -1.65 and 1.65. The p-value indicates the significance level and demonstrates spatial randomness with values greater than 0.10 (ESRI).

To use the Spatial Autocorrelation tool, all HRUs in the watershed were converted from polygon shapefiles to point shapefiles (located at the respective centroid of each HRU). A new field was added to the attribute table of the point shapefile layer. In the field, zero (0) was used to indicate no changes to the baseline HRU values, whereas one (1) was used to indicate the modeling of tile drainage in the HRU (as selected by Excel). HRUs with tile drainage (1) and without tile drainage (0), were then analyzed with the Spatial Autocorrelation tool to determine their spatial pattern. This process was repeated five times to ensure all scenarios—15% to 75% tile-drained agricultural land—were distributed spatially randomly throughout the watershed. The spatial distribution of tile-drained agricultural HRUs used for scenario analysis can be viewed below, in Figure 3-13.

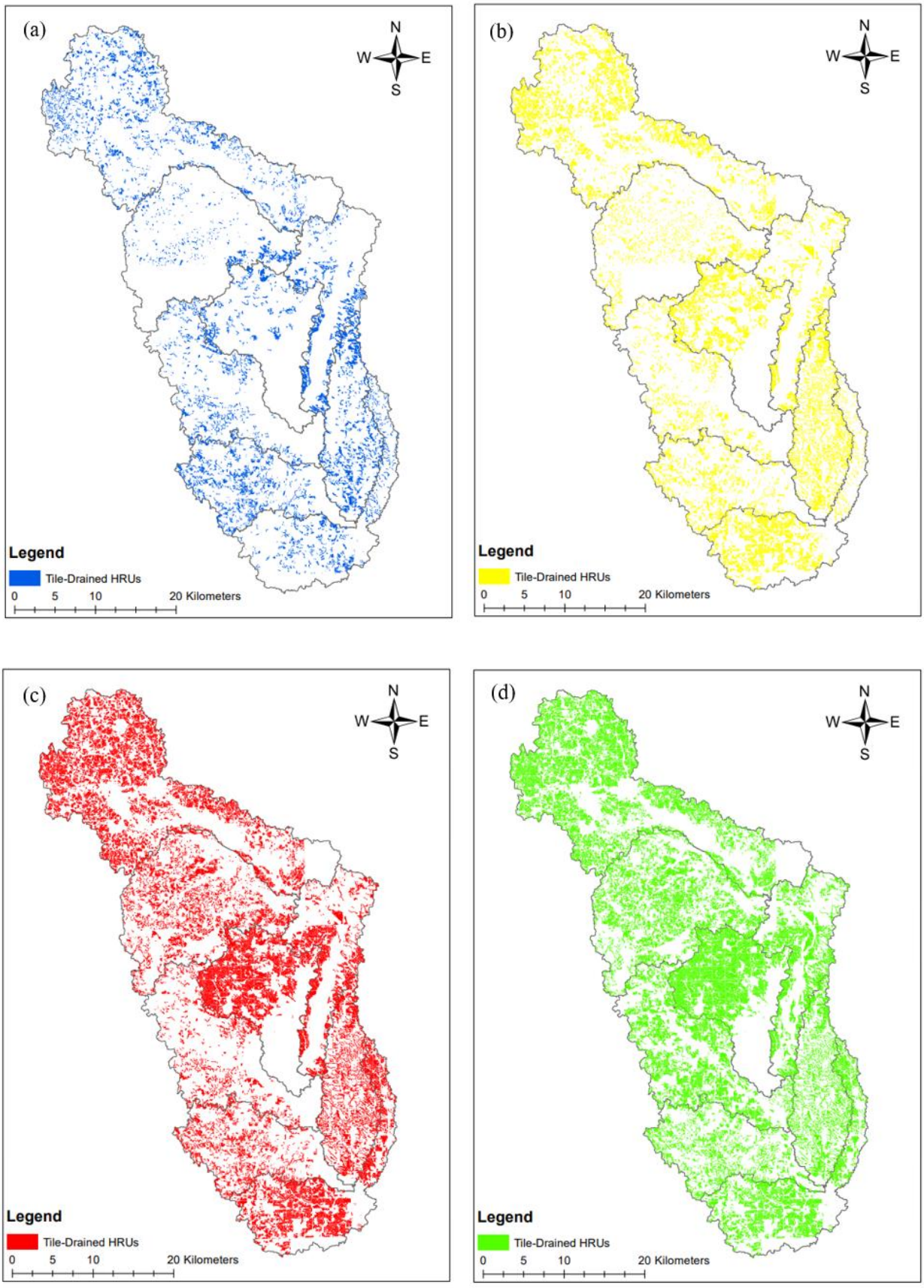
(a)
N
W
E
S
Legend
Tile-Drained HRUs
0 5 10 20 Kilometers
(b)
N
W
E
S
Legend
Tile-Drained HRUs
0 5 10 20 Kilometers
(c)
N
W
E
S
Legend
Tile-Drained HRUs
0 5 10 20 Kilometers
(d)
N
W
E
S
Legend
Tile-Drained HRUs
0 5 10 20 Kilometers

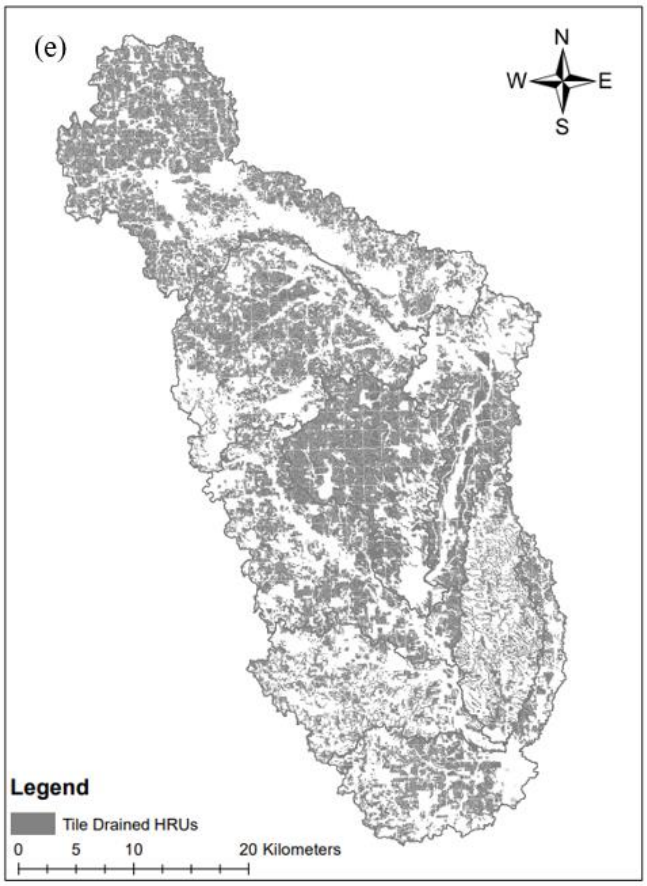

Figure 3-13: Map showing spatial distribution of tile drainage scenarios in Skunk Creek watershed, where: (a) Scenario 1, (b) Scenario 2, (c) Scenario 3, (d) Scenario 4, and (e) Scenario 5.

As the distribution of tile-drained agricultural land is based on total watershed area, and thus non-uniform throughout the sub-basins (Figure 3-13), the percentage of each sub-basin modeled with tile drainage, as well as the total area of each sub-basin modeled with tile drainage, is presented in Appendix A. In total, the area of agricultural land modeled with tile drainage ranged from 173.4 km^2 in Scenario 1 to 851.9 km^2 in Scenario 5, respectively (Table 3-9). As a reminder, Skunk Creek watershed has an area of approximately 1,606 km^2. Therefore, the total area of tile-drained agricultural land modeled during scenario analysis accounts for approximately 10.8% to 53.0% of the total watershed area.

Table 3-9: Total watershed area modeled with tile drainage during scenario analysis.

Scenario	Area (km^2)
Scenario 1	173.4
Scenario 2	344.0
Scenario 3	511.9
Scenario 4	685.2
Scenario 5	851.9

To ensure simulated tile flow was an accurate representation of the study area, a review of previously published papers was completed to identify a reasonable, expected range of tile flow (Appendix B). From these studies, tile flow was found to range from 8.5% to 16.2% of annual precipitation (with an outlier of 39%) and from 6% to 89.7% of annual water yield. However, most published studies focus on watersheds with areas less than or equal to 150 km^2 (Arenas Amado et al., 2017; Boles, 2013; Golmohammadi et al., 2017; King et al., 2015; Macrae et al., 2007; Moloney, 2016; Moriasi et al., 2013; Rahman et al., 2014; Schilling et al., 2019; Sloan et al., 2016; Thomas, 2015). When considering scale, Schilling et al., (2019) compared Boone River watershed (2370 km^2) and Lyons Creek watershed (42 km^2) in north-central Iowa. The authors found the contribution of tile flow to annual water yield to diminish with increasing scale. More specifically, Boone River watershed received approximately 12% less water yield from tile flow than Lyons Creek watershed.

Therefore, as 15% to 75% of Skunk Creek watershed is simulated with tile drains in this study, and the effects of tile drainage diminish with increasing scale, reasonable, expected values of tile flow should comprise approximately 2.11% to 10.56% of annual precipitation and 4.88% to 24.40% of annual water yield. While there is variability in tile drain depth and spacing

(drainage density) and soil types in the referenced studies, these ranges represent approximate targets of tile flow for scenario analysis (Boles, 2013).

3.7.1 Watershed Water Balance Evaluation

To evaluate the impacts of the flood assessment (tile drainage) scenarios on the watershed water balance, the SWAT output.std file (located in Scenarios, Default, TxtInOut) was used. The output.std file is the standard output summary file of the SWAT model. The file provides average daily, monthly, or annual watershed loadings from HRUs to the streams. During analysis, the average annual basin values were used. Average annual basin values include water balance as well as nutrient balance variables. In this study, analyzed variables include precipitation (PRECIP), surface runoff (SURFACE RUNOFF Q), lateral flow (LATERAL SOIL Q), tile flow (TILE Q), groundwater flow (GROUNDWATER Q), deep aquifer recharge (DEEP AQ RECHARGE), percolation (PERCOLATION OUT OF SOIL), evapotranspiration (ET), and water yield (TOTAL WATER YLD) (see Table 3-10).

Table 3-10: Average annual basin values used in watershed water balance evaluation of tile drainage scenarios.

SWAT Variable	SWAT Definition
PRECIP	Average amount of precipitation in the watershed for the simulation (mm).
SURFACE RUNOFF Q	Surface runoff generated in the watershed for the simulation (mm).
LATERAL SOIL Q	Lateral flow contribution to streamflow in watershed for the simulation (mm).
TILE Q	Drainage tile flow contribution to stream in watershed for the simulation (mm).
GROUNDWATER Q	Groundwater contribution to stream in watershed for the simulation (mm).

DEEP AQ RECHARGE	Deep aquifer recharge in watershed during simulation (mm).
PERCOLATION OUT OF SOIL	Water percolation past bottom of soil profile in watershed for the simulation (mm).
ET	Actual evapotranspiration in the watershed for the simulation (mm).
TOTAL WATER YLD	Water yield to streamflow from HRUs in a watershed for the simulation (mm).

Further analysis of the watershed water balance involved the calculation of the percentage change of the average annual basin values between the baseline and tile drainage scenarios. These variables include surface runoff, lateral soil flow, tile flow, groundwater flow, deep aquifer recharge, percolation, ET, and water yield. Percentage change was calculated as follows:

$$Percentage\ Change = \left(\frac{Final\ Value - Initial\ Value}{Initial\ Value}\right) x\ 100\%$$

where *Final Value* is the average annual basin value (mm) from a tile drainage scenario and *Initial Value* is the average annual basin value (mm) from the baseline scenario for all studied watershed water balance components.

Chapter 4 - Results and Discussion

4.1 Calibration and Validation of SWAT Model

4.1.1 Precipitation Assessment

The precipitation input (pcp1.pcp) file was manually modified to include missed daily precipitation data during the 2007-2021 study period. In general, the original simulated streamflow underestimated observed peak streamflow. However, the addition and redistribution of missed precipitation data (modified simulated streamflow) allowed observed daily peak flow events to be more accurately simulated by the SWAT model (e.g., April 2007, March 2010, July 2010, September 2018, March 2019, September 2019) (Figure 4-1).

The observed maximum daily streamflow during the 2007-2021 study period was 194.5 m^3/s, whereas the original simulated maximum daily streamflow was 159.2 m^3/s. Following the precipitation assessment, the modified simulated maximum daily streamflow increased to 190.7 m^3/s. When comparing original simulated streamflow to modified simulated streamflow during the July 2010 peak flow event, maximum flow increased from 54.49 m^3/s to 113.5 m^3/s (with an observed streamflow of 110.2 m^3/s). Similarly, the March 2019 peak streamflow increased from 159.2 m^3/s to 190.7 m^3/s (with an observed streamflow of 194.5 m^3/s), whereas the September 2019 peak streamflow increased from 107.1 m^3/s to 186.6 m^3/s (with an observed streamflow of 176.4 m^3/s) (Figure 4-1). From this analysis, it can be said that the precipitation assessment enabled the model to simulate peak streamflow events more appropriately in the watershed.

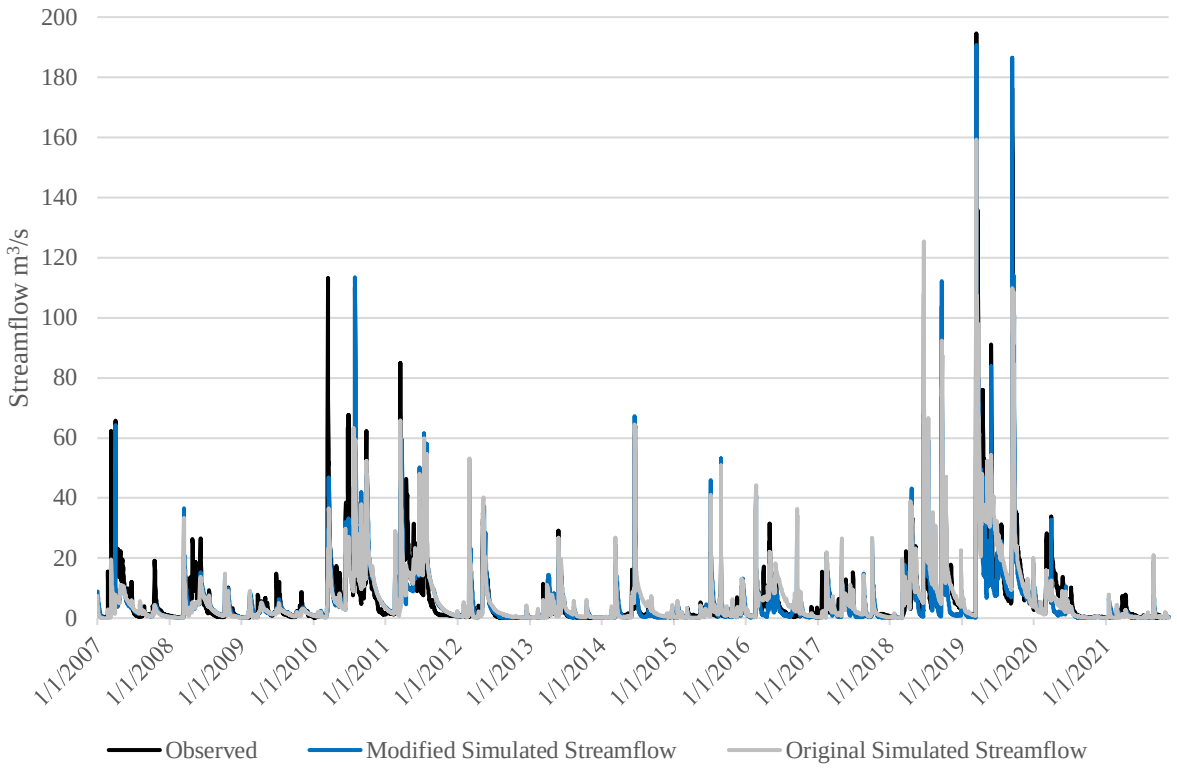

Figure 4-1: Comparison of observed streamflow, original simulated streamflow, and modified simulated streamflow (following precipitation assessment).

4.1.2 Indicators of Hydrologic Alteration

To further ensure the model accurately simulated peak flow events (flood days) in the watershed, the Indicators of Hydrologic Alteration (IHA) tool was used to visualize the observed and simulated streamflow. The observed streamflow had a total of 560 Extreme Low Flow days, 3,551 Low Flow days, and 741 High Flow Pulse days (Figure 4-2a), whereas the simulated streamflow had a total of 0 Extreme Low Flow days, 4,110 Low Flow days, and 846 High Flow Pulse days (Figure 4-2b).

In addition to low flow days and high pulse days, the model was found to effectively simulate the observed July 2010, September 2018, March 2019, May 2019, and September 2019 flood events in the watershed (Figure 4-2). For example, the maximum observed daily streamflow of the July 2010 Action flood event was 110.2 m^3/s (Figure 4-2a), whereas the

simulated streamflow was 113.5 m^3/s (Figure 4-2b). During the September 2018 Action flood event, maximum observed daily streamflow was 85.5 m^3/s, whereas maximum simulated streamflow was 112.3 m^3/s. Similarly, the maximum observed and simulated March 2019 daily peak streamflow were 194.5 m^3/s and 190.7 m^3/s, and the September 2019 peak streamflow were 176.4 m^3/s and 186.6 m^3/s, respectively. From this analysis, the model was found to accurately simulate daily peak streamflow, hence flood days, at the outlet of the watershed.

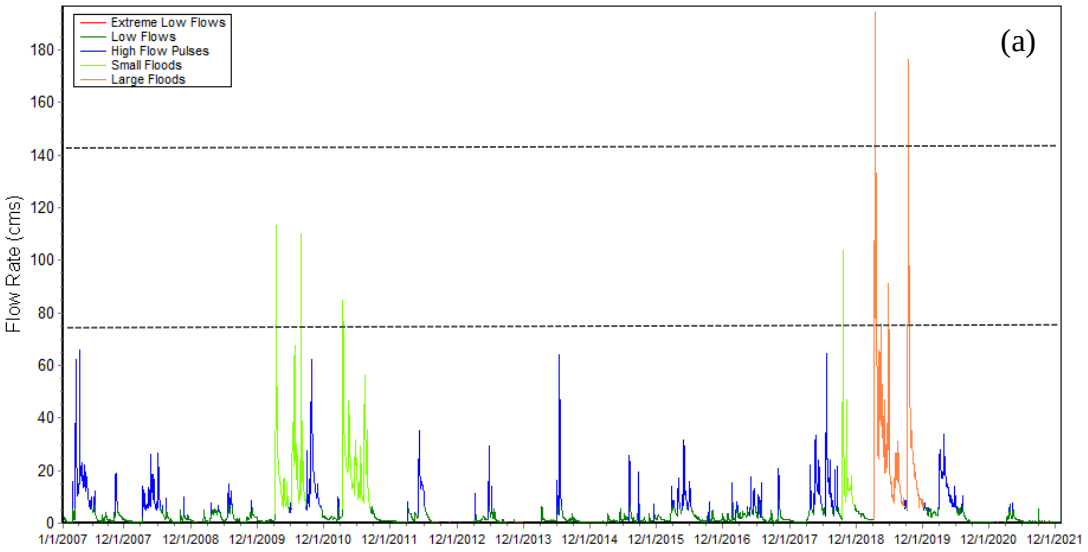

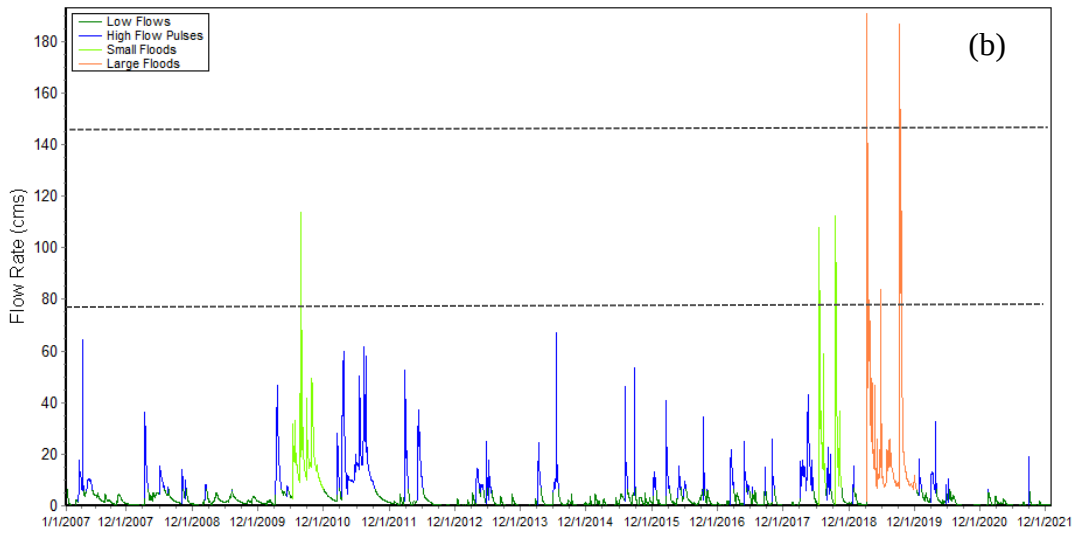

Figure 4-2: (a) Observed streamflow and (b) simulated streamflow with Action Flood Stage (78 m^3/s) and Minor Flood Stage (144 m^3/s) from the Indicators of Hydrologic Alterations tool.

4.1.3 Calibrated and Validated SWAT Model

Statistical indices and soft, qualitative data were evaluated regarding the performance of the model. Observed daily streamflow data from the watershed outlet was compared with simulated daily streamflow to ensure the calibrated model accurately represented the watersheds' hydrologic characteristics. The soft data value of ET was achieved with an average annual watershed value of 608.0 mm (Paul et al., 2016). Similarly, the percentage of baseflow as streamflow was within the expected range at 27% (USGS, 2003).

In general, the nineteen calibrated and validated parameters, as well as the manual addition of missed precipitation data, allowed the simulated streamflow to match well with the observed streamflow data, except for several high-flow events (e.g., March 2010 and March 2011; Figure 4-3). These findings are similar to previous studies conducted across different parts of the world where the researchers have found inconsistencies in SWAT model performance under extreme flow conditions (e.g., Oeurng et al., 2011; Qui & Wang, 2013; Rajib et al., 2016,

Rajib et al., 2016a; Wang et al., 2008). For example, in a study conducted in the Upper Red River of the North Basin, Rahman et al., (2014) found the SWAT model to under-predict peak flows as a result of spring snowmelt.

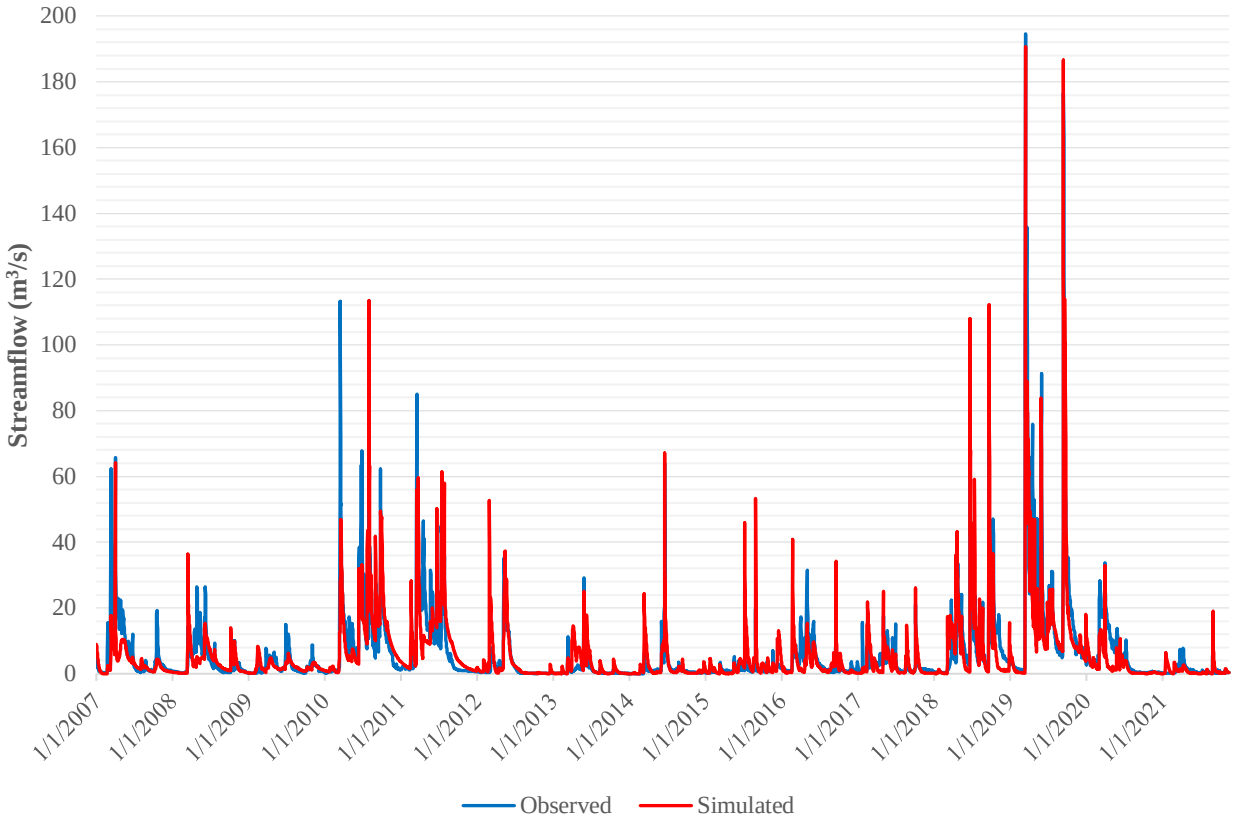

Figure 4-3: Comparison of observed and simulated daily streamflow for Skunk Creek watershed during the calibration (2007-2018) and validation (2019-2021) period.

However, in general, the simulated streamflow resulted in acceptable objective function, or model performance, statistics. The daily NSE ranged from 0.595 to 0.790, the PBIAS ranged from -2.588 to 25.808, and the RSR ranged from 0.636 to 0.458 during the calibration and validation period. Validation statistics generally demonstrated model performance improvement from calibration statistics, and most of the values, except PBIAS, were satisfactory (Table 4-1; Moriasi et al., 2007). Although the SWAT model performed reasonably well according to the NSE and RSR, a high positive daily PBIAS during the validation period is concerning. This high

positive PBIAS indicates that the total volume of flow was overestimated at the watershed outlet (Krause et al., 2005). The overestimation of daily streamflow during the validation period (2019-2021) could be attributed to 2019 having the maximum observed annual precipitation during the study period. Additionally, it could be due to the issue of frequent snowmelt flash flows during spring in the study area and the prevalence of low-flow conditions during the rest of the year. Given the inherent complexity of simulating daily flows and the frequency of spring snowmelt, it can be said that the model performed satisfactorily during the calibration and validation time periods.

Table 4-1: Comparison statistics of daily, monthly, and annual simulated streamflow in Skunk Creek watershed to observed streamflow during the calibration and validation periods.

	Calibration (2007-2018)			Validation (2019-2021)		
	NSE	PBIAS	RSR	NSE	PBIAS	RSR
Daily	0.595	-2.588	0.636	0.790	25.808	0.458
Monthly	0.681	-2.659	0.562	0.874	25.774	0.350
Annual	0.929	-2.588	0.256	0.887	25.671	0.274

4.2 Baseline and Tile Drainage Scenarios

4.2.1 Spatial Autocorrelation

The HRUs randomly selected for tile drainage scenario analysis were verified to be spatially random by using the Spatial Autocorrelation (Moran's I) tool to obtain the z-score and p-value, or spatial pattern, of the selection. When comparing across all tile drainage scenarios (Scenario 1 to Scenario 5) the Moran's Index ranged from 0.014 to 0.053, the z-score ranged

from 0.250 to 0.879, and the p-value ranged from 0.803 to 0.379. Due to these statistics, the respective spatial pattern of each tile drainage scenario was determined to be random and can be viewed below in Table 4-2 and Figure 4-4.

Table 4-2: Spatial autocorrelation statistics and respective spatial pattern for modeled tile drainage scenarios.

	Scenario 1	**Scenario 2**	**Scenario 3**	**Scenario 4**	**Scenario 5**
Moran's Index	0.014	0.023	0.037	0.045	0.053
z-score	0.250	0.398	0.626	0.761	0.879
p-value	0.803	0.691	0.531	0.447	0.379
Spatial Pattern	Random	Random	Random	Random	Random

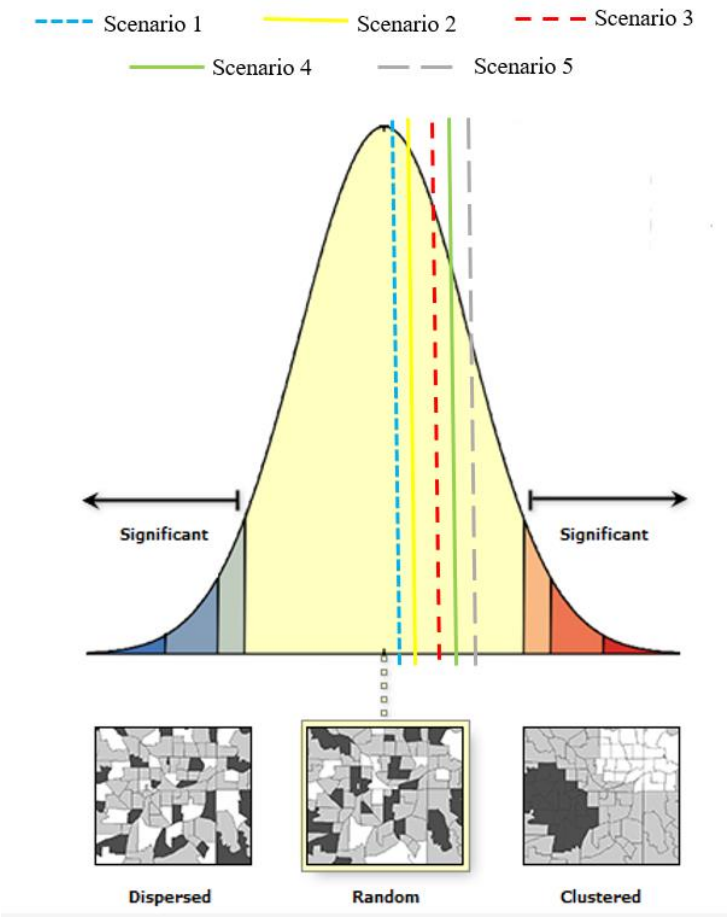

Figure 4-4: Global Moran's Index distribution (z-score) for tile drainage scenarios, indicating spatial randomness (Adapted from ESRI).

4.2.2 Watershed Water Balance

When observing the watersheds' average annual water budget for the baseline scenario during the entire 2007-2021 study period, evapotranspiration (ET) had the highest share, followed by surface runoff, percolation, groundwater flow, lateral soil flow, and deep aquifer recharge. As tile drainage was introduced in the watershed, surface runoff, groundwater flow, deep aquifer recharge, and percolation decreased, whereas lateral soil flow, tile flow, ET, and water yield all increased. More specifically, from the baseline scenario (0.0% tile-drained agricultural land) to scenario 5 (75% tile-drained agricultural land), surface runoff decreased by 17.80 mm/year, groundwater flow decreased by 14.77 mm/year, deep aquifer recharge decreased

by 1.45 mm, and percolation decreased by 28.93 mm/year. In contrast, lateral soil flow increased by 10.32 mm/year, tile flow increased by 35.25 mm/year, ET increased very slightly by 1.2 mm/year, and water yield increased by 12.97 mm/year (Table 4-3). These results are similar to those observed by Golmohammadi et al., (2017) in Canagagigue Creek watershed; as tile drainage was introduced, surface runoff and groundwater flow decreased, whereas lateral soil flow increased. Similarly, in a field study by Rahman et al., (2014) in the Upper Red River of the North Basin, as tile drainage was introduced in the field, surface runoff decreased, and total water yield increased.

Table 4-3: Average annual watershed water budget (mm) of the baseline and tile drainage scenarios.

Hydrologic Component	Baseline	Scenario 1	Scenario 2	Scenario 3	Scenario 4	Scenario 5
Precipitation	727.8					
Surface Runoff	75.41	72.19	69.48	66.69	61.92	57.61
Lateral Soil Flow	4.480	5.900	8.130	9.920	12.27	14.80
Tile Flow	0.000	6.410	12.36	18.49	27.02	35.25
Groundwater Flow	26.08	23.67	20.73	18.05	14.79	11.31
Deep Aquifer Recharge	2.510	2.260	1.980	1.720	1.390	1.060
Percolation	50.16	45.29	39.66	34.35	27.87	21.23
Evapotranspiration	608.0	608.2	608.4	608.6	608.9	609.2
Water Yield	106.02	108.22	110.73	113.18	116.04	118.99

Similarly, upon calculation of the percentage change between the baseline scenario and scenario 5, surface runoff had a percent decrease of approximately 24%, groundwater flow had a percent decrease of approximately 57%, deep aquifer recharge had a percent decrease of

approximately 58%, and percolation had a percent decrease of approximately 58%. In contrast when comparing the baseline scenario and scenario 5, lateral soil flow had a percent increase of approximately 230%, tile flow had a percent increase of 0.00% (as the initial value of tile flow was 0 mm), ET had a percent increase of approximately 0.20%, and water yield had a percent increase of approximately 12% (Table 4-4).

Table 4-4: Percentage change of average annual watershed water budget (mm) between baseline scenario and tile drainage scenarios.

Hydrologic Component	Baseline - Scenario 1	Baseline - Scenario 2	Baseline - Scenario 3	Baseline - Scenario 4	Baseline - Scenario 5
Precipitation	727.8				
Surface Runoff	-4.27%	-7.86%	-11.6%	-17.9%	-23.6%
Lateral Soil Flow	31.7%	81.5%	121%	174%	230%
Tile Flow	0.00%	0.00%	0.00%	0.00%	0.00%
Groundwater Flow	-9.24%	-20.5%	-30.8%	-43.3%	-56.6%
Deep Aquifer Recharge	-9.96%	-21.1%	-31.5%	-44.6%	-57.8%
Percolation	-9.71%	-20.9%	-31.5%	-44.4%	-57.7%
Evapotranspiration	0.03%	0.07%	0.10%	0.15%	0.20%
Water Yield	2.10%	4.44%	6.75%	9.45%	12.2%

The average annual simulated tile flow in Skunk Creek watershed ranged from 6.41 mm in Scenario 1 (15% tile-drained agricultural land) to 32.25 mm in Scenario 5 (75% tile-drained agricultural land) (Table 4-3). These results indicate that the contribution of tile flow ranges from 0.88% to 4.84% of annual precipitation and from 5.92% to 29.62% of annual water yield in the watershed (Table 4-5). In general, the targeted ranges of 2.11% to 10.56% of total annual

precipitation and 4.88% to 24.40% of annual water yield were met (Arenas Amado et al., 2017; Boles, 2013; Golmohammadi et al., 2017; King et al., 2015; Macrae et al., 2007; Moloney, 2016; Moriasi et al., 2013; Rahman et al., 2014; Schilling et al., 2019; Sloan et al., 2016; Thomas, 2015). The percentage of precipitation as tile flow in Scenarios 1 and 2 were slightly lower than the expected range, and the percentage of tile flow as water yield in Scenario 5 was slightly higher than the expected range (Table 4-5). However, given the scale of Skunk Creek watershed, as well as the variability in drainage distribution, density, and local soil types, it can be inferred that the simulated tile flow is an accurate representation of tile flow in the study region of the Midwest (Boles, 2013; Schilling et al., 2019).

Table 4-5: Percentage of average annual tile flow as precipitation and as water yield in Skunk Creek watershed for the baseline and tile drainage scenarios.

	Baseline	**Scenario 1**	**Scenario 2**	**Scenario 3**	**Scenario 4**	**Scenario 5**
Tile Flow / Precipitation	0.00	0.88%	1.70%	2.54%	3.71%	4.84%
Tile Flow / Water Yield	0.00	5.92%	11.16%	16.33%	23.29%	29.62%

Additional analysis of simulated streamflow demonstrated the contribution of tile flow, as well as the redistribution of surface runoff, groundwater flow, and lateral soil flow, to the average annual water yield. When comparing the baseline scenario to scenario 5, as tile drainage was introduced into the watershed, surface runoff contributed 23% less to the average annual water yield while groundwater flow contributed 15% less. In contrast, lateral soil flow contributed 8% more to the average annual water yield, while tile flow contributed 30% more (Figure 4-5). These results are similar to those observed by Golmohammadi et al., (2017); when comparing a scenario with no tile drainage to a scenario with 65% tile drainage, the contribution of surface runoff and groundwater flow to average annual water yield decreased, whereas the contribution of lateral flow and tile flow to average annual water yield increased.

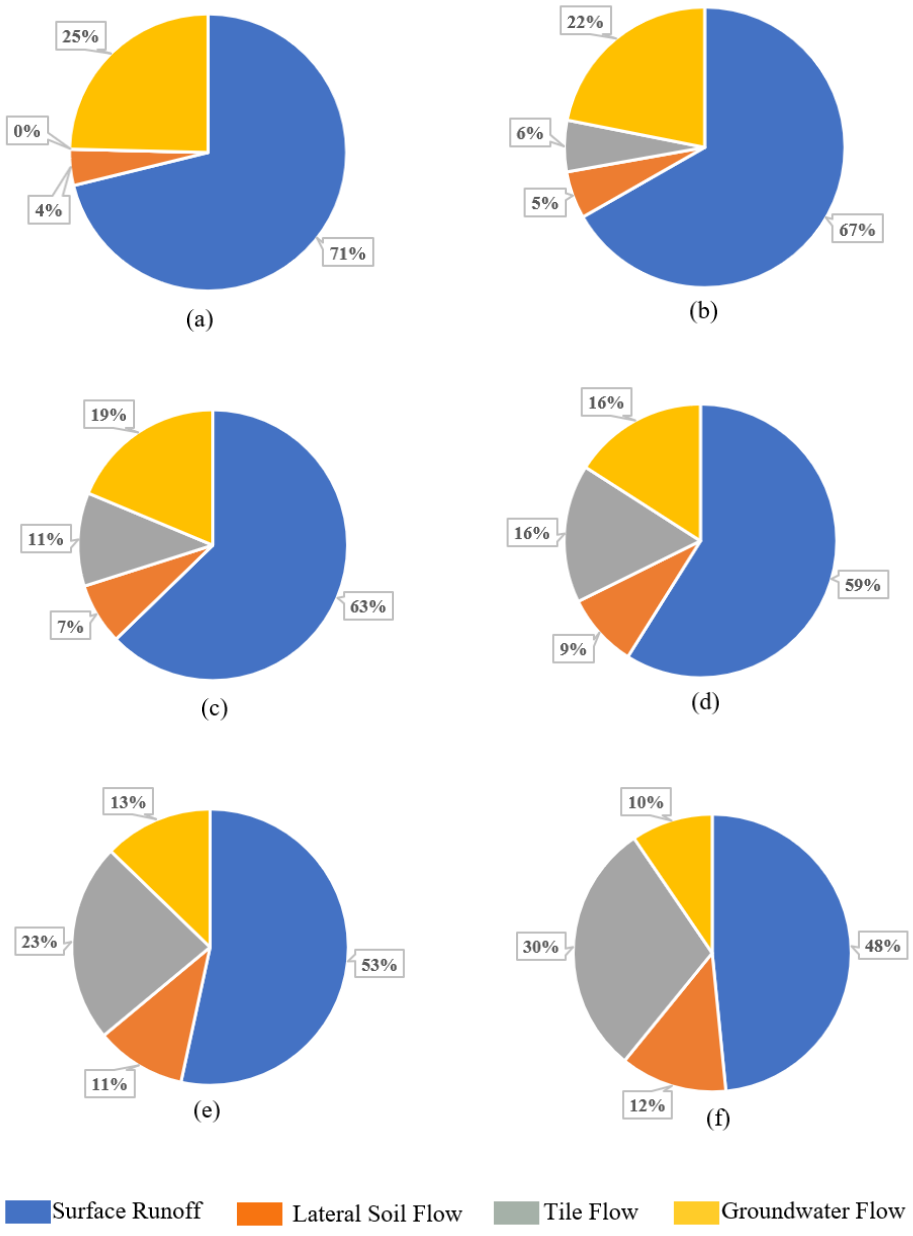

Figure 4-5: Average annual water yield budgets for 2007-2021 study period in Skunk Creek watershed, where: (a) Baseline Scenario, (b) Scenario 1, (c) Scenario 2, (d) Scenario 3, (e) Scenario 4, and (f) Scenario 5.

Further investigation of the contribution of tile flow to streamflow showed a pronounced seasonality and varied from month to month (Figure 4-6). It is interesting to note that high tile flows occurred from March to October, whereas almost no tile flow occurred from November to

February, or the colder, late fall and winter months. These results are similar to those obtained by Schilling et al., (2019) for a study conducted in Iowa. The authors found that the sources of water yield varied from month to month, with tile flow being minimal in the colder months (February) and increasing in the late spring and early summer months (March to June).

The late spring and early summer months are dominant periods of tile flow in the Midwestern United States due to a combination of factors such as high spring precipitation, snowmelt, and decreased ET (Ikenberry et al., 2014). The slight spike in simulated tile flows from August to October could be attributed to the senescence of corn and soybean crops during that time frame, leading to replenished soil moisture conditions; thus, the resumption of tile flows (Schilling et al., 2019).

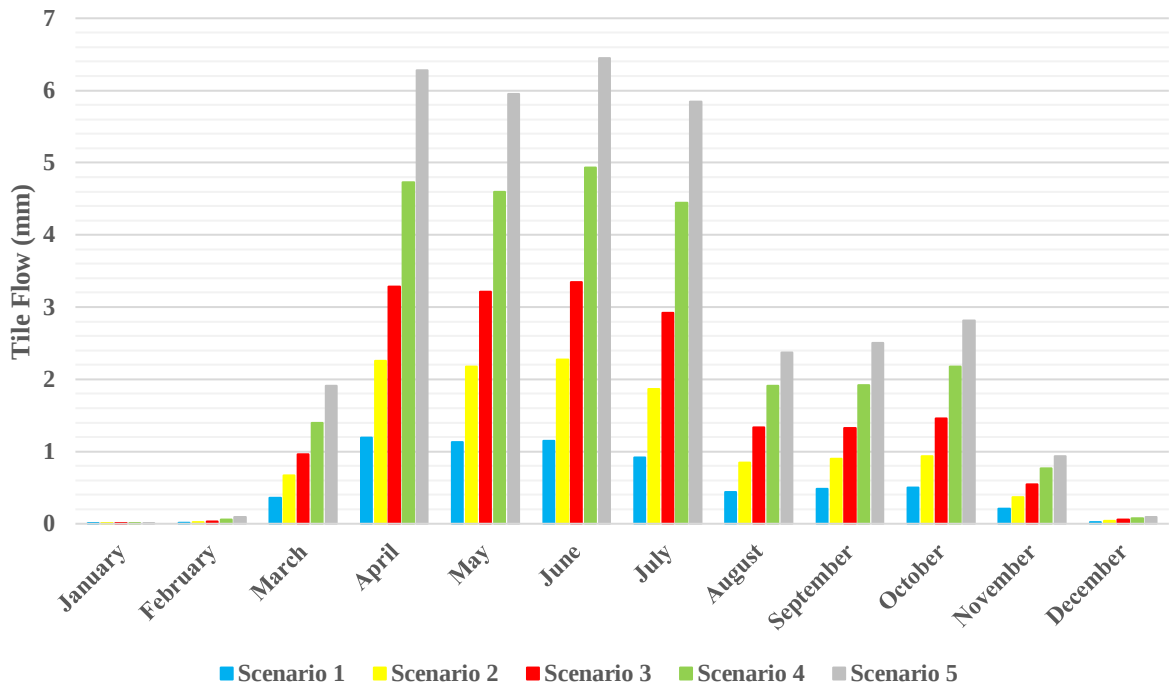

Figure 4-6: Average tile flow for each month of the year for the 2007-2021 study period for tile drainage scenarios.

A comparison of scenarios to study the impact of varied extents of tile-drained agricultural land on streamflow showed that the larger the percentage of tile-drained, agricultural

land in the watershed, the larger the corresponding depth of tile flow. Scenario 5, with 75% tile-drained agricultural land, resulted in the largest depth of flow, whereas scenario 1, with 15% tile-drained agricultural land, resulted in the smallest depth of tile flow during the study period. The flows varied temporally over the 2007-2021 study period, with the highest variation among tile flow depths occurring in years with the highest flows (e.g., 2010, 2011, 2018, and 2019) (Figure 4-7).

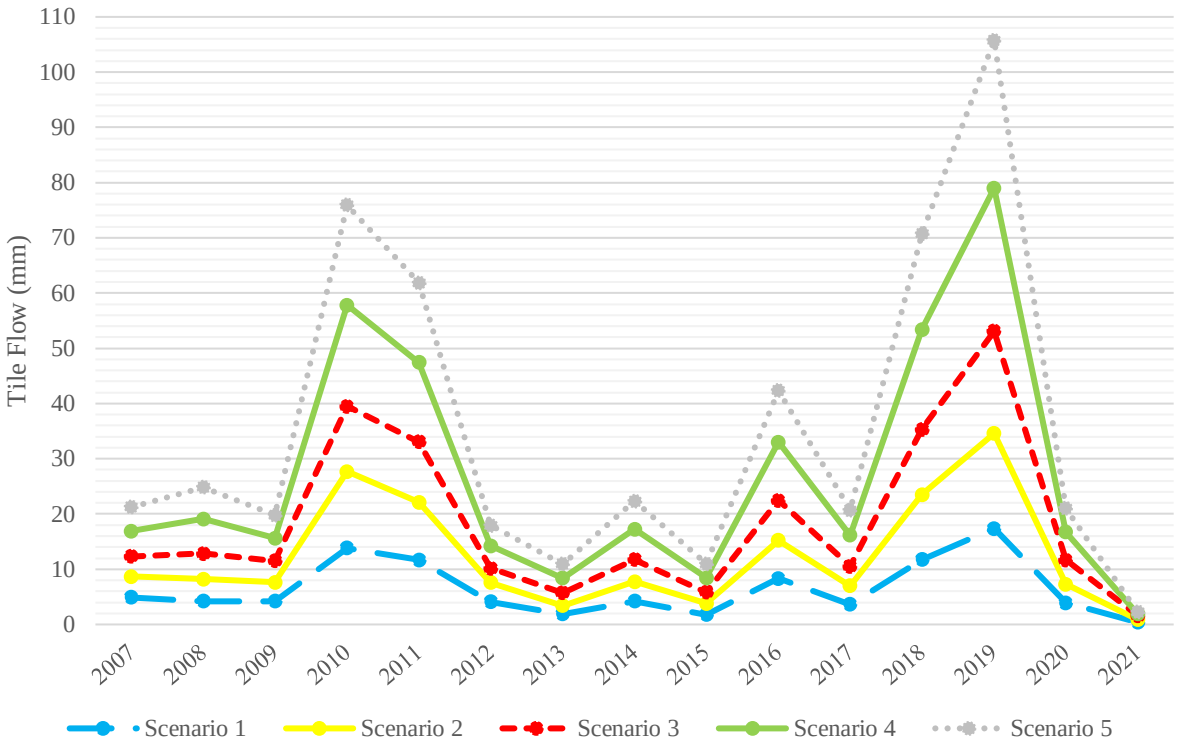

Figure 4-7: Annual tile flow showing the impact of increasing tile-drained agricultural land in the watershed during the 2007-2021 study period.

4.3 Flood Assessment

4.3.1 Baseline Scenario

Analysis indicated that the total annual precipitation during the baseline scenario (i.e., 2007 to 2021), that contains no tile drainage, varied from approximately 461 mm (2020) to 1182 mm (2019), while observed daily streamflow varied from approximately 0.04 m^3/s to 195 m^3/s,

with an average of 5.84 m^3/s during the study period. In comparison, simulated streamflow varied from approximately 0.01 m^3/s to 190.7 m^3/s, with an average of 5.44 m^3/s during the study period (Figure 4-8).

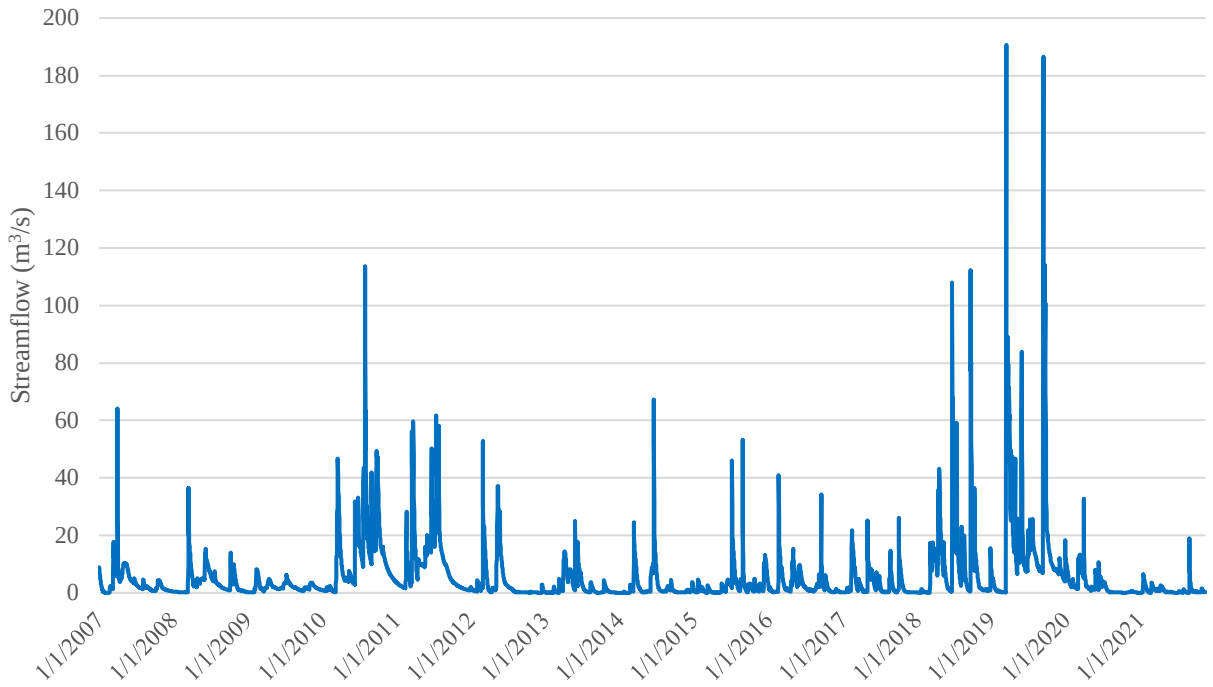

Figure 4-8: Simulated daily streamflow for the baseline scenario.

Daily simulated streamflow in the baseline scenario resulted in 22 flood days. Of the flood days, 20 were Action flood events (i.e., streamflow greater than 78 m^3/s), while two (2) were Moderate flood events (i.e., streamflow greater than 184 m^3/s) (Table 4-6). Flood events ranged from an average daily streamflow of 78.3 m^3/s on March 24, 2019, to 190.7 m^3/s on March 14, 2019. There were both zero Minor flood days and zero Major flood days in the baseline scenario. Simulated flood events occurred in July 2010, June 2018, September 2018, March 2019, and September 2019. It is important to note that the July 2010, September 2018, March 2019, and September 2019 events were observed flood events and were simulated by the model, hence adding to the validity of the model.

4.3.2 Tile Drainage Scenarios

When 15% of the agricultural land in the watershed was simulated with tile drainage (Scenario 1), daily simulated streamflow ranged from approximately 0.01 m^3/s to 190.6 m^3/s, with an average value of 5.56 m^3/s over the study period. While the minimum streamflow was not impacted when compared to the baseline scenario, maximum streamflow decreased by 0.10 m^3/s, and average streamflow increased by approximately 0.12 m^3/s during the study period. Daily simulated streamflow resulted in 19 flood days (three less than the baseline scenario). Of the flood days, 17 were Action flood events, while two (2) were Moderate flood events (Table 4-6). Flood days ranged from an average daily flow of 78.3 m^3/s on September 22, 2018, to 190.6 m^3/s on September 12, 2019. There were both zero Minor flood events and zero Major flood events with tile drainage simulated in 15% of the watershed agricultural land.

When 30% of the agricultural land in the watershed was simulated with tile drainage (Scenario 2), daily simulated streamflow ranged from approximately 0.01 m^3/s to 194.8 m^3/s, with an average of 5.69 m^3/s over the study period. When compared to the baseline scenario, the minimum study period streamflow was not impacted by tile drainage, however, the maximum streamflow increased by approximately 4.10 m^3/s. Similarly, the average study period streamflow increased by approximately 0.25 m^3/s. Daily simulated streamflow resulted in 20 flood days (two less than the baseline scenario). Of the flood days, 18 were Action flood events, while two (2) were Moderate flood events (Table 4-6). Flood events ranged from an average daily flow of 78.3 m^3/s on May 30, 2019, to 194.8 m^3/s on September 12, 2019. There were zero Minor flood events and zero Major flood events with tile drainage simulated in 30% of the watershed agricultural land.

When 45% of the agricultural land in the watershed was simulated with tile drainage (Scenario 3), daily simulated streamflow varied from 0.02 m^3/s to 194.3 m^3/s, with an average of 5.82 m^3/s during the study period. When compared to the baseline scenario, minimum streamflow increased by approximately 0.01 m^3/s, maximum streamflow increased by 3.60 m^3/s, and average streamflow increased by 0.38 m^3/s. Daily simulated streamflow resulted in 20 flood days (two less than the baseline scenario). It is important to note that the 20 simulated flood days slightly differ from the flood days simulated by Scenario 2. Of the flood days, 18 were Action flood events, while two (2) were Moderate flood events (Table 4-6). Flood events ranged from a daily average streamflow of 78.1 m^3/s on September 22, 2018, to 194.3 m^3/s on September 12, 2019. There were zero Minor flood events and zero Major flood events with tile drainage simulated in 45% of the watershed agricultural land.

When 60% of the agricultural land in the watershed was simulated with tile drainage (Scenario 4), daily simulated streamflow values ranged from 0.01 m^3/s to 190.9 m^3/s, with an average of 5.97 m^3/s during the study period. Values of minimum streamflow did not differ from the baseline scenario. However, maximum streamflow increased by 0.20 m^3/s and average streamflow increased by 0.53 m^3/s. Daily simulated streamflow resulted in 20 flood days (two less than the baseline scenario). It is important to note that the dates of the 20 simulated flood days differ slightly from both the flood days simulated in Scenario 2 and Scenario 3. Of the flood days, 18 were Action flood events, while two (2) were Moderate flood events (Table 4-6). Flood events ranged from a daily average streamflow of 79.5 m^3/s on March 22, 2019, to 190.9 m^3/s on September 12, 2019. During the study period, there were both zero Minor flood events and zero Major flood events with 60% of the agricultural land simulated with tile drainage.

When 75% of the agricultural land in the watershed was simulated with tile drainage (Scenario 5), daily streamflow values ranged from 0.01 m^3/s to 193.1 m^3/s, with an average of 6.12 m^3/s during the 2007-2021 study period. The minimum streamflow did not vary from the baseline scenario. However, maximum streamflow increased by 2.40 m^3/s and average streamflow increased by 0.68 m^3/s. Daily simulated streamflow resulted in 16 flood days (six less than the baseline scenario). Of the simulated flood days, 14 were Action flood events, while two (2) were Moderate flood events (Table 4-6). Of the flood events, streamflow ranged from 79.6 m^3/s on September 23, 2019, to 193.1 m^3/s on March 14, 2019. During the study period, zero Minor flood events and zero Major flood events resulted from 75% tile-drained agricultural land. It is interesting to note that from the baseline scenario to Scenario 5, the total number of Action flood days decreased, whereas the number of Moderate flood days remained the same across all scenarios (Table 4-6).

Table 4-6: Total number of Action Flood days (streamflow greater than 78 m^3/s) and Moderate Flood days (streamflow greater than 144 m^3/s) during the 2007-2021 study period for the baseline and tile drainage scenarios.

Scenario	Action Flood Days	Moderate Flood Days	Total Flood Days
Baseline	20	2	22
Scenario 1	17	2	19
Scenario 2	18	2	20
Scenario 3	18	2	20
Scenario 4	18	2	20
Scenario 5	14	2	16

Further analysis of the presence of flood days were found to vary by date across the baseline and tile drainage scenarios. During the 2007-2021 study period, twelve flood events

were simulated across all scenarios (i.e., baseline scenario to Scenario 5). These events occurred on July 30-31, 2010; June 21, 2018; September 20, 2018; March 14-15, 2019; September 12-14, 2019; September 16, 2019; and September 19, 2019; and September 21, 2019. Two flood days (March 24, 2019, and June 28, 2019) were simulated by the baseline scenario, but were not simulated by any tile drainage scenario. In contrast, three flood days (May 29-30, 2019, and September 23, 2019) were not simulated by the baseline scenario but were simulated by various tile drainage scenarios (Table 4-7). It is important to note that the variability by date of flood days is relative to Action flood events, whereas the date of the two Moderate flood events remains the same across all scenarios.

Table 4-7: Simulated flood days and respective values of streamflow (m^3/s) during the 2007-2021 study period, where --- indicates the absence of a flood day.

Date	Baseline	Scenario 1	Scenario 2	Scenario 3	Scenario 4	Scenario 5
7/30/2010	114	113	112	111	109	108
7/31/2010	87.0	86.0	85.2	84.4	82.8	81.5
6/21/2018	108	109	110	111	116	115
9/20/2018	112	112	113	113	114	112
9/22/2018	80.2	78.3	80.2	78.1	---	---
3/14/2019	191	190	190	189	188	193
3/15/2019	90.7	95.6	93.9	92.3	88.5	89.1
3/16/2019	87.3	87.3	84.3	81.4	80.0	---
3/21/2019	89.0	---	---	81.4	---	---
3/22/2019	---	84.1	81.5	---	79.5	---
3/23/2019	79.5	---	---	78.6	---	---
3/24/2019	78.3	---	---	---	---	---

5/28/2019	83.9	---	---	---	---	---
5/29/2019	---	---	83.2	89.5	91.6	95.0
5/30/2019	---	---	78.3	83.9	86.4	90.0
9/12/2019	187	191	195	194	191	187
9/13/2019	121	123	123	122	120	116
9/14/2019	96.1	96.1	94.5	92.8	90.5	87.4
9/15/2019	86.4	86.2	83.8	82.4	80.5	---
9/16/2019	82.6	82.3	80.1	112	110	108
9/17/2019	83.9	83.7	115	---	---	---
9/18/2019	84.3	84.3	---	---	---	---
9/19/2019	114	114	106	106.3	101	100
9/21/2019	101	102	97.3	91.4	87.9	88.8
9/22/2019	88.9	90.7	87.9	87.1	83.5	---
9/23/2019	---	---	---	---	---	79.6

To further examine the relationship between tile drainage and downstream flood days, several properties were analyzed, including precipitation, the distribution of tile-drained HRUs in the watershed, and the respective soil types of the tile-drained HRUs. The total precipitation received by the watershed during the first day of each flood event in the baseline scenario is shown below, in Table 4-8. It is important to note that each daily flood event corresponds to a precipitation event greater than 300 mm/day, except for the May 2019 flood event. The day

before the start of the May 2019 Action Flood event, 94.7 mm of precipitation fell on the watershed, causing wet antecedent moisture conditions.

Table 4-8: Total daily watershed precipitation and corresponding flood flow for the first day of simulated flood events in the baseline scenario.

Date	Total Watershed Precipitation (mm)	Streamflow (m^3/s)
7/30/2010	315.6	114
6/21/2018	381.3	108
9/20/2018	460.6	112
3/14/2019	313.3	191
5/28/2019	75.00	83.9
9/12/2019	406.2	187

In addition to daily precipitation, the distribution of randomly selected tile-drained HRUs were analyzed. As a reminder, Subbasin 1 is located the furthest away from the watershed outlet, whereas Subbasin 8 contains the watershed outlet. In all tile-drainage scenarios, Subbasin 1 was found to contain the largest percentage of tile-drained agricultural land in the watershed. Additionally, the percentage of each subbasin simulated with tile drainage never decreases, and generally increases across all tile drainage scenarios (Table 4-9).

Table 4-9: Respective percent of watershed agricultural area simulated with tile drainage during scenario analysis.

	Scenario 1	**Scenario 2**	**Scenario 3**	**Scenario 4**	**Scenario 5**
Subbasin 1	3.88%	8.42%	12.70%	15.47%	19.00%
Subbasin 2	1.05%	2.90%	6.40%	9.58%	12.99%
Subbasin 3	1.96%	2.60%	4.19%	5.86%	7.49%
Subbasin 4	0.93%	3.43%	6.09%	7.60%	10.66%

Subbasin 5	1.61%	2.25%	2.41%	7.62%	9.78%
Subbasin 6	2.14%	3.82%	3.82%	3.92%	3.92%
Subbasin 7	2.25%	2.46%	3.01%	3.85%	4.50%
Subbasin 8	1.46%	4.42%	6.49%	6.49%	6.74%
Total	15.28%	30.31%	45.12%	60.39%	75.09%

Finally, the composition of the soil types in the tile drainage scenarios were analyzed. In all tile drainage scenarios, Hydrologic Soil Group B accounted for the greatest percentage of tile-drained agricultural HRUs (Table 4-10). It is interesting to note that in Scenario 1, group D soils were the second largest tile-drained soil; however, following Scenario 2, group C soils became the second largest tile-drained soil.

Table 4-10: Percentage of each soil group in tile-drained agricultural HRUs, as simulated in scenario analysis.

Hydrologic Soil Group	Scenario 1	Scenario 2	Scenario 3	Scenario 4	Scenario 5
A	0.00%	0.00%	0.00%	0.00%	0.74%
B	72.4%	74.0%	74.8%	75.0%	78.1%
C	10.9%	16.4%	19.3%	19.9%	17.1%
D	16.7%	9.61%	5.98%	5.09%	4.10%

The function of tile drainage systems in downstream peak flood flows were found to differ across studied events. The first observed impact of tile drainage systems on downstream flooding can be interpreted from the July 2010 Action flood event (Figure 4-9). On the first day of the flood event, a total of 315.6 mm of precipitation fell on the watershed. During the event, water was able to infiltrate into the soil profile more readily (due to increased subsurface storage from tile drainage systems), causing a decrease in surface runoff. From the baseline scenario (no

tile-drained agricultural land) to scenario 5 (75% tile-drained agricultural land), it was observed that the larger the area of tile-drained agricultural land, the larger the reduction in peak runoff, hence, flood flows. These results are similar to those obtained by Sloan, (2013); when observing flood flows at the catchment scale, the addition of drainage systems was found to reduce the amount of surface runoff entering the stream, therefore, decreasing the hydrograph peak. Similarly, in a field study by Rahman et al., (2014), extensive drainage was found to decrease the magnitude of large peak flows.

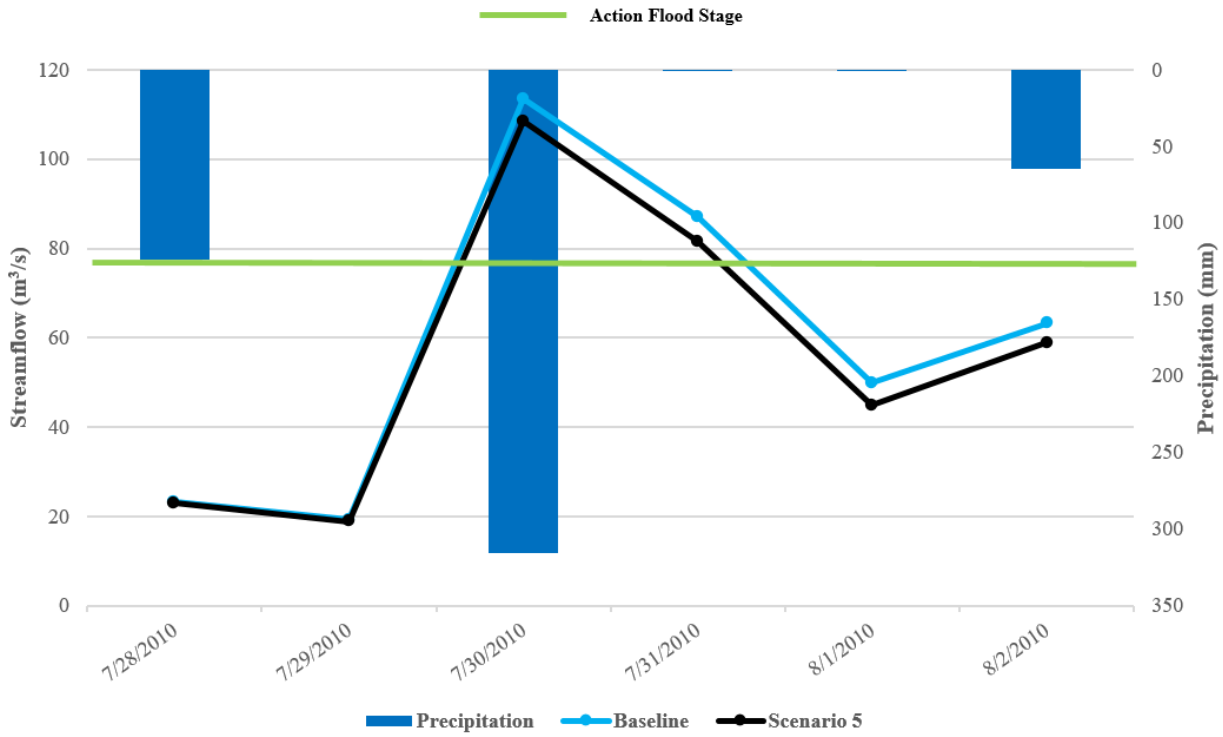

Figure 4-9: July 2010 Action Flood event for Baseline Scenario and Scenario 5.

An alternative, contrasting impact of tile drainage and daily downstream flood events is represented by the May 2019 flood event. The May 2019 flood event is unique due to the antecedent moisture conditions of the watershed. It is important to note that May 2019 was a wet month during the study period, with the watershed receiving slightly over 874 mm of total precipitation. The day before the Action flood event (May 27, 2019) a total of 94.7 mm of

precipitation fell on the watershed. The following day, (May 28, 2019), 75 mm of precipitation fell on the watershed. When considering the baseline scenario, it can be inferred that the day of the flood event, the soil moisture content was high (due to the occurrence of the precipitation event the proceeding day). As the soil moisture content was high from the previous rainfall event, the occurrence of another medium-sized precipitation event caused surface runoff to be the primary mechanism of water transportation in the watershed. Therefore, high soil moisture content, decreased infiltration, and increased surface runoff contributed to the Action flood day on May 28, 2019, with a streamflow of 83.9 m^3/s.

In contrast, the commencement of the May 2019 Action flood event experienced a one-day delay across all tile drainage scenarios. The delay could be attributed to the increased soil water storage capacity caused by the tile drainage systems. However, as several consecutive days (May 27, 28, and 29, 2019) of total precipitation greater than 70 mm/day occurred in the watershed, the soil profile likely became saturated. The saturated soil profile likely caused both tile flow and surface runoff to occur, contributing to the delayed flood day. Additionally, a unique feature of the May 2019 Action flood event is that in contrast to the July 2010 Action flood event, the larger the area of tile-drained agricultural land, the larger the corresponding volume of daily peak streamflow (Figure 4-10).

This relationship between tile drainage and downstream flood days can be attributed to the wet antecedent moisture conditions of the watershed. The occurrence of regular precipitation events allowed both tile flow and increased surface runoff to occur due to high soil moisture content. It has been observed that during multiple, consecutive precipitation events, antecedent moisture conditions can dictate the rate at which soil storage fills, allowing for more surface runoff and higher peak flows (Skaggs et al., 1994). Therefore, during the May 2019 flood events,

it can be said that the frequent precipitation events and wet antecedent moisture conditions caused an increase in both tile flow and surface runoff to total streamflow (Skaggs et al., 1994; Sloan, 2013). Due to these discussed properties and conditions, the larger the area of tile-drained land, the larger the volume of corresponding streamflow and number of downstream flood days.

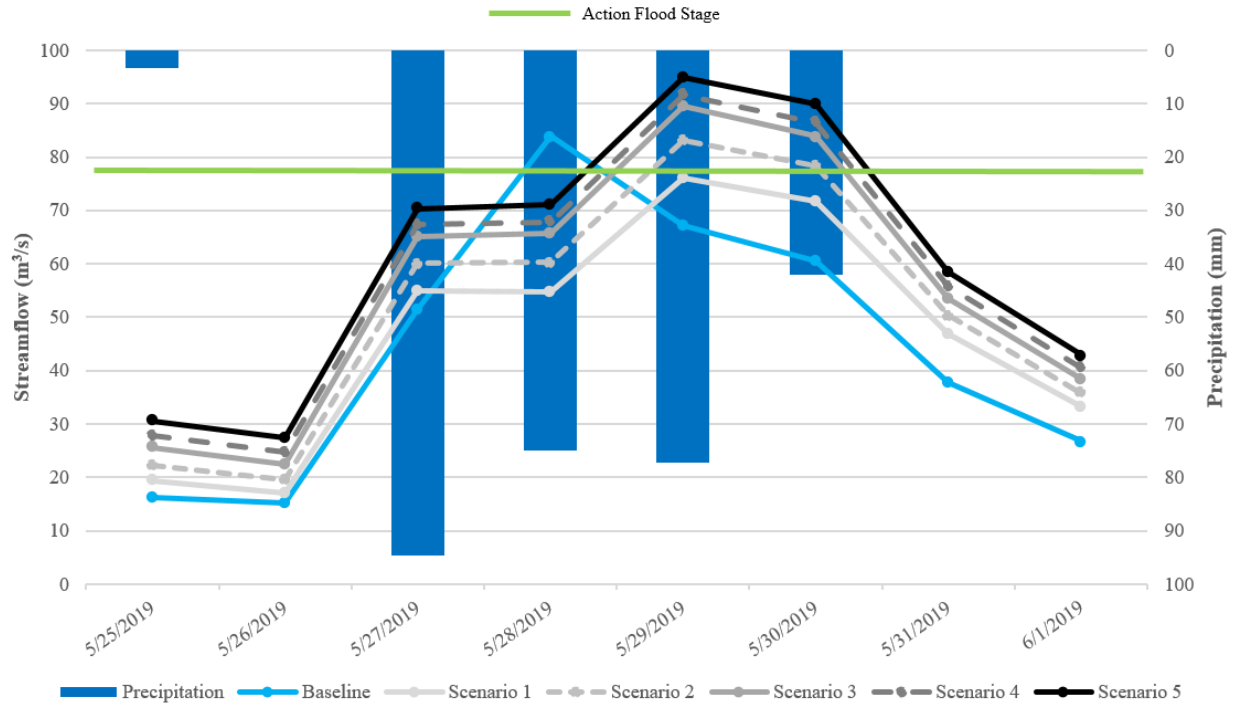

Figure 4-10: May 2019 Action Flood event for the baseline and tile drainage scenarios.

Finally, a third pattern observed by the impact of tile drainage on downstream flooding can be visualized by the September 2019 Moderate flood event and the succeeding Action flood events. It is important to note that in the baseline scenario and tile drainage scenarios, the peak streamflow of the Moderate flood event is largely unimpacted. The day of the Moderate flood event (September 12, 2019), the watershed received 406.2 mm of precipitation, and the day before (September 11, 2019), the watershed received 370.9 mm of total precipitation. Given the observed, daily precipitation, it can be inferred that surface runoff was the primary mechanism contributing to the Moderate flood day.

Following the Moderate flood day, the average daily streamflow in the baseline scenario and Scenario 1 followed similar patterns, whereas the average daily streamflow in Scenario 3 and Scenario 4 followed similar patterns. In contrast, Scenario 2 was observed to have a one-day delayed Action flood peak flow on September 17, 2019, whereas Scenario 5 was observed to have a decreased peak flow (and absence of a flood day) on September 22, 2019 (Figure 4-11). However, generally speaking, the hydrographs of the September 2019 Moderate Flood event and succeeding Action flood events follow similar patterns across the baseline and tile drainage scenarios.

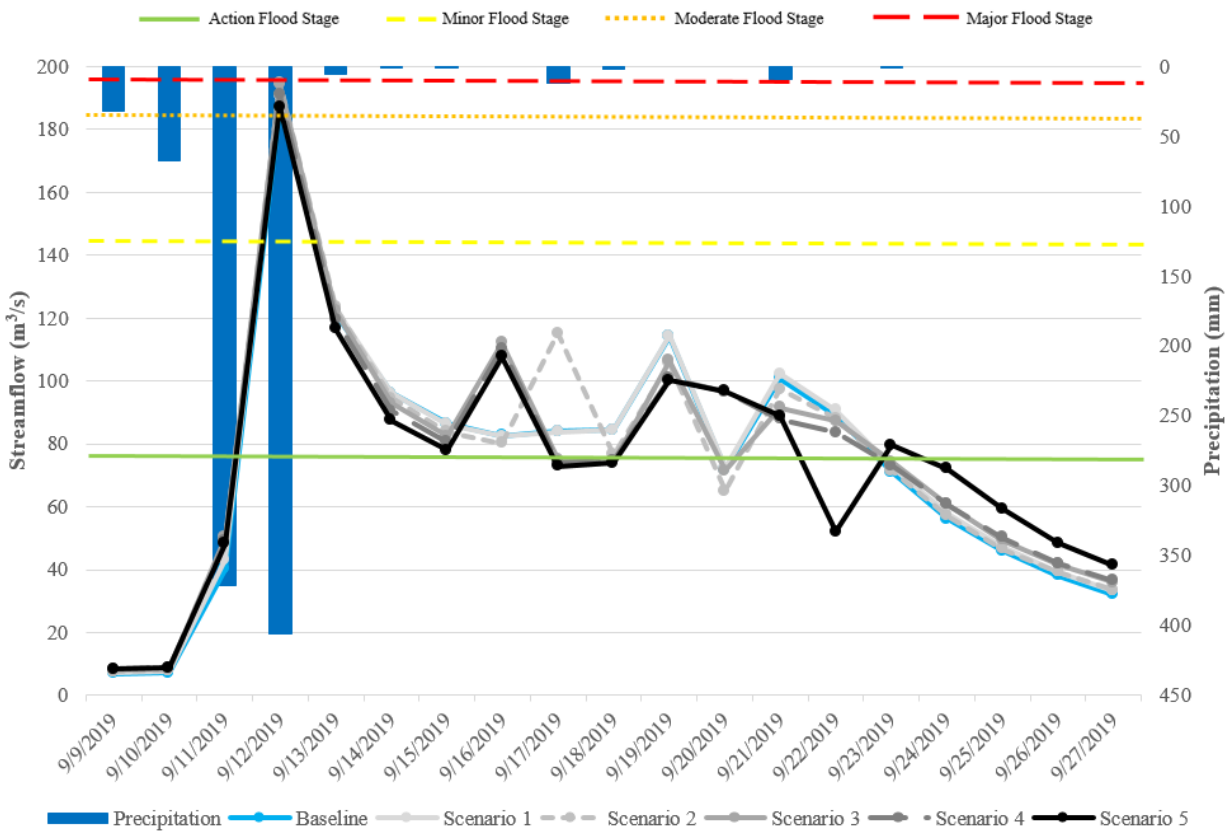

Figure 4-11: September 2019 Moderate Flood event and Action Flood events for the baseline and tile drainage scenarios.

Upon the evaluation of simulated flood days at the outlet of the watershed, precipitation and antecedent moisture conditions were determined to be the most influential factors in

inducing downstream flood days. All flood days simulated by the model occurred when daily watershed precipitation was greater than 300 mm (except the May 2019 event, which had high antecedent moisture conditions). Specific hydrologic soil group properties were not considered to be a significant contributor to daily flood events, as during large precipitation events, different soil types have similar hydrographs due to the dominance of surface runoff (Sloan, 2013). Additionally, due to the random distribution of tile-drained HRUs modeled in the tile drainage scenarios (i.e., tile-drained HRUs in each subbasin never decrease and generally increase), the drainage network distribution was not determined to be as influential in daily downstream flood flows, as distribution would remain relatively similar across all modeled scenarios.

In this study, the impact of varied extents of tile-drained agricultural land on streamflow was found to both decrease peak flows (Figure 4-9) and increase peak flows (Figure 4-10) and be primarily a function of precipitation. These results are similar to those obtained by Sloan, (2013). The author found that the reduction of peak flows caused by tile drainage at the watershed scale were not universal for all precipitation events. These results are drawn from the fact that during large storms, precipitation is either so intense or so great in volume that surface runoff is the dominant mechanism. Therefore, for some large events that cause downstream flooding, subsurface tile drainage systems have little to no impact on streamflow volumes.

Additionally, while the results indicate a reduction in total flood days due to the implementation of tile drainage, it is important to note the scale of the study. The simulated flooding occurring with the level of tile implementation in this study may be causing flash flood events which are generally noticeable at time-step smaller than daily. The analysis conducted in this study focused on daily flood events which did not account for flash flooding. An extension of this study should consider running the scenarios on sub-daily time step to capture these flash

flood events which are common in the upper Midwest. It is hoped that this study would generate discussions and interests to replicate the approach herein utilized with sub-daily time step for SWAT simulations and various implementation levels of tile drainage scenarios.

Chapter 5 - Summary, Conclusions, and Recommendations for Future Work

5.1 Summary

In this study, a SWAT model was developed for Skunk Creek watershed in southeastern South Dakota to study the potential influence of subsurface tile drainage systems on daily downstream flood events in a Midwestern, predominantly agricultural watershed. The model was calibrated and validated both by SWAT-CUP and through the manual addition and redistribution of missed, observed precipitation data. The performance of the model was evaluated using the statistics NSE (0.595 to 0.790), PBIAS (-2.588 to 25.808), and the RSR (0.636 to 0.458), which demonstrated satisfactory agreement between simulated and observed daily streamflow. The model was found to be reliable in predicting average daily streamflow at the outlet of Skunk Creek watershed, although several high spring peak flows were less satisfactory.

The calibrated and validated model was used as the baseline scenario and contained no tile drainage systems. A total of five tile drainage scenarios—ranging from 15% to 75% tile-drained agricultural land—were developed to model the influence of tile drainage systems on daily downstream flooding. The baseline scenario and tile drainage scenarios were evaluated over a study period of 18-years (2007-2021). In all tile drainage scenarios, the Kirkham and Hooghoudt Drainage Equations were used to model tile drainage in the watershed, as well as a commonly adopted drain depth and drain spacing. Similarly, the curve number was reduced in all tile-drained agricultural HRUs to model infiltrated water contributing to tile flow. The location and distribution of tile-drained agricultural HRUs were randomly selected throughout the watershed and were evaluated to ensure spatial randomness.

The hydrologic response to the installation of subsurface tile drainage in Skunk Creek watershed was evaluated through the comparison of the average annual water budget of the baseline and tile drainage scenarios. The increased installation of tile drainage systems in the watershed indicates a decrease in surface runoff, groundwater flow, deep aquifer recharge, and percolation, whereas lateral soil flow, tile flow, ET, and water yield increase. The overall contribution of average annual tile flow ranged from 6.41 mm to 32.25 mm across the five scenarios, ranging from 0.88% to 4.84% of annual precipitation and from 5.92% to 29.62% of annual water yield in the watershed. These results were validated against an expected range from previously published studies. Additionally, the analysis of seasonal variability of tile flow showed that flow primarily occurred from March to October, with little to no tile flow occurring from November to February.

The effect of increased tile-drained agricultural land suggests that tile flow seems to reduce the number of daily flood events (flood days) across the studied scenarios. However, the impact of tile drainage systems on peak downstream flood flows were found to vary by event. For example, the impact of varied extents of tile-drained agricultural land on streamflow were found to both decrease peak flows and increase peak flows, as primarily a function of precipitation and watershed antecedent moisture conditions. Large precipitation events (greater than 300 mm/day) in the watershed were found to initiate flood days with similar peak flows across all scenarios. In some instances, the increased extent of tile-drained agricultural land allowed increased infiltration and reduced surface runoff, decreasing downstream flood peak flows. In contrast, under wet antecedent moisture conditions, the increased extent of tile-drained agricultural land caused both tile flow and surface runoff to occur, from saturated soil conditions.

5.2 Conclusions

Specific conclusions of this study are as follows:

- A SWAT model was set up, calibrated, and validated, with the daily NSE ranging from 0.595 to 0.790, the PBIAS ranging from -2.588 to 25.808, and the RSR ranging from 0.636 to 0.458 during the calibration and validation time periods.
- Five tile drainage scenarios—ranging from 15% to 75% tile-drained agricultural land—were incorporated into the model, with average annual simulated tile flow ranging from 6.41 mm to 32.25 mm across the scenarios.
- Increased tile-drained agricultural land caused a decrease in surface runoff, groundwater flow, deep aquifer recharge, and percolation, as well as an increase in lateral soil flow, tile flow, ET, and water yield.
- The effect of increased tile-drained agricultural land suggests that tile flow reduces the number of daily flood events (flood days) across the studied scenarios. Large precipitation events (greater than 300 mm/day) in the watershed initiate flood days with tile drainage causing both decreases and increases in downstream peak flood flows.

5.3 Recommendations for Future Work

Given the limitations of the study, there are several recommendations for future work regarding tile drainage systems and downstream flooding, including:

1. The current SWAT model missed several peak flow (flood) events due to the difficulty of simulating snowmelt flash flows. Further evaluation of SWAT snow hydrology in the watershed water balance would improve streamflow simulation in the study watershed.

2. This study focused on flooding at the daily time step. There is a need to study tile drainage scenarios on a sub-daily time-step to capture flash flood events which are common in the upper Midwest.
3. This study evaluated tile drainage systems distributed spatially randomly throughout the watershed. Additional scenarios with tile drainage systems implemented in upland, middle, and lower watershed areas would provide additional information and relationships regarding tile drainage and downstream flooding.
4. This study evaluated a commonly adopted tile drain depth and spacing for all scenarios. The evaluation of various tile drain depth and spacing combinations could provide further insight regarding tile drainage and downstream flooding events.
5. This study focuses on the presence of flood days with respect to tile drainage scenarios. The analysis of nutrient export through and from tile drainage systems would provide valuable insight regarding the water quality impacts of tile drainage systems in relation to downstream flood days.
6. This study considered historical climatic data (2004-2021) for scenario analyses. Evaluating the effects of climate change, hence extreme precipitation events, in the watershed would provide necessary information regarding the effects of climate change on the relationship between tile drainage and downstream flooding.

It is hoped that this study would generate further discussions and interests to replicate the approach for SWAT simulations, various tile drainage scenarios, and climate change impacts, as the continued development and understanding of the contribution of tile flow to river discharge and downstream flooding is necessary.

References

Abbaspour, K. C., Rouholahnejad, E., Vaghefi, S., Srinivasan, R.,Yang, H., Klove, B. (2015). A continental-scale hydrology and water quality model for Europe: Calibration and uncertainty of a high-resolution large-scale SWAT model. *Journal of Hydrology, 524.* 733-752. http://dx.doi.org/10.1016/j.jhydrol.2015.03.027.

Ahiablame, L., Sheshukov, A. Y., Mosase, E., Hong, J. (2019). Modelling the impacts of grassland to cropland conversion on river flow regimes in Skunk Creek watershed, Upper Midwest United States. *River Research and Applications, 35*(9), 1454-1465. https://doi.org/10.1002/rra.3512.

ArcSWAT Google Groups. [mka…@umich.edu]. (2014, August 22). A manual on tile drainage? Retrieved from https://groups.google.com/g/arcswat/c/poWWA2LY4Kk.

Arnold, J., Gassman, P., King, K., Saleh, A., and Sunday, U. (1999). Validation of the subsurface tile flow component in the SWAT model, Transactions of ASAE, 99–2138.

Arnold, J. G., Youssef, M. A., Yen, H., White, M. J., Sheshukov, A.Y., Sadeghi, A. M., Moriasi, D. N., Steiner, J. L., Amatya, D. M., Skaggs, R. W., Haney, E. B., Jeong, J., Arabi, M., Gowda, P.H. (2015). Hydrological processes and model representation: impact of soft data on calibration. *Transactions of the ASABE, 58*(6). 1637–1660.

Ayivi, F. & Jha, M. K. (2018). Estimation of water balance and water yield in the Reedy Fork-Buffalo Creek Watershed in North Carolina using SWAT. *International Soil and Water Conservation Research, 6*. 203-213. https://doi.org/10.1016/j.iswcr.2018.03.007.

Bailey, R. T., Park, S., Bieger, K., Arnold, J. G., Allen, P. M. (2020). Enhancing SWAT+ simulation of groundwater flow and groundwater-surface water interactions using MODFLOW routines. *Environmental Modelling & Software, 126.* https://doi.org/10.1016/j.envsoft.2020.104660.

Blann, K. L., Anderson, J. L., Sands, G. R., Vondracek, B. (2009). Effects of Agricultural Drainage on Aquatic Ecosystems: A Review. *Critical Reviews in Environmental Science and Technology, 39.* 909-1001. DOI: 10.1080/10643380801977966.

Boles, C. M. W. (2013). *Swat Model Simulation of Bioenergy Crop Impacts in a Tile-Drained Watershed.* [Master's thesis, Purdue University]. Purdue e-Pubs.

Brazos River Authority. (n.d.). *What is flood stage?* Retrieved from https://brazos.org/About-Us/Education/Water-School/ArticleID/269.

Carlson C. G., Clay, D. E., Reese, C. L. (2016). Chapter 28: Common Fertilizers Used in Corn Production. In Clay, D.E., Carlson, C.G. Clay, S.A., Byamukama, E. (eds). iGrow corn: Corn Best Management Practices. South Dakota State University.

Cihacek L. J., Kalwar, N., Scherer, T. (2020, July). Evaluation of Soils for Suitability for Tile Drainage Performance. *NDSU Extension.* Retrieved from https://www.ag.ndsu.edu/publications/crops/evaluation-of-soils-for-suitability-for-tile-drainage-performance.

Cooke, R.A., Badiger, S., Garcia, A.M. (2001, June 21). Drainage equations for random and irregular tile drainage systems. *Agricultural Water Management, 48.* (3), 207-224. https://doi.org/10.1016/S0378-3774(00)00136-0.

Cooke, R., Chun, J. A., Christopher, K. (n.d.). Illinois Drainage Guide (Online). Department of Agricultural and Biological Engineering, University of Illinois. Retrieved from http://www.wq.illinois.edu/DG/.

Eller, D. (2015, September 13). *How do we fix Iowa's nitrate pollution?* Retrieved from desmoinesregister.com/story/money/agriculture/2015/09/13/tiling-pollution-nitrates/72103422/.

ESRI, n.d. *How Spatial Autocorrelation (Global Moran's I) works.* ArcGIS Pro. Retrieved from https://pro.arcgis.com/en/pro-app/latest/tool-reference/spatial-statistics/h-how-spatial-autocorrelation-moran-s-i-spatial-st.htm.

Fahlquist, L., & Hopkins, C. (2023, February 27). Why We Use Gage Height. USGS. Retrieved from https://waterdata.usgs.gov/blog/gage_height/.

Frankenberger, J., Boles, C., Moriasi, D. (2013). *Tile Drainage in SWAT. (Plus a little about our Lake Erie Basin projects).* [PowerPoint slides]. Department of Agricultural & Biological Engineering, Purdue University. https://graham.umich.edu/media/files/watercenter/Frankenberger_Tile-drainage-in-SWAT.pdf.

Fraser, H., Fleming, R., Eng, P. (2001). Environmental benefits of tile drainage. Prepared for: LICO. Land Improvement Contractors of Ontario. Ridgetown College, University of Guelph.

Gao, Y., Vogel, R. M., Kroll, C. N., LeRoy Poff, N., Olden, J. D. (2009). Development of representative indicators of hydrologic alteration. *Journal of Hydrology, 374*. 136-147. DOI: 10.1016/j.jhydrol.2009.06.009.

Getis, A., & Ord, J. K. (1992). The Analysis of Spatial Association by Use of Distance Statistics. *Geographical Analysis, 24*(3).

Golmohammadi, G., Rudra, R., Prasher, S., Madani, A., Youssef, M., Goel, P., Mohammadi, K. (2017). Impact of tile drainage on water budget and spatial distribution of sediment generating areas in an agricultural watershed. *Agricultural Water Management, 184.* 124-134. http://dx.doi.org/10.1016/j.agwat.2017.02.001.

Guo, T., Gitau, M., Merwade, V., Arnold, J., Srinivasan, R., Hirschi, M., Engel, B. (2018). Comparison of performance of tile drainage routines in SWAT 2009 and 2012 in an extensively tile-drained watershed in the Midwest. *Hydrology and Earth System Sciences, 22*. 89-110. https://doi.org/10.5194/hess-22-89-2018.

Hall, R. G., Reitsma, K. D., Clay, D. E. (2016). Appendix A: Corn Planting Guide. In Clay, D.E., Carlson, C.G., Clay, S.A., Byamukama, E. (eds). iGrow Corn: Best Management Practices. South Dakota State University.

Hamilton, E. (2021, June 28). *Tile Drainage Impacts Yield and Nitrogen.* Soil Science Society of America. Retrieved from https://www.soils.org/news/science-news/tile-drainage-impacts-yield-and-nitrogen/.

Hofstrand, D. (2010). *Understanding the Economics of Tile Drainage.* Iowa State University Ag Decision Maker. Retrieved from https://www.extension.iastate.edu/agdm/wholefarm/html/c2-90.html.

Hong, Jiyeong. (2017). Modeling Streamflow and Water Quality Impacts of Grassland Establishment, Conversion, and Management in Skunk Creek Watershed. [Master's thesis, South Dakota State University]. Electronic Theses and Dissertations. https://openprairie.sdstate.edu/etd/1705?utm_source=openprairie.sdstate.edu%2Fetd%2F1705&utm_medium=PDF&utm_campaign=PDFCoverPages.

Hooghoudt, S. B. (1940). Bijdragen tot de kenins van enige natuurkundige grootheden van de ground. No. 7. Versl. Landbouwk. Onderz. (Contributions to the knowledge of some physical constants of the soil. No.7. Report Agric. Res.). 46, 515-707.

Hutchinson, K. J. & Christiansen, D. E. (2013). *Use of the Soil and Water Assessment Tool (SWAT) for Simulating Hydrology and Water Quality in the Ceder River Basin, Iowa, 2000-10.* (Report No. 2013-5002). U.S. Department of the Interior and U.S. Geological Survey. https://doi.org/10.3133/sir20135002.

Ikenberry, C. D., Soupir, M. L., Schilling, K. E., Jones, C. S., Seeman, A. (2014). Nitrate-nitrogen export: magnitude and patterns from drainage districts to downstream river basins. *Journal of Environmental Quality, 43*(6). 2024–2033.

Irwin, R.W., Whiteley, H.R. (1983). Effects of land drainage on stream flow. *Canadian Water Resources Journal, 8*. 88-103.

Jha, M. K. (n.d.). Lesson 9 Materials for Pipe Drainage Systems [e-Krishi Shiksha Online Lecture]. Department of Agricultural and Food Engineering, IIT Kharagpur. http://ecoursesonline.iasri.res.in/course/view.php?id=550.

Jha, M., Gassman, P. W., Secchi, S., Gu, R., Arnold, J. (2004). Effect of Watershed Subdivision on SWAT Flow, Sediment, and Nutrient Predictions. *Journal of the American Water Resources Association, 40*(3). 811-825. https://www.card.iastate.edu/products/publications/pdf/02wp315.pdf.

Kim, B-S., Kim, B-K., Kwon, H-H. (2011). Assessing the impact of climate change on the flow regime of the Han River Basin using indicators of hydrologic alteration. *Hydrological Processes, 25*. 691-704. DOI: 10.1002/hyp.7856.

King, K.W., Fausey, N.R., Williams, M.R. (2014). Effect of subsurface drainage on streamflow in an agricultural headwater watershed. *Journal of Hydrology, 519*. 438-445. DOI: 10.1016/j.jhydrol.2014.07.035.

Kirkham, D., (1957). Theory of Land Drainage, In "Drainage of Agricultural Lands Agronomy Monograph No. 7, American Soc. Agron", Madison, Wisconsin.

Konyha, K., Skaggs, R., Gilliam, J. (1992). Effects of drainage and water-management practices on hydrology. *Journal of irrigation and drainage engineering, 118*. 807-819.

Krause, P., Boyle, D. P., Bäse, F. (2005). Comparison of different efficiency criteria for hydrological model assessment. *Advances in Geosciences, 5*. 89-97.

Kringen, D., Hay, C., Trooien, T., Karki, G. (2021, August). *Optimal Design Drainage Rates for Eastern South Dakota.* South Dakota State University Extension. Retrieved from https://extension.sdstate.edu/sites/default/files/2021-08/P-00220.pdf.

Lou, Y., Arnold, J., Allen, P., Chen, X. (2012). Baseflow simulation using SWAT model in an inland river basin in Tianshan Mountains, Northwest China. *Hydrology and Earth System Sciences, 16.* 1259-1267. doi:10.5194/hess-16-1259-2012.

Maalim, F.K., & Melesse, A.M. (2013). Modelling the impacts of subsurface drainage on surface runoff and sediment yield in the Le Sueur Watershed, Minnesota, USA. *Hydrological Sciences Journal, 58*. 570-586. DOI: 10.1080/02626667.2013.774088.

Macrae, M. L., English, M. C., Schiff, S. L., Stone, M. (2007). Intra-annual variability in the contribution of tile drains to basin discharge and phosphorous export in a first-order agricultural catchment. *Agricultural Water Management, 92*. 171-182. DOI: 10.1016/j.agwat.2007.05.015.

Mathews, R., Richter, B. D. (2007, December). Applications of the Indicators of Hydrologic Alteration Software in Environmental Flow Setting. *Journal of the American Water Resources Association, 43*(6). 1400-1413. DOI: 10.1111/j.1752-1688.2007.00099.x.

Mehan, S., Kannan, N., Neupane, R. P., McDaniel, R., Kumar, S. (2016). Climate Change Impacts on the Hydrological Processes of a Small Agricultural Watershed. *Climate, 4*(56). DOI:10.3390/cli4040056.

Mehan, S., Neupane, R. P., Kumar, S. (2017, August). Coupling of SUFI 2 and SWAT for Improving the Simulation of Streamflow in an Agricultural Watershed of South Dakota. *Hydrology Current Research, 8*(3). 10.4172/2157-7587.1000280.

Mengel, D. (1996). *Some Questions and Answers on Applying Nitrogen to Corn After Planting*. Retrieved from https://www.agry.purdue.edu/ext/corn/news/articles.96/dm9603.htm#:~:text=For%20most%20corn%20hybrids%20N,by%20or%20shortly%20after%20tasseling.

Moriasi, D. N., Arnold, J. G., Van Liew, M. W., Binger, R. L., Harmel, R. D., Veith, T. L. (2007). Model Evaluation Guidelines for Systematic Quantification of Accuracy in Watershed Simulations. *Transactions of the ASABE, 50*(3). 885-900. https://swat.tamu.edu/media/1312/moriasimodeleval.pdf.

Moriasi, D. N., Gowda, P. H., Arnold, J. G., Mulla, D. J., Ale, S., Steiner, J. L. (2013). Modeling the impact of nitrogen fertilizer application and tile drain configuration on nitrate leaching using SWAT. *Agricultural Water Management, 130.* 36-43. http://dx.doi.org/10.1016/j.agwat.2013.08.003.

Moriasi, D. N., Gitau, M. W., Pai, N., Daggupati, P. (2015). Hydrologic and water quality models: performance measures and evaluation criteria. *Transactions of the ASABE, 58*(6). 1763-1785.

Multi-Resolution Land Characteristics Consortium. (2019). Data. Retrieved from https://www.mrlc.gov/data.

National Research Council of the National Academies. (2015). *Tying Flood Insurance to Flood Risk for Low-Lying Structures in the Floodplain.* The National Academies Press. Retrieved from https://nap.nationalacademies.org/read/21720/chapter/1.

National Weather Service. (2022). Advanced Hydrologic Prediction Service [https://water.weather.gov/ahps2/]. Retrieved from https://water.weather.gov/ahps2/hydrograph.php?wfo=fsd&gage=sifs2.

National Weather Service. (n.d.). *High Water Level Terminology*. Retrieved from https://water.weather.gov/ahps2/hydrograph.php?wfo=FSD&gage=SIFS2.

NDSU. (n.d.). *Tile Drainage: Subsurface (Tile Drainage in North Dakota and the Red River Valley.* North Dakota State University. Retrieved from https://www.ag.ndsu.edu/tiledrainage.

Neitsch, S. L., Arnold, J. G., Kiniry, J. R., Williams, J. R. (2005, January). Soil and Water Assessment Tool Theoretical Documentation, Version 2005. Grassland, Soil and Water Research Laboratory. Agricultural Research Service, 808 East Blackland Road, Temple, Texas. 76502. https://swat.tamu.edu/media/1292/SWAT2005theory.pdf.

NOAA. (2022). National Weather Service, Advanced Hydrologic Prediction Service. Retrieved from https://water.weather.gov/ahps2/hydrograph.php?wfo=FSD&gage=SIFS2.

Oeurng, C., Sauvage, S., Sanchez-Perez, J. M. (2011). Assessment of Hydrology, Sediment and Particulate Organic Carbon Yield in a Large Agricultural Catchment Using the SWAT Model. *Journal of Hydrology, 401*(3-4). 145-153.

Pandey, A., Bishal, K. C., Kalura, P., Chowdary, V. M., Jha, C. S., Cerda, A. (2021). A Soil and Water Assessment Tool (SWAT) Modeling Approach to Prioritize Soil Conservation Management in River Basin Critical Areas Coupled With Future Climate Scenario Analysis. *Air, Soil and Water Research, 14*(1). https://doi.org/10.1177/11786221211021395.

Panuska, J. (2018). *The Basics of Agricultural Tile Drainage: Basic Dranage Science and Principles.* [PowerPoint slides]. Biological Systems Engineering Department, UW Madison. https://sheboygan.extension.wisc.edu/files/2018/08/Panuska-Drainage-PPT.pdf.

Pape, A. (2017, August 14). Nitrogen Transport in Tile Drainage Systems. Ag Water Exchange. Retrieved from https://agwaterexchange.com/2017/08/14/nitrogen-transport-tile-drainage-systems/.

Pual, M. (2016). Impacts of Land Use and Climate Changes on Hydrological Processes in South Dakota Watersheds. [Master's thesis, South Dakota State University]. Electronic Theses and Dissertations. https://openprairie.sdstate.edu/cgi/viewcontent.cgi?article=2018&context=etd.

Paul, M., Rajib, M. A., Ahiablame, L. (2016). Spatial and temporal evaluation of hydrological response to climate and land use change in three South Dakota watersheds. *Journal of the American Water Resources Association, 53(*1). 69-88.

PRISM Climate Group. (n.d.). *PRISM Climate Data.* Northwest Alliance for Computational Science. Retrieved from https://www.prism.oregonstate.edu/.

Qiu, Z., Wang, L. (2013). Hydrological and Water Quality Assessment in a Suburban Watershed with Mixed Land Uses Using the SWAT Model. *Journal of Hydrologic Engineering, 19*(4). 816-827.

Rahman, M. M. (2011, November). Application of SWAT for Impact Analysis of Subsurface Drainage on Streamflows in a Snow Dominated Watershed. [Master's thesis, North Dakota State University]. https://library.ndsu.edu/ir/bitstream/handle/10365/29555/Rahman%2C%20Mohammed_Agriculture%20and%20Biosystems%20MS_2011.pdf?sequence=1&isAllowed=y.

Rahman, M. M., Lin, Z., Moriasi, D. N. (2011, August 7-10). *Applying SWAT for Impact Analysis of Tile Drainage on Streamflow in a Snow Dominated Watershed.* [Paper Presentation]. 2011 ASABE Annual International Meeting, Louisville, Kentucky. 10.13031/2013.37343

Rahman, M. M., Lin, Z. (2013). Impact of Subsurface Drainage on Stream Flows in the Red River of the North Basin. Technical Report No: ND13-05, North Dakota Water Resources Research Institute.

Rahman, M. M., Lin, Z., Jia, X., Steele, D. D., DeSutter, T. M. (2014). Impact of subsurface drainage on streamflows in the Red River of the North basin. *Journal of Hydrology, 511.* 474-483. http://dx.doi.org/10.1016/j.jhydrol.2014.01.070.

Rajib, M. A., Ahiablame, L., Paul, M. (2016, November). Modeling the effects of future land use change on water quality under multiple scenarios: A case study of low-input agriculture with hay/pasture production. *Sustainability of Water Quality and Ecology, 8.* 50-66. https://doi.org/10.1016/j.swaqe.2016.09.001.

Rajib, M. A., Merwade, V. Yu, Z. (2016a). Multi-Objective Calibration of a Hydrologic Model Using Spatially Distributed Remotely Sensed/In-Situ Soil Moisture. *Journal of Hydrology, 536.* 192-207. DOI: 10.1016/j.jhydrol.2016.02.037.

Ransom, J. (2020). Corn Growth and Management Quick Guide. Retrieved from https://www.ndsu.edu/agriculture/ag-hub/publications/corn-growth-and-management-quick-guide.

Richter, B. D., Baumgartner, J. V., Powell, J., Braun, D. P. (1996). A Method for Assessing Hydrologic Alteration within Ecosystems. *Conservation Biology, 10*(4). 1163-1174.

Robinson, M., Rycroft, D. (1999). In RW Skaggs and J. van Schifgaarde (eds.) "Agricultural Drainage." Agronomy Monograph: 767-800.

Rupp, D. E., Daly, C., Doggett, M. K., Smith, J. I., Steinberg, B. (2022). Mapping an Observation-Based Global Solar Irradiance Climatology across the Conterminous United States. *Journal of Applied Meteorology and Climatology, 61*(7). 857-876. https://doi.org/10.1175/JAMC-D-21-0236.1

Saha, P. P., Zeleke, K., Hafeez, M. (2019). Chapter 15- Impacts of land use and climate change on streamflow and water balance of two sub-catchments of the Murrumbidgee River in South Eastern Australia. *Extreme Hydrology and Climate Variability.* 175-190. Elsevier.

Sanghun, L & Reicks, G. (2013). Chapter 26: Management recommendations for soybean Fe, K, Cl, and S. In Clay, D.E., Carlson, C.G., Clay, S. A., Wagner, L., Deneke, D., Hay, C. (eds). iGrow Soybeans: Best Management Practices for Soybean Production. South Dakota State University, SDSU Extension.

Scherer, T., Sands, G., Kandel, H., Hay, C. (2015, March). *Frequently Asked Questions About Subsurface (Tile) Drainage.* AE1690. Retrieved from https://northcentralwater.org/wp-content/uploads/sites/317/2016/02/Frequently-Asked-Questions-About-Subsurface-Tile-Drainage.pdf.

Schilling, K. E., Gassman, P. W., Kling, C. L., Campbell, T., Jha, M. K., Wolter, C. F., Arnold, J. G. (2013). The potential for agricultural land use change to reduce flood risk in a large watershed. *Hydrological Processes, 28*(8). 3314-3325. https://doi.org/10.1002/hyp.9865.

Schilling, K. E., Gassman, P. W., Arenas-Amada, A., Jones, C. S., Arnold, J. (2019). Quantifying the contribution of tile drainage to basin-scale water yield using analytical and numerical models. *Science of the Total Environment, 657.* 297-309. https://doi.org/10.1016/j.scitotenv.2018.11.340.

Sharma, A. (2018). Application of Drainage Water Management and Saturated Buffers for Conservation Drainage in South Dakota. [Master's thesis, South Dakota State University]. Electronic Theses and Dissertations. https://openprairie.sdstate.edu/cgi/viewcontent.cgi?article=3714&context=etd.

Sheshukov, A. (2012, April 25). K-State Calibration Utility for ArcSWAT. Kansas State University. Retrieved from http://www.bae.ksu.edu/watershed.

Skaggs, R., Broadhead, R. (1982). Drainage strategies and peak flood flows. ASAE, Paper, St. Joseph, MI.

Skaggs, R.W., Breve, M., Gilliam, J. (1994). Hydrologic and water quality impacts of agricultural drainage∗. *Critical reviews in environmental science and technology, 24*. 1-32.

Sloan, B. P. (2013). *Hydrologic impacts of tile drainage in Iowa.* [Master's thesis, University of Iowa]. Iowa Research Online.

Sloan, B. P., Basu, N. B., Mantilla, R. (2015). Hydrologic impacts of subsurface drainage at the field scale: Climate, landscape and anthropogenic controls. *Agricultural Water Management, 165.* 1-10. http://dx.doi.org/10.1016/j.agwat.2015.10.008.

Soil Survey Staff, Natural Resources Conservation Service, United States Department of Agriculture. Soil Survey Geographic (SSURGO) Database for [Skunk Creek Watershed, South Dakota]. Available online. Accessed [04/22/2022].

South Dakota's Conservation Districts. (n.d.). *Cropland.* Retrieved from https://www.sdconservation.org/index.asp.

Stika, J. (2019, December 4). *The connection between a tile drainage system and healthy soil.* Retrieved from https://www.agdaily.com/insights/tile-drainage-system-healthy-soil/.

Stokes, T. (n.d.). *Removal of Nitrogen and Phosphorous from Tile Drainage Water.* [PowerPoint slides]. Crop Adviser Institute, Iowa State University. https://masters.agron.iastate.edu/files/stokesthomas-cc.pdf.

Susquehanna Flood Forecast and Warning System. (n.d.). *Types of Flooding.* Retrieved from https://www.susquehannafloodforecasting.org/flood-types.html.

Teshager, A. D., Gassman, P. W., Secchi, S., Schoof, J. T., Misgna, G. (2016). Modeling Agricultural Watersheds with the Soil and Water Assessment Tool (SWAT): Calibration and Validation with a Novel Procedure for Spatially Explicit HRUs. *Environmental Management, 57.* 894-911. 10.1007/s00267-015-0636-4.

The Nature Conservancy. (n.d.). Indicators of Hydrologic Alteration (IHA). *Conservation Gateway*. Retrieved from https://www.conservationgateway.org/ConservationPractices/Freshwater/EnvironmentalFlows/MethodsandTools/IndicatorsofHydrologicAlteration/Pages/indicators-hydrologic-alt.aspx.

Thomas, N. W. (2015). *Simulating the hydrologic impact of distributed flood mitigation practices, tile drainage, and terraces in an agricultural catchment.* [Ph.D. Thesis, University of Iowa]. Iowa Research Online.

Tyagi, J. V. & Rao, Y. R. S. (n.d.). *Evaluation of SWAT for modelling the water balance and water yield in Yerrakalva River Basin, A. P.* [PowerPoint slides]. National Institute of Hydrology, Roorkee. https://swat.tamu.edu/media/115946/3-jaivir-tyagi-e3-session.pdf.

United States Department of Agriculture Natural Resources Conservation Service. (2007). Chapter 7 Hydrologic Soil Groups. *Part 630 Hydrology, National Engineering Handbook.* (7-ii-7-5). Retrieved from https://directives.sc.egov.usda.gov/OpenNonWebContent.aspx?content=17757.wba.

United States Department of Agriculture Soil Conservation Service. (1971). National Engineering Handbook. Section 16, Drainage of Agricultural Land. Chapter 4, Subsurface Drainage. Washington, D.C.: U.S. Dept. of Agriculture, Soil Conservation Service.

University of Minnesota Extension. (2018). *Designing a subsurface drainage system.* Retrieved from https://extension.umn.edu/agricultural-drainage/designing-subsurface-drainage-system#drain-depth-and-spacing-1367612.

USDA-NRCS. (2014, April). Cropping Systems in South Dakota: A 2013 Inventory and Review. Retrieved from SD-2013CroppingSystemsInventory_Final.pdf.

USDA-NRCS. (2022, April 22). Geo Spatial Data Gateway. Retrieved from https://datagateway.nrcs.usda.gov/GDGOrder.aspx.

USDA-NRCS. (n.d.). Web Soil Survey. Retrieved from https://websoilsurvey.sc.egov.usda.gov/App/WebSoilSurvey.aspx.

U.S. Geological Survey, 2022, *National Water Information System data available on the World Wide Web* (Water Data for the Nation), accessed [June 10, 2022], at https://waterdata.usgs.gov/nwis/dv?referred_module=sw&site_no=06481500.

USGS. (2022). *USGS 06481500 SKUNK CR AT SIOUX FALLS, SD.* Retrieved from https://waterdata.usgs.gov/nwis/dv?referred_module=sw&site_no=06481500.

USGS. (2003). Fraction of Streamflow derived from baseflow. *US Baseflow Fractions*. Retrieved from http://water.usgs.gov/GIS/metadata/usgswrd/XML/bfi48grd.xml#stdorder.

USGS. (2023). WaterWatch. Customized Rating Curve Builder. Retrieved from https://waterwatch.usgs.gov/index.php?sno=06481500&btnGo=Go&pw=650&ph=500&fm=0&fmn=100&fmy=&fml%5B%5D=4&fml%5B%5D=8&fla=30&yt=1&ymin=&ymax=&xt=1&xmin=&xmax=&m=mkrc&rrm=0.

Vidon, P., Cuadra, P. (2010). Impact of precipitation characteristics on soil hydrology in tile-drained landscapes. *Hydrological Processes, 24*. 1821-1833.

Vidon, P., Cuadra, P. E. (2011). Phosphorus dynamics in tile-drain flow during storms in the US Midwest. *Agricultural Water Management, 98*. 532-540. DOI: 10.1016/j.agwat.2010.09.010.

Wang, S., Kang, S. Zhang, L., Li, F. (2008). Modelling Hydrological Response to Different Land-Use and Climate Change Scenarios in the Zamu River Basin of Northwest China. *Hydrological Processes, 22*(14). 2502-2510.

Werner, B., Tracy, J., Johnson, W. C., Voldseth, R. A., Guntenspergen, G. R., Millet, B. (2016, December). Modeling the Effects of Tile Drain Placement on the Hydrologic Function of Farmed Prairie Wetlands. *Journal of the American Water Resources Association, 52*. (6), 1482-1492. https://doi.org/10.1111/1752-1688.12471.

Wesström, I., Joel, A., Messing, I. (2014). Controlled drainage and subirrigation – A water management option to reduce non-point source pollution from agricultural land. *Agriculture, Ecosystems & Environment, 198*. 74-82. DOI: https://doi.org/10.1016/j.agee.2014.03.017.

Whiteley, H.R. (1979). Hydrologic Implications of Land Drainage. *Canadian Water Resources Journal, 4*. 12-19. DOI: 10.4296/cwrj0402012.

Winchell, M., Srinivasan, R., Di Luzio, M., Arnold, J. (2013). ArcSWAT Interface For SWAT2012, User's Guide. Grassland, Soil, and Water Research Laboratory. USDA Agricultural Research Service, 808 East Blackland Road, Temple, Texas. 76502.

Wiskow, E., van der Ploeg, R. R. (2003). Calculation of drain spacings for optimal rainstorm flood control. *Journal of Hydrology, 272*. 163-174.

Woo, D. K., Song, H., Kumar, P. (2019, June 1). Mapping subsurface tile drainage systems with thermal images. *Agricultural Water Management, 218.* 94-101. https://doi.org/10.1016/j.agwat.2019.01.031.

Yang, Y., Anderson, M., Gao, F., Hain, C., Kustas, W., Meyers, T., Crow, W., Finocchiaro, R., Otkin, J., Sun, L., Yang, Y. (2017). Impact of Tile Drainage on Evapotranspiration in South Dakota, USA, Based on High Spatiotemporal Resolution Evapotranspiration Time Series from a Multisatellite Data Fusion System. *IEEE Journal of Selected Topics in Applied Earth Observations and Remote Sensing, 10*. 2550-2564. DOI: 10.1109/jstars.2017.2680411.

Zucker, L. A., Brown, L. C. (1998). Agricultural drainage: Water quality impacts and subsurface drainage studies in the Midwest. Ohio State University Extension.

Appendix A – Area of Tile Drainage Scenarios

Table A-1: Percent of subbasin agricultural land modeled with tile drainage during scenario analysis.

	Scenario 1	Scenario 2	Scenario 3	Scenario 4	Scenario 5
Subbasin 1	17.3%	37.4%	56.4%	68.8%	84.5%
Subbasin 2	6.36%	17.6%	38.8%	58.0%	78.8%
Subbasin 3	19.3%	25.6%	41.2%	57.5%	73.6%
Subbasin 4	7.54%	27.9%	49.5%	61.7%	86.6%
Subbasin 5	13.1%	18.3%	19.6%	62.0%	79.5%
Subbasin 6	24.4%	43.6%	43.6%	44.7%	44.7%
Subbasin 7	26.3%	28.9%	35.3%	45.1%	52.7%
Subbasin 8	16.4%	49.5%	72.7%	72.7%	75.6%

Table A-2: Area of subbasin agricultural land modeled with tile drainage during scenario analysis.

	Scenario 1	Scenario 2	Scenario 3	Scenario 4	Scenario 5
Subbasin 1	44.0 km^2	95.5 km^2	144.1 km^2	175.6 km^2	215.6 km^2
Subbasin 2	11.9 km^2	32.9 km^2	72.7 km^2	108.6 km^2	147.4 km^2
Subbasin 3	22.3 km^2	29.5 km^2	47.6 km^2	66.5 km^2	85.0 km^2
Subbasin 4	10.5 km^2	39.0 km^2	69.1 km^2	86.3 km^2	121.0 km^2
Subbasin 5	18.3 km^2	25.6 km^2	27.4 km^2	86.5 km^2	110.9 km^2
Subbasin 6	24.3 km^2	43.3 km^2	43.3 km^2	44.5 km^2	44.5 km^2
Subbasin 7	25.5 km^2	27.9 km^2	34.2 km^2	43.6 km^2	51.0 km^2
Subbasin 8	16.6 km^2	50.1 km^2	73.6 km^2	73.6 km^2	76.5 km^2

Appendix B – Literature Review Used to Develop Expected Tile Flow Ranges

Table B-1: Tile drainage papers used to develop expected range of tile flow per average annual precipitation and per average annual water yield.

Study	Authors	Watershed Location	Watershed Size	Percent Drained	Soil Type	Tile Flow
SWAT Model Simulation of Bioenergy Crop Impacts in a Tile-Drained Watershed	Boles, (2013)	Matson Ditch watershed Dekalb County, Indiana	47 km^2	50.9%	Silt loam, Clay loam	8.5%-16.2% annual precipitation 20.3%-48.2% annual water yield
Impact of Subsurface Drainage on Streamflows in the Red River of the North Basin	Rahman et al., (2014)	Upper Red River of the North Basin Part of MN, ND, SD, USA and Manitoba, Saskatchewan, Canada	0.20 km^2 field	Observed field: 100%	Lake deposits (clay and silt) Glacial Drift (mixture of clay, silt, sand, and gravel)	16% annual precipitation 37% water yield
Modeling the impact of nitrogen fertilizer application and tile drain configuration on nitrate leaching using SWAT	Moriasi et al., (2013)	Monitoring study from University of Minnesota's Agricultural Experiment Station	--- Assumed small (study plot)	Assumed 100%	Clay loam	39% annual precipitation
Quantifying the contribution of tile drainage to basin-scale water yield	Schilling et al., (2019)	Boone River watershed	2370 km^2	All cropland <2% slope	Silty and loamy soils	EMMA: 46% water yield

using analytical and numerical models		North-central Iowa Lyons Creek watershed	 42 km^2	 84% cropland	 “ “	SWAT: 54% water yield 58%-66% water yield
Impact of tile drainage on water budget and spatial distribution of sediment generating areas in an agricultural watershed	Golmohammadi et al., (2017)	Canagagigue Creek Ontario, Canada	143 km^2	65%	Loam, Silty Loam	11.9% annual precipitation 25.45% water yield
Hydrologic impacts of subsurface drainage at the field scale: Climate, landscape, and anthropogenic controls	Sloan et al., (2016)	Iowa State University’s experimental plots	-- Assumed small (study plot)	100%	Clay Silt	19.0% precipitation 16.9% precipitation
Simulating the hydrologic impact of distributed flood mitigation practices, tile drainage, and terraces in an agricultural catchment	Thomas, (2015)	Beaver Creek watershed Iowa (central US)	45 km^2	100%	Loam, Clay Loam	6%-71% water yield
Applying SWAT for Impact Analysis of Tile Drainage on Streamflow in a Snow Dominated Watershed	Rahman et al., (2011)	Upper Red River of the North Basin Southeastern ND, midwestern MN,	16,576 km^2	0.75%	---	Essentially 0% of annual precipitation and water yield
Simulation of flow and water quality from tile drains at the watershed and field scale	Moloney, (2016)	“Watershed B” located in Upper Big	3.8 km^2	89%	Silt loam, Silty clay loam	45.3%-89.7% water yield

		Walnut Creek Watershed Central Ohio				
Contributions of Systematic Tile Drainage to Watershed-Scale Phosphorous Transport	King et al., (2015)	Headwater watershed of Upper Big Walnut Creek watershed Central Ohio	3.8 km^2	80%	Silt loam, clay loam	47% of water yield
Estimation of tile drainage contribution to streamflow and nutrient loads at the watershed scale based on continuously monitored data	Arenas Amado et al., (2017)	Otter Creek watershed Northeast Iowa	122 km^2	Not available	Not available	15%-43% water yield
Intra-annual variability in the contribution of tile drains to basin discharge and phosphorous export in a first-order agricultural catchment	Macrae et al., (2007)	Strawberry Creek watershed Ontario, Canada	< 3km^2	45%	Loam, Silt loam	42% water yield